國立交通大學

應用化學研究所

博士論文

多面體聚矽氧烷與高分子複合材之氫鍵作用力與高分子電解質之研究

The Study on Hydrogen Bonding Interactions and Polyelectrolyte Properties of Polyhedral Oligomeric Silsesquioxane/Polymer Composites

研 究 生：嚴英傑

指導教授：張豐志　教授

中 華 民 國 九 十 七 年 十 月

多面體聚矽氧烷與高分子複合材之氫鍵作用力與高分子電解質之研究

The Study on Hydrogen Bonding Interactions and Polyelectrolyte Properties of Polyhedral Oligomeric Silsesquioxane/Polymer Composites

研 究 生：嚴英傑　　Student：Ying-Chieh Yen

指導教授：張豐志　　Advisor：Feng-Chih Chang

國 立 交 通 大 學

應 用 化 學 系

博 士 論 文

A Thesis

Submitted to Department of Applied Chemistry

College of Science

National Chiao Tung University

in partial Fulfillment of the Requirements

for the Degree of

Doctor of Philosophy

in

Applied Chemistry

October 2008

Hsinchu, Taiwan, Republic of China

中華民國九十七年十月

多面體聚矽氧烷與高分子複合材之氫鍵作用力與高分子電解質之研究

學生：嚴英傑　　指導教授：張豐志 教授

國立交通大學應用化學研究所 博士班

摘　要

多面體聚矽氧烷 (POSS) 衍生物於許多領域均有應用性。然而，探討其於高分子電解質及質子傳導膜方面(能源儲存及來源方面)應用之論文卻十分稀少。本論文中，改質後之多面體矽氧烷經由共價鍵結(化學鍵)及非共價鍵結(物理鍵)之方法導入高分子中，形成新型高分子電解質及質子傳導膜。此外，我們也利用 Painter-Coleman association model (PCAM) 理論計算改質後多面體聚矽氧烷分子內作用力常數及其與高分子間作用力常數。

本研究首先探討具八酚官能基多面體聚矽氧烷分別與聚甲基丙烯酸甲酯 [poly(methyl methacrylate) (PMMA)]、聚乙烯必咯烷酮 [poly(vinyl pyrrolidone) (PVP)]，及兩者之共聚物 (PMMA-*co*-PVP) 形成摻合物之相溶性及作用力機制。二相混摻系統中，具八酚官能基多面體聚矽氧烷與聚甲基丙烯酸甲酯間之作用力

常數為 29，此常數小於聚乙烯苯酚 [poly(vinyl phenol) (PVPh)] 與聚甲基丙烯酸甲酯間之作用力常數 (37) 及乙基苯酚 [ethyl phenol (EPh)] 與聚甲基丙烯酸甲酯間之作用力常數 (101)。由上述可知，具八酚官能基多面體聚矽氧烷之酚官能基與聚甲基丙烯酸甲酯之羰基作用之機率較其他二者低。此外，我們也發現，具八酚官能基多面體聚矽氧烷之摻入可增加過氯酸鋰 ($LiClO_4$) 與甲基丙烯酸甲酯－乙烯必咯烷酮共聚物 (PMMA-*co*-PVP) 高分子電解質之離子導電度。

接著觀察具八酚官能基多面體聚矽氧烷摻入過氯酸鋰與聚甲基丙烯酸甲酯高分子電解質後對於熱性質、形態，及作用力之影響。具八酚官能基多面體聚矽氧烷與聚甲基丙烯酸甲酯二相摻合物中，具八酚官能基多面體聚矽氧烷傾向自身聚集。因此，導致整體玻璃轉移溫度 (glass transition temperature) 下降。但於聚甲基丙烯酸甲酯、過氯酸鋰，與具八酚官能基多面體聚矽氧烷三相摻合物中，具八酚官能基多面體聚矽氧烷可形成約 20 奈米大小之聚集，導致整體之玻璃轉移溫度上升。傅立葉轉換紅外線光譜 (FTIR) 量測結果指出，過氯酸鋰有助於增加具八酚官能基多面體聚矽氧烷與聚甲基丙烯酸甲酯形成氫鍵作用力之機率。場發射掃描式電子顯微鏡 (SEM) 、熱示差掃瞄卡量計 (DSC) ，及 X 光繞射儀 (XRD) 之結果均指出，過氯酸鋰之摻入是可改善具八酚官能基多面體聚矽氧烷於聚甲基丙烯酸甲酯中之分散情形並使具八酚官能基多面體聚矽氧烷之物理效應由稀釋之角色轉為物理交聯之角色。

在本研究之最後一部分中，我們將多面體聚矽氧烷導入磺化聚醚醚酮

[sulfonated poly(ether ether ketone) (SPEEK)] 中，形成一新型交聯型質子傳導膜。在傳導膜中，奈米級交聯劑之分散性受其上有無磺酸根之影響而產生不同之分散程度，導致親水區域之分散及聯結程度不同。其中，含 17.5 wt% 交聯劑之新型質子傳導膜，具有高質子導電度 (0.0153 S/cm) 、低甲醇穿透率 (1.34×10^{-7} cm^2/s) ，以及高選擇率 (0.0011 Ss/cm^3) 之特性。

The Study on Hydrogen Bonding Interactions and Polyelectrolyte Properties of Polyhedral Oligomeric Silsesquioxane/Polymer Composites

Student：Ying-Chieh Yen Advisors：Dr. Feng-Chih Chang

Department of Applied Chemistry
National Chiao Tung University

ABSTRACT

Polyhedral oligomeric silsequioxane (POSS) derivatives have the potential for the application in several fields, however, they had rarely been used in the filed of polyelectrolyte and proton exchange membrane which play a critical role in the people's life because of the need for energy storage and cleaning energy source. In this thesis, POSSs were modified to be non-covalently and covalently incorporated into polymer matrix to form the new polyelectrolyte and proton exchange membrane. In addition, the Painter–Coleman association model (PCAM) was employed to theoretically study the intra-association and inter-association between the modified POSS and polymer.

Firstly, we investigated the miscibility behavior and mechanism of interaction of poly(methyl methacrylate) (PMMA), poly(vinyl pyrrolidone) PVP, and PMMA-*co*-PVP blends with octa(phenol)octasilsequioxane (OP-POSS). For the PMMA/OP-POSS binary blend, the value of the association constant (K_A = 29) was smaller than that in the poly(vinyl phenol) (PVPh)/PMMA (K_A = 37.4) and ethyl phenol (EPh)/PMMA (K_A = 101) blend systems, implying that the phenol groups of the OP-POSS units in the PMMA/OP-POSS blends interacted to a lesser degree with the C=O groups of PMMA than they did in the other two systems. In addition, the ionic conductivity of a $LiClO_4$/PMMA-*co*-PVP polymer electrolyte was increased after blending with OP-POSS.

Secondly, the thermal properties, morphologies, and interactions within the binary and ternary blends of poly(methyl methacrylate) (PMMA), octa(phenol)octasilsesquioxane (OP-POSS), and $LiClO_4$ were described. In the binary PMMA/OP-POSS blends, the OP-POSS molecules tend to aggregate and result in a decrease (19 °C) in the glass transition temperature. In the ternary PMMA/$LiClO_4$/OP-POSS blends, however, the OP-POSS molecules form small sphere-like domains (20 nm) leading to the composite's glass transition temperature increasing by up to 30 °C. Based on these FTIR spectra, the addition of $LiClO_4$ influenced the probability of hydrogen bonds formed between PMMA and OP-POSS and these SEM micrographs, DSC, and XRD data indicated that the addition of $LiClO_4$ is a convenient and simple approach toward dispersing the OP-POSS nanoparticles within PMMA,

where the presence of $LiClO_4$ changes the physical effect of OP-POSS from that of a diluent role to a cross-linker role.

Finally, polyhedral oligomeric silsequoixane (POSS) was incorporated into sulfonated poly(ether ether ketone) (SPEEK), forming a new cross-linked proton exchange membrane (PEM). The distribution of these nano-scale cross-linkers were affected by their sulfonic acid groups and dictated the water behavior and the dispersion and connectivity of hydrophilic domains within these PEMs. A PEM formed by incorporating 17.5 wt% of the cross-linkers (containing POSS molecules and sulfonic acid groups) into SPEEK exhibited high proton conductivity (0.0153 S/cm), low methanol permeability (1.34×10^{-7} cm^2/s), and high selectivity (0.0011 Ss/cm^3).

Acknowledgment

經過 2004 年夏天的研究所考試，我考上了交大應化所，從沒離開過家的我，帶著簡單的行李來到交大展開研究生涯。幸運地，張豐志老師願意收留我這個考試生，大學成績十分不理想的考試生。碩一時，在老師及郭紹偉學長的指導下，進行高分子間氫鍵作用力的研究。當時，老師經常和我說一個故事，一個博士和碩士有何不同的故事（這故事我到現在都還常和學弟提起），且經過和最支持我的家人，爸爸和媽媽，討論後，我報名了直升博士班的甄試，於 2005 年順利直升博士班。從直升後到現在，已有三年半的時間，期間老師對於我的影響非常大，無論是課業、人生觀，甚至我對未來的計畫。在老師自由的學風下，我對研究的興趣及渴望與日俱增，這種感覺，我想是其他實驗室的同學無法體會的。因此，我也決定繼續在老師的實驗室進行博士後研究，繼續做我喜歡做的事。我更希望，這就是我未來的職業。此外，老師待人處事豁達的態度，讓我對人生有了不同的體會，也學會了忍讓。謝謝老師這四年來的指導，未來的日子裡，也請老師多多指教。

這四年中間，林振隆學長及邱俊毅學長是幫助我最大最大的人，沒有你們二位，就沒有今天的我，雖相處時間只有短短二年，但無論實驗及生活上你們都給了我極大的幫助。智嘉及昀昇學弟，如果沒有你們，我也不會有現在多元化的成果，我相信我們的堅持是對的，希望可以一直合作下去，也期待未來會磨擦出更多火花。我的好朋友，振華，謝謝你在課業上及生活中的幫助，希望你也能順利地走下去。同學們及其他實驗室學弟

妹和學長姊們，非常感謝大家的幫忙，讓我在研究及課業上均可順利進行。

感謝女友芝嫻八年半來的陪伴，容忍我的怪脾氣，過去的日子有歡笑也有淚水，我會努力，讓未來的日子只有歡笑。最後，謝謝我的家人，爸爸、媽媽、外婆、乾媽、弟弟、妹妹，有你們的支持，我才能專心地進行研究工作。僅以此論文獻給所有曾經幫助過我的人，謝謝你們，我會繼續努力，不辜負你們的期望。

Outline of Contents

List of Tables

List of Schemes

List of Figures

Chapter 1

Introduction

1.1. Introduction to Polyhedral OligomericSilsesquioxane (POSS)

Polyhedral oligomeric silsesquoixanes (POSSs), which have the general formula $(RSiO_{1.5})_n$, are prototypical organic/inorganic systems composed of inorganic cores with external organic substituents where R can be hydrogen or any alkyl, alkylene, aryl, and arylene groups, or their derivatives of which structure can be the random structure, ladder structure, cage structure, and partial cage structure as shown in Figure 1-1.[1] In 1946, Scott et al. first isolated the oligomeric organosilsesquioxanes through the co-hydrolysis of methyltrichlorosilane and dimethylchlorosilane.[2] However, the further development of POSS was started until the discovery of the polymerizable POSS and its related copolymer proposed by Lichtenhan and the American Air Force Research Laboratory in 1991.[3,4] Later, Feher, Laine, Sellinger,[5] and Mather et al.[6] incorporated these POSS derivatives into polymer systems, resulting improvement in the physical and mechanical property, sequentially, the interest in lowering the cost and enlarging the quantity of the production was also growing. In 1998, the start-up of Hybrid plastics in Fountain Valley, CA, turned the scale of the production of the material into large, the industrial production.

These ladder-like POSSs [Figure 1-1 (b)] proposed by Baney et al. and others possess outstanding thermal stability and oxidative resistance at high temperature (more than 500 ^oC),[6-12] thus it can be used in the filed, including photoresist for electronics and optical devices,[13,14] dielectrics and protective films for semiconductor,[15,16] liquid crystal display materials,[17] recording media,[18] gas separation film,[19] and ceramics binder.[20] Recently, the specific cage structures [Figure 1-1 (c)] have attracted great interest because it is a nanoparticle with diameter varied from 1 to 3 nm and organic substituents on its outer surface leading to the formation of miscible blend with polymers, biological systems, and surfaces.

Through appropriate designing of the functionality of these organic substituents, it is possible to create both mono- and octa-functional macromonomers for desired applications. These functionalized POSS derivatives can be blended[21-23] or attached covalently to linear thermoplastics[24-31] or thermosetting networks[25,26,32-37] to form high-performance hybrid materials.[38-43] Based on the above, these POSS derivatives have the potential for the application in several fields, however, they had rarely been used in the filed of polyelectrolyte and proton exchange membrane which play a critical role in the people's life because of the need for energy storage and cleaning energy source. In this thesis, POSS were modified to be non-covalently and covalently incorporated into polymer matrix to form the new polyelectrolyte and proton exchange membrane. In addition, the Painter–Coleman association model (PCAM) was employed to theoretically study the intra-association and inter-association between the modified POSS and polymer.

References

1. Pittman, Jr. C. U.; Li, G. Z.; Ni, H. *Macromol. Symp.* **2003**, *196*, 301.

2. Scott, D. W. *J. Am. Chem. Soc.* **1946**, *68*, 356.

3. Lichtenhan, J. D.; Feher, F. J.; Gilman, J. W. *Macromolecules* **1993**, *26*, 2141.

4. Lichtenhan, J. D.; Otonary, Y.; Carr, M. J. *Macromolecules* **1995**, *28*, 8435.

5. Laine, R. M.; Sellinger, A. *Macromolecules* **1996**, *29*, 2327.

6. Baney, R. H.; Itoh, M.; Sakakibara, A.; Suzuki, T. *Chem. Rev.* **1995**, *95*, 1409.

7. Zhang, X.; Shi, L. *Chin. J. Polym. Sci.* **1987**, *5*, 197.

8. Xie, Z.; He, Z.; Dai, D.; Zhang, R. *Chin. J. Polym. Sci.* **1989**, *7*, 183.

9. Maciel, G. E.; Sullivan, M. J.; Sindorf, D. W. *Macromolecules* **1981**, *14*, 1607.

10. Engelhavdt, G.; Jancke, H.; Lippmaa, E.; Samoson A. *J. Organomet. Chem.* **1981**, *210*, 295.

11. Frye, C. L.; Collins, W. T. *J. Am. Chem. Soc.* **1970**, *92*, 5586.

12. Belot, V.; Corriu, R.; Leclerq, D.; Mutin, P. H.; Vioux, A. *Chem. Mater.* **1991**, *3*, 127.

13. Adachi, H.; Hayashi, O.; Okahashi, K. Japanese Patent Kokoku-H-2-15863.

14. Adachi, H.; Hayashi, O.; Okahashi, K. Japanese Patent Kokai-S-60-108841.

15. Adachi, E.; Aiba, Y.; Adachi, H. Japanese Patent Kokai-H-2-277255.

16. Aiba, Y.; Adachi, E.; Adachi, H. Japanese Patent Kokai-H-3-6845.

17. Shoji, F.; Sudo, R.; Watanabe, T. Japanese Patent Kokai-S-56-146120.

18. Imai, E.; Takeno, H. Japanese Patent Kokai-S-59-129939.

19. Saito, Y.; Tsuchiya, M.; Itoh, Y. Japanese Patent Kokai-S-58-14928.

20. Mine, T.; Komasaki, S. Japanese Patent Kokai-S-60-210570.

21. Kuo, S. W.; Lin, H. C.; Huang, W. J.; Huang, C. F.; Chang, F. C. *J. Polym. Sci., Polym. Phys.* **2006**, *44*, 673.

22. Lee, Y. J.; Huang, J. M.; Kuo, S. W.; Chang, F. C. *Polymer* **2005**, *46*, 10056.

23. Zhang, H.; Kulkarni, S.; Wunder, S. L. *J. Phys. Chem. B* **2007**, *111*, 3583.

24. Kopesky, E. T.; Haddad, T. S.; Cohen, R. E.; McKinley, G. H. *Macromolecules* **2004**, *37*, 8992.

25. Li, G. Z.; Wang, L.; Toghiani, H.; Daulton, T. L.; Koyama, K.; Pittman, C. Y. *Macromolecules* **2001**, *34*, 8686.

26. Matejka, L.; Strachota, A.; Plestil, J.; Whelan, P.; Steinhart, M.; Slouf, M. *Macromolecules* **2004**, *37*, 9449

27. Lin, H. C.; Wang, C. F.; Kuo, S. W.; Tung, P. H.; Huang, C. F.; Lin, C. H.; Chang, F. C. *J. Phys. Chem. B* **2007**, *111*, 3404.

28. Leu, C. M.; Chang, Y. T.; Wei, K. H. *Chem. Mater.* **2003**, *15*, 2261.

29. Leu, C. M.; Chang, Y. T.; Wei, K. H. *Chem. Mater.* **2003**, *15*, 3721.

30. Phillips, S. H.; Haddad, T. S.; Tomcrzak, S. J. *Curr. Opin. Solid State Mater. Sci.* **2004**, *8*, 21.

31. Li, G. Z.; Wang, L. C.; Ni, H. L. *J. Inorg. Organomet. Polym.* **2001**, *11*, 123.

32. Chen, W. Y.; Wang, Y. Z.; Kuo, S. W.; Huang, C. F.; Tung, P. H.; Chang, F. C. *Polymer* **2004**, *45*, 6897.

33. Tamaki, R.; Choi, J.; Laine, R. M. *Chem. Mater.* **2003**, *15*, 793.

34. Lee, Y. J.; Huang, J. M.; Kuo, S. W.; Lu, J. S.; Chang, F. C. *Polymer* **2005**, *46*, 173.

35. Ye, Y. S.; Chen, W. Y.; Wang, Y. Z. *J. Polym. Sci., Part A: Polym. Chem.* **2006**, *44*, 5391.

36. Liu, Y. L.; Chang, G. P.; Hsu, K. Y.; Chang, F. C. *J. Polym. Sci., Part A: Polym. Chem.* **2006**, *44*, 3825.

37. Do Carmo, D. R.; Paim, L. L.; Dias, N. L. *Appl. Surf. Sci.* **2007**, *253*, 3683.

38. Voronkov, M. G.; Lavrent'ev, V. I. *Top. Curr. Chem.* **1982**, 102, 199.

39. Baney, R. H.; Itoh, M.; Sakakibara, A.; Suzuki, T. *Chem. Rev.* **1995**, 95, 1409.

40. Provatas, J. G. *Trends Polym. Sci.* 1997, 5, 327.

41. Loy, D. A.; Shea, K. J. Chem. Rev. 1995, 95, 1431.

42. Lichtenhan, J. D.; In Polymeric Materials Encyclopedia, Salamone, J. C. Ed.; CRC Press: Boca Raton, FL, 1996, 7768.

43. Ni, Y.; Zheng, S. *Chem. Mater.* **2004**, *16*, 5141.

Figure 1-1. Structures of POSS.

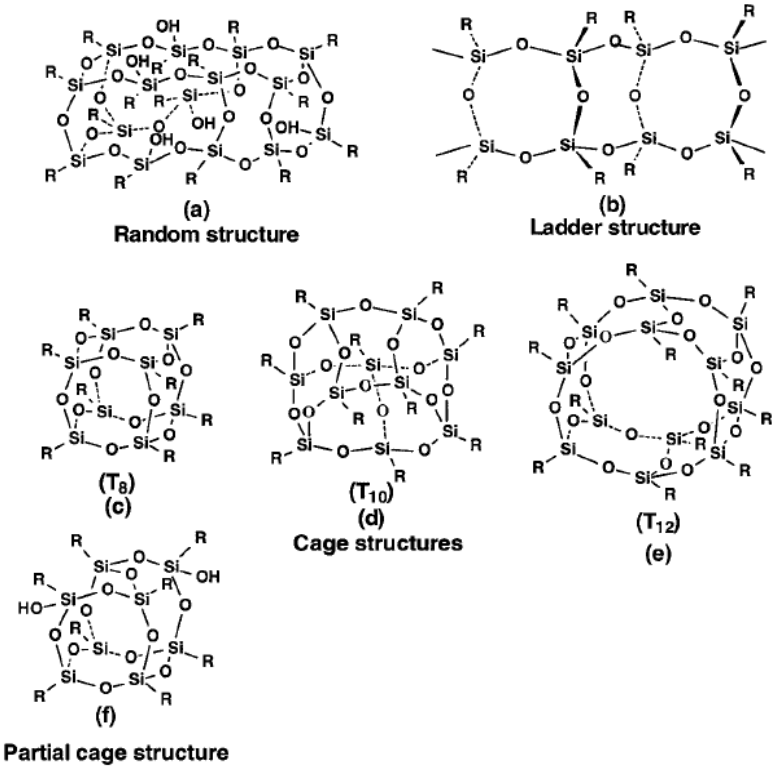

1.2. Introduction to Hydrogen Bonds in Polymer/POSS blends

1.2.1. Polymer/POSS blends

The production of polymers was growing rapidly in the past 50 years and their versatility guarantees that they are suitable for not only the traditional use but also the use in high technology. Because covalent copolymerization can be a complicated and time-consuming process, polymer blending is usually considered to be a simpler and more convenient means of preparing new polymer materials with improved properties and has been developed for a long time. Recently, the incorporation of nanoparticle into polymer matrix has attracted great interest because the resulted composite exhibited the advantage over both inorganic and organic compounds with the unique physical properties of POSS nanoparticle. The properties of these polymer/POSS composites are strongly depend on the miscibility between the incorporated polymer and POSS derivatives which can be affected by the correlation between the polymer matrix and the externally covered functionality of POSS. The correlation in the polymer/POSS composite is similar to that in polymer blend which has been widely concerned with the following intermolecular or inter-segment forces:

(a) Strong dipoles

(b) Hydrogen bonds

(c) Charge transfer complexes

(d) Ionic interactions in ionomers

The most common and important correlation are the strong hydrogen bond and/or strong dipole interactions. Coleman and Painter proposed the association models and the related theories in 1995,[1] resulting in significant progress in the field of hydrogen bonded in polymer blends. In this thesis, the model proposed by them was employed to obtain the equilibrium association constant.

1.2.2. Introduction to Painter-Coleman Association Model

In the Painter-Coleman association model proposed by Painter and Coleman, a contribution of hydrogen bonding interaction was added to the Flory-Huggins equation for the free energy of mixing:

$$\frac{\Delta G_m}{RT} = N_B \ln \Phi_B + N_A \ln \Phi_A + n_B \Phi_A \chi + \frac{\Delta G_H}{RT} \qquad (1\text{-}1)$$

where N_B and N_A are the number of polymer molecules and n_B is the total number of B segments. The first four terms correspond to the classic Flory-Huggins equation. The contribution of hydrogen bonds (the last term of the equation) can be derived from a simple model:

$$B_h + B_1 \xleftrightarrow{K_B} B_{h+1}$$

$$B_h + A \xleftrightarrow{K_A} B_h A$$

where K_B and K_A correspond to the "chain like" self-association and inter-association equilibrium constant, respectively, thus $\frac{\Delta G_H}{RT}$ can be expressed as:

$$\frac{\Delta G_H}{RT} = \sum n_{B_h} \ln(\frac{\Phi_{B_h}}{h}) + \sum n_{B_h A} \ln(\frac{\Phi B_{h A}}{h+r}) + n_{A_1} \ln(\frac{\Phi_{A_1}}{r}) + n_{BB}^h + n_{AB}^h +$$

$$(\text{terms in z and } \sigma) - [n_B \ln \Phi_B + n_A \ln \Phi_A] - n_{BB}^h \ln K_B - n_{AB}^h \ln K_A \qquad (1\text{-}2)$$

where the square bracket corresponded the excess entropy term. The association model describes the mixing of small molecules, or in effect, describes the mixing of disconnected polymer segments. With the "physical" force derived from these solubility parameters, ΔG_H can be obtained from the equilibrium constants and enthalpies of hydrogen bond formation. As the combinatorial entropy is very small, the free energy of mixing (the miscibility) is dominated by the "physical" force and enthalpy of hydrogen bond formation.

1.2.3. Ternary Polymer Blends

The reasonable development of the association model is the extension of the model to describe the phase behavior of ternary blend. However, the accuracy and the unambiguous

interpretation of experiment become problems when changing the system from binary to ternary blends.

Considering a ternary blend system composed of three polymers, including PolyA, PolyB, and PolyC, PolyB is self-associated and contains proton donor groups and PolyA and PolyC are both not self-associated and both exhibit acceptor groups [there are no strong intermolecular interactions (hydrogen bond) PolyA and PolyC]. These hydrogen bonds within this ternary blend can be described through the equilibrium conastnts, K_A, K_B, and K_C.

$$B_h + B_1 \xleftrightarrow{K_B} B_{h+1}$$

$$B_h + A \xleftrightarrow{K_A} B_h A$$

$$B_h + C \xleftrightarrow{K_C} B_h C$$

The equation describing the mixing free energy of the ternary blend is very similar to that of the binary blend, except the extra terms corresponded to the additional component of the blend:

$$\frac{\Delta G_m}{RT} = \frac{\Phi_A}{r_A N_A}\ln\Phi_A + \frac{\Phi_B}{r_B N_B}\ln\Phi_B + \frac{\Phi_C}{r_C N_C}\ln\Phi_C + \Phi_A\Phi_B\chi_{AB} + \Phi_A\Phi_C\chi_{AC} + \Phi_B\Phi_C\chi_{BC} + \frac{\Delta G_H}{RT} \quad (1\text{-}3)$$

where Φ_A, Φ_B, and Φ_C correspond to the volume fractions of PolyB, PolyA, and PolyC, respectively, and N_i is the degree of polymerization. These parameters, $r_A = \frac{V_A}{V_B}$ and $r_C = \frac{V_C}{V_B}$ are the ratios of the segment molar volumes of PolyA to PolyB and PolyC to PolyB, respectively. Because the interaction parameter, χ_{ij}, obtained from the group molar attraction and molar volume constant designed to specifically exclude contributions from hydrogen bonding is positive or equal to zero,[2] the term, $\frac{\Delta G_H}{RT}$, becomes a favorable contribution to

the mixing free energy from the hydrogen bonding interaction.[3-12] The further study on the calculation of these equilibrium constants within these binary and ternary blends is described in chapter 2.

References

1. Coleman, M. M.; Painter, P. C. *Prog. Polym. Sci.* **1995**, *20*, 1.

2. Coleman, M. M.; Graf, J. F.; Painter, P. C. *Specific Interactions and the Miscibility of Polymer Blends*; Technomic Publishing, Inc.; Lancaster, PA, 1991.

3. Painter, P. C.; Park, Y.; Coleman, M. M. *Macromolecules* **1988**, *21*, 66.

4. Painter, P. C.; Park, Y.; Coleman, M. M. *Macromolecules* **1989**, *22*, 570.

5. Painter, P. C.; Park, Y.; Coleman, M. M. *Macromolecules* **1989**, *22*, 580.

6. Coleman, M. M.; Xu, Y.; Painter, P. C. *Macromolecules* **1994**, *27*, 127.

7. Coleman, M. M.; Pehlert, G. J.; Painter, P. C. *Macromolecules* **1996**, *29*, 6820.

8. Pehlert, G. J.; Painter, P. C.; Veytsman, B.; Coleman, M. M. *Macromolecules* **1997**, *30*, 3671.

9. Painter, P. C.; Veytsman, B.; Kumar, S.; Shenoy, S.; Graf, J. F.; Xu, Y.; Coleman, M. M. *Macromolecules* **1997**, *30*, 932.

10. Coleman, M. M.; Painter, P. C. *Macromol. Chem. Phys.* **1998**, *199*, 1307.

11. Zeman, L.; Patterson, D. *Macromolecules* **1972**, *5*, 513.

12. Patterson, D. *Polym. Eng. Sci.* **1982**, *22*, 64.

1.3. Introduction to Polyelectrolytes

Rechargeable Li-ion cells are key components of the portable, entertainment, computing and telecommunication equipment required by today's information-rich, mobile life. Polymer electrolytes formed through dissolving salts into polar and high-molecular-weight polymers are the subject of intensive research because of their potential for use as the solid polymer electrolyte (SPE) in rechargeable lithium batteries.[1-6] Both the salt and the neat polymer are solids and the complex-forming reaction can be expressed as follows:[7]

$$mMX + (-RY-)_n \rightarrow (MX)_m \bullet (-RY-)_n \qquad (1\text{-}4)$$

where (–RY–) corresponds to the repeat unit of polymer. The kinetics of eq (1-4) are unfavorable, even when the complex is stable. The most commonly used method to dissolve or suspend both the MX salt and the host polymer is dissolving them in a common solvent and then removing the solvent, producing the solvent-free polymer electrolyte.[8] Obviously, the dissolving reaction will be thermodynamically favorable (negative $\Delta G°$) only if the Gibbs energy of dissolving the salt into polymer is large enough to overcome the lattice energy of the salt, thus three parameters are important for the controlling these salt/neutral molecule interactions: (a) electron pair donicity, (b) acceptor number, and (c) an entropy term. The electro pair donicity is corresponded to the ability of the solvent donating electrons to solvate the cation as Lewis acid, thus the incorporated polymer should exhibit donor site such as oxygen, sulfur, or nitrogen either in the backbone or in the side chain. The acceptor number represents the possibility for anion (base) solvation. For instance, PEO, a polyether, exhibits strong donor and its donicity is close to 20, additionally, ethers are very poor acceptors because they lack hydrogen bonding for anion salvation.[9] Thus, PEO can effectively solvate cation possessing bulky delocalized counter anions such as I^-, ClO_4^-, BF_4^- or $CF_3SO_3^-$which require little or no salvation.

The use of these electrolytes for high-energy-density batteries and other solid state

electrochemical devices spurred considerable interest in the ion-transport properties of these materials.[10-15] Besides the advantage of flexibility, polyelectrolyte can also be cast into thin films and since thin films while minimizing the resistance of the electrolyte also reduces the volume and the weight, use of polymer electrolytes can increase the energy stored per unit weight and volume. As shown in Figure 1-2, the polyelectrolyte serves as a medium to transport the ions in the cell. In addition, a separator isolating the anode from the cathode electronically can be ceramic or polymeric separator as using liquid electrolytes. Both functions, ion conduction and separation, can be realized in a single thin membrane when polymer electrolytes are used.

The goal for the SPE research is the development of highly ionic conductive (ca. 10^{-4} S/cm), dimensionally stable, and flexible SPE materials under ambient condition. Since Wright reported that poly(ethylene oxide) (PEO) can be the candidate for use in the SPEs at 1975, it has became one of the most studied materials[16] and polymer electrolytes were proposed for batteries in 1978 because they exhibited the advantages of solid state electrochemistry with the ease of processing inherent to plastic materials.[17] Since that time, the number of contributions to the field of SPEs related to PEO has grown enormously, these PEO based polyelectyrolytes were prepared through numerous physical and chemical procedures including non-covalent blending,[10-15] covalent copolymerization,[18-21] and grafting[22] for studying their interaction mechanism and for improving their flexibility and chemical and physical properties without detrimentally affecting the ionic conductivity. The ionic conductivity σ can be roughly expressed by the following equation:

$$\sigma = \sum_i n_i z_i \mu_i \qquad (1\text{-}5)$$

where n_i, z_i, and μ_i are the effective number of mobile ions, the elementary electric charge, and the ion mobility, respectively, indicating that the fraction of “free” ions is an important parameter, a high degree of dissociation of the salt in the polymer is needed for obtaining

highly ionic conductive polyelectrolyte. High Li^+ transference number is also needed, i.e., a high ratio of the charge transfer which has been an important subject of research in recent years.[23-24] The molecular dynamic simulation shown in Figure 1-3 indicated that the Li^+ ions are complexed to PEO through approximately five ether oxygens of the PEO chain, and thus mobility of the cations is decreased considerably,[25] implying that the mobility of the Li^+ cation is related to the motion of the complexed PEO chain. In summary, the polymer required for the SPE application should possess that (1) high concentration of polar (basic) groups and (2) low cohesive energy and high flexibility to solvate the salt effectively, resulting high ionic conductivity.[26-30]

References

1. Croce, F.; Appetecchi, G. B.; Persi, L.; Scrosati, B. *Nature* **1998**, ***394***, 456.

2. Gray, F. M. *Polymer Electrolytes* (RSC Materials Monographs, The Royal Society of Chemistry, Cambridge, 1997).

3. Scrosati, B. (ed.) *Applications of Electroactive Polymers* (Chapman & Hall, London, 1993).

4. Bruce, P. G. (ed.) *Solid State Electrochemistry* (Cambridge University Press, Cambridge, 1995).

5. Fenton, D. E.; Parker, J. M.; Wright, P. V. *Polymer* **1973**, *14*, 589.

6. Ratner, M. A. in *Polymer Electrolytes Reviews*—1 (eds MacCallum, J. R.; Vincent, C. A.) 173–236 (Elsevier Applied Science, London, New York, 1987).

7. Ratner, M. A.; Shriver, D. F. *Chem. Rev*. **1988**, *88*, 109.

8. LaNest, J. F.; Cheradame, H.; Dalard, F.; Deroo, D. *J. Appl. Electrochem*. **1986**, *16*, 75.

9. Gutmann, V. *The Donor Acceptor Approach to Molecular Interactions*; Plenum Press: New York, **1978**.

10. Druger, S. D.; Ratner, M. A.; Nitzan, A. *Solid State Ionics* **1983**, *9/10*, 1115.

11. Armand, M. B.; Chabango, J. M.; Duclot, M. J. in *Fast Ion Transport in Solids* (eds Vashishta, P., Mundy, J. N.; Shenoy, G. K.) 131–136 (North-Holland, Amsterdam, 1979).

12. Chiu, C. Y.; Yen, Y. J.; Kuo, S. W.; Chen, H. W.; Chang, F. C. *Polymer* **2007**, *48*, 1329.

13. Gorecki, W. *Solid State Ionics* **1998**, *28***,** 1018.

14. Chiu, C. Y.; Hsu, W. H.; Yen, Y. J.; Kuo, S. W.; Chang, F. C. *Macromolecules* **2005**, *38*, 6640.

15. Chiu, C. Y., Chen, H. W., Kuo, S. W. & Chang, F. C. *Macromolecules* **2004**, *37*, 8424.

16. Wright, P. V. *Br. Polym. J.* **1975**, *7*, 319.

17. Armand, M.; Duclot, M. *French Patent* **1978**, *7832976*.

18. Cho, B. K.; Jain, A.; Gruner, S. M.; Wiesner, U. *Science* **2004**, *305*, 1598.

19. Epps, T. H.; Bailey, T. S.; Waletzko, R.; Bates, F. S. *Macromolecules* **2003**, *36*, 2873.

20. Singh, M.; Odusanya, O.; Wilmes, G. M.; Eitouni, H. B.; Gomez, E. D.; Patel, A. J.; Chen, V. L.; Park, M. J.; Fragouli, P.; Iatrou, H.; Hadjichristidis, N.; Cookson, D.; Balsara, N. P. *Macromolecules* **2007**, *40,* 4578.

21. Zhang, H.; Kulkarni, S.; Wunder, S. L. *J. Phys. Chem. B* **2007**, *111*, 3583.

22. Gavelin, P.; Jannasch, P.; Wessle´n, B. *J. Polym. Sci. Part A: Polym. Chem.* **2001**, *39*, 2223.

23. Armand, M. *Solid State Ionics* **1994**, *69*, 309.

24. Bruce, P. G.; Vincent, C. A. *Faraday Discuss. Chem. Soc.* **1989**, *88*, 43.

25. Müller-Plathe, F.; Van Gunsteren, W. F. *J. Chem. Phys.* **1995**, *103*, 4745.

26. Vincent, C. A.; MacCallum, J. R. In *Polymer Electrolyte Reviews*; Mac Callum, J. R., Vincent, C. A., Eds., Elsevier: London, 1987.

27. Armand, M. B.; Chabagno, J. M.; Duclot, M. J. In *Fast Ion Transport in Solids*; Duclot, M. J., Vashishta, P., Mundy, J. N., Shenoy, G. K., Eds.; North-Holland: New York, 1979.

28. Shriver, D. F.; Papke, B. L.; Ratner, M. A.; Dupon, R.; Wong, T.; Brodwin, M. *Solid State Ionics* **1981**, *5*, 83.

29. Paper, B. L.; Ratner, M. A.; Shrever, D. F. *J. Phys. Chem. Solids* **1981**, *42*, 493.

30. Paper, B. L.; Ratner, M. A.; Shrever, D. F. *J. Electrochem. Soc.* **1982**, *129*, 1694.

Figure 1-2. Schematic illustration of a lithium rocking chair battery with graphite and spinel as intercalation electrodes and its electrode reactions.

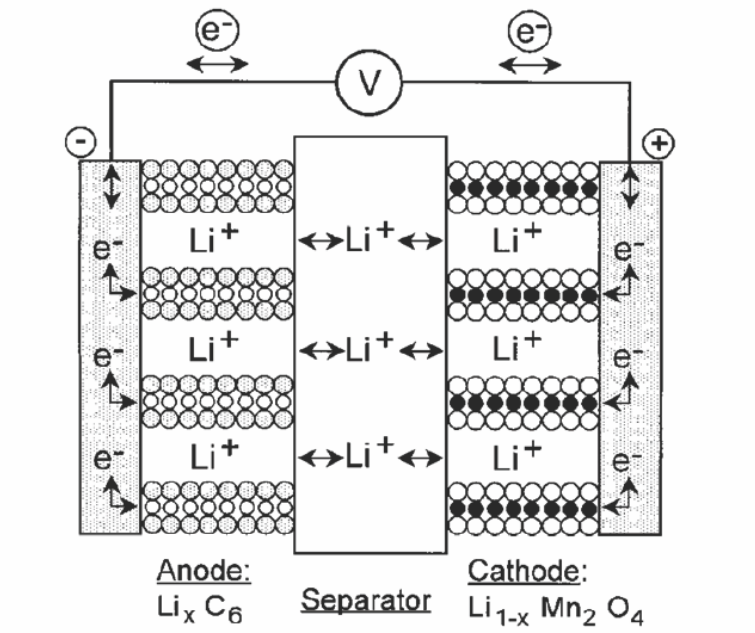

anode reaction: $Li_xC_6 \Leftrightarrow xLi^+ + xe^- + C_6$

cathode reaction: $xLi^+ + xe^- + Li_{1-x}Mn_2O_4 \Leftrightarrow LiMn_2O_4$

charging $\Leftrightarrow$ discharging

Figure 1-3. Schematic of the segmental motion assisted diffusion of Li^+ in the PEO matrix. The circles represent the ether oxygen atoms of PEO.

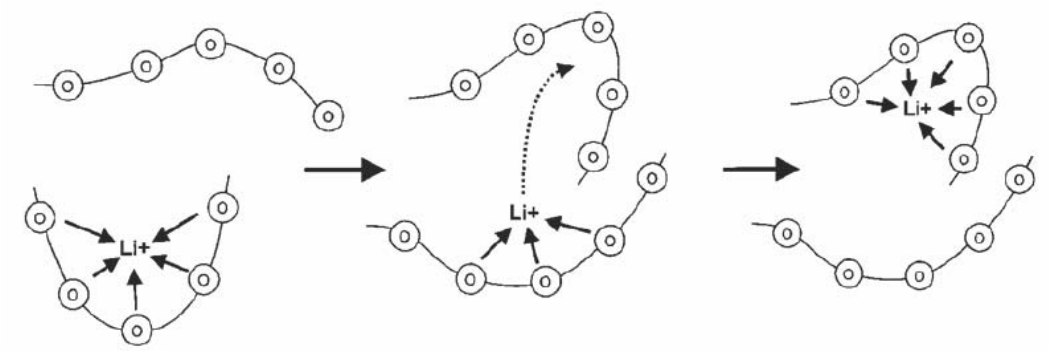

1.4. Introduction to Proton Exchange Membrane (PEM) Applied in Direct Methanol Fuel Cell (DMFC)

Recently, advanced energy technology reducing fossil fuel consumption and keeping the environment clean for human activities is becoming intensively important because of the worldwide concern about the environmental consequences of fossil fuel use in the day-to-day production of electricity and for the propulsion of vehicles. More importantly, the societal awareness concerning issues of environmental pollution increased over the last few decades. Therefore, the renewable energy sources such as wind, sun, and water were proposed and developed, but one has to remember that the complete generation process should be taken into account that these sources are not suited to satisfy the base demand. Fuel cell exhibits the potential to become an important energy conversion technology because it is a clean energy producing only water (hydrogen fuel cell) or water and carbon dioxide (direct methanol fuel cell) to overcome drawbacks of the previous energy generation. Fuel cells can usually classified by temperature and electrolyte employed in the cell, thus there are low temperature fuel cells such as Alkaline Fuel Cell (AFC), Phosphoric Acid Fuel Cell (PAFC), and DMFC, etc and high temperature fuel cells, including Molten Carbonate Fuel Cell (MCFC) and Solid Oxide Fuel Cell (SOFC), etc.[1-10]

In this thesis, we tried to focus on the polymer employed for the application in DMFC, a promising power source in today's society because of its convenient power generation procedure which is suited to today's mobile life. The basic membrane electrode assembly of DMFC was shown in Figure 1-4,[10] displaying that the proton exchange membrane plays a critical role to separate the fuel from the oxidant. These reactions involved in the power generation within DMFC were expressed as follows:

Anode:

$$CH_3OH + H_2O \rightarrow CO_2 + 6H^+ + 6e^-$$

Cathod:

$$\frac{3}{2}O_2 + 6H^+ + 6e^- \rightarrow 3H_2O$$

Overall:

$$CH_3OH + \frac{3}{2}O_2 \rightarrow CO_2 + 2H_2O$$

where the overall reaction only produced water and carbon dioxide representing that DMFC was a clean energy. The proton exchange membrane suitable for the application in DMFC should possess (1) high protonic conductivity, (2) low electronic conductivity, (3) low permeability to fuel and oxidant, (4) low water transport through diffusion and electro-osmosis, (5) oxidative and hydrolytic stability, (6) good mechanical properties in both the dry and hydrated states, (7) cost, and (8) capability for fabrication into MEA.[10] Nafion, one of the most studied material for application as PEM, exhibits both chemical and physical stability at moderate temperature and high proton conductivity through its highly interconnected hydrophilic channels.[10] Sulfonated polymers, such as sulfonated poly(ether sulfone) (SPES), poly(benzimidazole) (SPBI), poly(ether ether ketone) (SPEEK), and polyimide (SPI), are also potential candidates for use in PEMs,[11-22] but their high cost and high methanol permeability limit their applications.[10-22] To overcome these drawbacks, numerous new materials possessing reinforced sulfnoated polymers are often employed.[23-30] Cross-linked PEMs have shown significant advantages in controlling the water behavior, improving the dimension stability, and thermal stability.[31-40] The incorporation of inorganic materials into sulfonated polymers by cross-linking reaction has also been reported.[41-48] Although numerous works to develop proton exchange membrane had been done, the development of more-efficient methods for improving the chemical and mechanical stabilities of sulfonated polymer membranes—without detrimentally affecting the proton conductivity and methanol crossover—remains an important challenge.

References

1. Carrette, L.; Friedrich, K. A.; Stimming, U. *CHEMPHYSCHEM* 2000, *1*, 162.

2. Barnett, B. M.; Teagan, W. P. *J. Power Sources* **1992**, *37*, 15.

3. Melle, F. D. *J. Power Sources* **1998**, *71*, 7.

4. Hart, D. *J. Power Sources* **2000**, *86*, 23.

5. Gallow, G. D. *J. Power Sources* **1999**, *80*, xvii.

6. Bauen, A.; Hart, D. *J. Power Sources* **2000**, *86*, 482.

7. "Clean fuel cell energy for today": *Platinum Met. Rev.* **1999**, *43*, 14.

8. Chalk, S. G.; Miler, J. F.; Wanger, F. W. *J. Power Sources* **2000**, *86*, 40.

9. Dufour, A. U. *J. Power Sources* **1998**, *71*, 19.

10. Hickner, M. A.; Ghassemi, H.; Kim, Y. S.; Einsla, B. R.; McGrath, J. E. *Chem. Rev.* **2004**, *104*, 4587.

11. Wang, F.; Hickner, M.; Kim, Y. S.; Zawodzinski, T. A.; McGrath, J. E. *J. Membrane. Sci.* **2002**, *197*, 231.

12. Rozière, J.; Jones, D. J.; *Annu.Rev. Mater. Res.* **2003**, *33*, 503.

13. Xing, P. X.; Robertson, G. P.; Guiver, M. D.; Mikhailenko, S. D. Kaliaguine, S. *Macromolecules* **2004**, *37*, 7960.

14. Wang, Z.; Ni, H. Z.; Zhao, C. J.; Li, X. F.; Zhang, G.; Shao, K.; Na, H. *J. Membrane. Sci.* **2006**, *285*, 239.

15. Schönberger, F.; Jochen Kerres, J. *J. Polym. Sci Pol Chem.* **2007**, *45*, 5237.

16. Patric Jannasch, P. *Curr. Opin. Colloid. Interface Sci.* **2003**, *8*, 96.

17. Fu, Y. Z.; Manthiram, A. Guiver, M. D. *Eelctrochem. Commun.* **2007**, *9*, 905.

18. Xing, P. X.; Robertson, G. P.; Guiver, M. D.; Mikhailenko, S. D.; Wang, K. P.; Kaliaguine, S. *J. Membrane. Sci.* **2004**, *229*, 95.

19. Fang, J. H.; Guo, X. X.; Harada, S.; Watari, T.; Tanaka, K.; Kita, H.; Okamoto, K.

Macromolecules **2002**, *35*, 9022.

20. Zhou, Z. L.; Dominey, R. N.; Rolland, J. P.; Maynor, B. W.; Pandya, A. A.; M. DeSimone, J. M. *J. Am. Chem. Soc.* **2006**, *128*, 12963.
21. Miyatake, K.; Chikashige, Y.; Eiji Higuchi, E.; Masahiro Watanabe, M. *J. Am. Chem. Soc.* **2007**, *129*, 3879.
22. Asano, N.; Aoki, M.; Suzuki, S.; Miyatake, K.; Uchida, H.; Watanabe, M. *J. Am. Chem. Soc.* **2006**, *128*, 1762.
23. Xu, K.; Li, K.; Khanchaitit, P.; Wang, Q. *Chem. Mater.* **2007**, *19*, 5937.
24. M. Tsui, E. M.; Cortalezzi, M. M.; Wiesner, M. R. *J. Membrane. Sci.* **2007**, *306*, 8.
25. Subbaraman, R.; Ghassemi, H.; Zawodzinski, T. A. *J. Am. Chem. Soc.* **2007**, *128*, 2238.
26. Yamaguchi, T.; Zhou, H.; Nakazawa, S.; Hara, N.; *Adv. Mater.* **2007**, *19*, 592.
27. Grunzinger, S. J.; Watanabe, M.; Fukagawa, K.; Kikuchi, R.; Tominaga, Y.; Hayakawa, T.; Kakimoto, M. *J. Power. Sources.* **2008**, *175*, 120.
28. Yang, Y. S.; Shi, Z. Q.; Holdcroft, S. *Macromolecules* **2004**, *37*, 1678.
29. Shi, Z. Q.; Holdcroft, S. *Macromolecules* **2005**, *38*, 4193.
30. Farhat, T. R.; Hammond, P. T. *Adv. Funct. Mater.* **2005**, *15*, 945.
31. Ding, F. C.; Wang, S. J.; Xiao, M.; Meng Y. Z. *J. Power. Sources.* **2007**, *164*, 488.
32. Cho, K. Y.; Jung, H. Y.; Shin, S. S.; Choi, N. S.; Sung, S. J.; Park, J. K.; Choi, J. H.; Park, K. W.; Sung, Y. E. *Electrochim. Acta*. **2004**, *50*, 589.
33. Lee, C. H.; Park, H. B.; Chung, Y. S.; Lee, Y. M.; Freeman, B. D. *Macromolecules* **2006**, *39*, 755.
34. Fu, T. Z.; Zhao, C. J.; Zhong, S. L.; Zhang, G.; Shao, K.; Zhang, H. Q.; Wang, J.; Na, H. *J. Power. Sources.* **2007**, *165*, 708.
35. Qiao, J. L.; Hamaya, T.; Okada, T. *Chem. Mater.* **2005**, *17*, 2413.
36. Zhong, S. L.; Fu, T. Z.; Dou, Z. Y.; Zhao, C. J.; Na, H. *J. Power. Sources.* **2006**, *162*, 51.

37. Gasa, J. V.; Boob, S.; Weiss, R. A.; Shaw, M. T. *J. Membrane. Sci.* **2006**, *269*, 177.

38. Yamaki, T.; Kobayashi, K.; Asano, M.; Kubota, H.; Yoshida, M. *Polymer* **2004**, *45*, 6569.

39. Park, H. B.; Lee, C. H.; Sohn J. Y.; Lee, Y. M.; Freeman, B. D.; Kim, H. J. *J Membrane. Sci.* **2006**, *285*, 432.

40. Kim, D. S.; Guiver, M. D.; Nam, S. Y.; Yun, T. I.; Seo, M. Y.; Kim, S. J.; Hwang, H. S.; Rhim, J. W. *J. Membrane. Sci.* **2006**, *281*, 156.

41. Kim, D. S.; Liu, B. J.; Guiver, M. D. *Polymer* **2006**, *47*, 7871.

42. Chen, W. F.; Kuo, P. L. *Macromolecules* **2007**, *40*, 1987.

43. Shahi, V. K. *Solid. State. Ionics.* **2007**, *177*, 3395.

44. Vona, M. L. D.; Marani, D. D'Ottavi, C.; Trombetta, Marcella.; Traversa, E.; Beurroies, I.; Knauth, P.; Licoccia, S. *Chem. Mater.* **2006**, *18*, 69.

45. Kim, D. S.; Park, H. B.; Rhim, J. W.; Lee, Y. M. *J. Membrane. Sci.* **2004**, *240*, 37.

46. Su, Y. H.; Liu, Y. L.; Sun, Y. M.; Lai, J. Y.; Wang, D. M.; Gao, Y. Liu, B.; Guiver, M. D. *J. Membrane. Sci.* **2007**, *296*, 21.

47. Chen, S. W.; Holmberg, B.; Li, W. Z.; Wang, X.; Deng, W. Q.; Munoz, R.; Yan Y. S. *Chem. Mater.* **2006**, *18*, 5669.

48. Chang, Y. W.; Wang, E.; Shin, G.; Han, J. E.; Mather, P. T. *Polym. Adv. Technol.* **2007**, *18*, 535.

Figure 1-4. Basic membrane electrode assembly of DMFC.

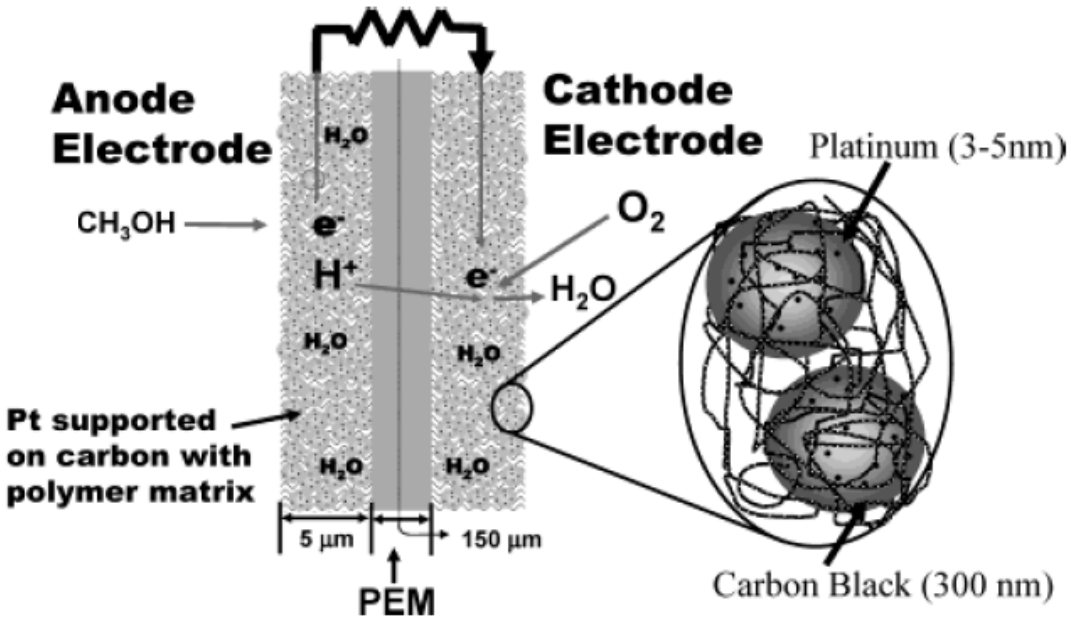

Chapter 2

Miscibility and Hydrogen Bonding Behavior in Organic/Inorganic Polymer Hybrids Containing Octaphenol Polyhedral Oligomeric Silsesquioxane

Abstract In this study, we investigated the miscibility behavior and mechanism of interaction of poly(methyl mechacrylate) (PMMA), poly(vinyl pyrrolidone) PVP, and PMMA-*co*-PVP blends with octa(phenol)octasilsequioxane (OP-POSS). For the PMMA/OP-POSS binary blend, the value of the association constant (K_A = 29) was smaller than that in the poly(vinyl phenol) (PVPh)/PMMA (K_A = 37.4) and ethyl phenol (EPh)/PMMA (K_A = 101) blend systems, implying that the phenol groups of the OP-POSS units in the PMMA/OP-POSS blends interacted to a lesser degree with the C=O groups of PMMA than they did in the other two systems. In addition, the ionic conductivity of a $LiClO_4$/PMMA-*co*-PVP polymer electrolyte was increased after blending with OP-POSS.

2.1. Introduction

Composite materials comprising organic polymers and inorganic materials have attracted great interests in recent years for both their fundamental scientific behavior and industrial applications. Polyhedral oligomeric silsesquoixanes (POSSs), which have the general formula $(RSiO_{1.5})_n$, are prototypical organic/inorganic systems composed of inorganic cores with external organic substituents. Through appropriate designing of the functionality of these organic substituents, it is possible to create both mono- and octa-functional macromonomers for desired applications. These functionalized POSS derivatives can be blended[1-3] or attached covalently to linear thermoplastics[4-11] or thermosetting networks[5,6,12-17] to form high-performance hybrid materials.[18-23] The physical properties of POSS/polymer hybrid materials are strongly influenced by the miscibility of the host polymer and the POSS derivative. Hydrogen bonds are often exploited as a favorable interaction to improve the miscibility of blend systems[24–26]. In a previous study,[27] we observed a dramatic increase in the

glass transition temperature when strong hydrogen bonds existed between the POSS moieties and polymer containing proton acceptors.

In this study, the POSS was functionalized as a strong proton donor [i.e., octa(phenol)octasilsesquioxane (OP-POSS)] to improve its miscibility with polymers containing proton acceptors. In previous studies,[27,28] the thermal properties of poly(methyl methacrylate) (PMMA) and poly(vinylpyrrolidone) (PVP) polymers were enhanced through copolymerization with POSS derivatives. Because covalent copolymerization can be a complicated and time-consuming process, polymer blending is usually considered to be a simpler and more convenient means of preparing POSS/polymer hybrid materials. Our aim in this present study was to compare the miscibility and hydrogen bonding behavior of the PMMA/OP-POSS, PVP/OP-POSS, and PMMA-*co*-PVP/OP-POSS blends. Furthermore, POSS-based electrolytes for rechargeable lithium batteries have been reported:[29] the incorporation of POSS derivatives improved their potential applicability of these systems as solid state electrolytes. Thus, the ionic conductivity of the $LiClO_4$/OP-POSS/ PMMA-*co*-PVP ternary blends was also investigated. We employed differential scanning calorimetry (DSC), Fourier transform infrared (FTIR) spectroscopy, and ac impedance measurement as a battery of techniques to investigate the hydrogen bonding, miscibility, and ionic conductivity behavior of these systems.

2.2. Experimental Part

2.2.1. Materials. Ethyl ether, benzene, *N*,*N*-dimethylformamide (DMF), tetrahydrofuran (THF), azobisisobutyronitrile (AIBN), *N*-vinyl-2-pyrrolidone (VP), platinum divinyltetramethyldisiloxane complex [Pt(dvs)], 4-acetoxystyrene (AS), lithium perchlorate ($LiClO_4$), and methyl methacrylate (MMA) were purchased from Aldrich Chemical Co. $\mathbf{Q_8M_8^H}$ was obtained from Hybrid Plastics Co. AIBN was purified through recrystallization from ethanol. Benzene and DMF were fractionally distilled from calcium hydride. The MMA

and VP monomers were purified through vacuum distillation from calcium hydride. Ethyl ether, THF, $\mathbf{Q_8M_8^H}$, Pt(dvs), and AS were used as received.

2.2.2. Synthesis of Octa(phenol)octasilsequioxane-POSS (OP-POSS) Oligomer. The $\mathbf{Q_8M_8^H}$ oligomer (1.96 mmol) was placed in a dry 50-mL round-bottom flask equipped with a stirrer bar. Toluene (30 mL), AS (16.66 mmol), and Pt(dvs) (one drop) were added sequentially over 10 min. The reaction mixture was then heated to 80 °C under a nitrogen atmosphere for 4h. After cooling to room temperature, the solution was filtered and then evaporated, and finally the residue was dried under vacuum until reaching a constant weight. The product, octa(acetoxystyryl)octasilsequioxane (AS-POSS, Scheme 2-1, yield was calculated to be 80%), was obtained as a colorless, viscous liquid.[30] AS-POSS was dissolved in THF under a nitrogen atmosphere and then NaOH (10 %) was added dropwise. The mixture was stirred for 48 h at room temperature. After the reaction, ethyl ether and deionized water (1:1) were added; then aqueous hydrochloric acid (10 %) was added dropwise to the mixture with stirring until the pH reached 8. Residual ethyl ether and water were evaporated under vacuum to provide octa(phenol)octasilsequioxane (OP-POSS, yield was calculated to be 82%). The final product, OP-POSS (Scheme 2-1), which is a lightly brown and viscous liquid was filtered and dried in a vacuum oven for 96 h at 80 °C.[30]

2.2.3. Syntheses of PMMA-*co*-PVP Random Copolymers. The PMMA-*co*-PVP random copolymers were prepared through the free radical polymerization using AIBN as the initiator (Scheme 2-2). The reactions were performed in benzene at 80 °C under a nitrogen atmosphere in a dry 100-mL round-bottom flask equipped with a stirrer bar. To determine the reactivity ratio, samples of the copolymers were removed from the reaction mixture during the early stages of the copolymerization, when the degrees of conversion remained relatively low (between 4–9%).[31] After 24 h, the mixtures were cooled to room temperature and the product copolymers were purified through precipitation into ethyl ether. The filtered product

copolymers were dried until they reached a constant weight. The molecular weights and molecular weight distributions of the PMMA-*co*-PVP copolymers were characterized through GPC at 50 °C using DMF as the eluent and polystyrene standards for calibration. The compositions of the copolymers were characterized using ^{1}H NMR spectroscopy and elementary analysis (EA).

The ^{1}H NMR spectrum of the copolymer was recorded from a $CDCl_3$ solution at 25 °C using a Varian UNITY INOVA-400 NMR spectrometer. EA was performed in an oxidative atmosphere at 1021 °C using a Heraeus CHN-O Rapid Elementary Analyzer. The MMA and VP units in the PMMA-*co*-PVP copolymers correspond to repeating units of $C_5H_8O_2$ and C_6H_9NO, respectively, thus, the MMA content (mol%) was determined using the Eq. (2-1), based on the contents of C and N atoms.[32]

$$MMA(mol\%) = 1 - \frac{30N}{7C - 6N} \times 100 \qquad (2\text{-}1)$$

where N and C refer to the contents of N and C atoms, respectively, in the copolymer.

2.2.4. Blend Preparations. Several binary PMMA/OP-POSS, PVP/OP-POSS, and PMMA-*co*-PVP/OP-POSS blends were prepared. Desired amounts of PMMA, PVP, PMMA-*co*-PVP, and OP-POSS were dissolved in DMF and stirred continuously for 24 h at 60 °C. The solutions were cast into Teflon dishes and maintained at 80 °C for 24 h to remove most of the solvent and then the blends were dried under vacuum maintained at 120 °C for 96 h.

2.2.5. Characterizations. Thermal analyses were performed using a DuPont TA2010 DSC instrument calibrated with indium standards. The analyses were conducted under a nitrogen atmosphere at a scan rate of 20 °C/min over a temperature range from –60 to 200 °C. The glass transition temperature (T_g) was obtained as the inflection point of the heat capacity jump. FTIR spectra of KBr disks were recorded over the range 4000–400 cm^{-1} using a Nicolet Avatar 320 FT-IR spectrometer, 32 scans were collected at room temperature and a resolution

of 1 cm^{-1}. Each DMF solution was cast onto a KBr disk and then most of the solvent was evaporated at 80 °C for 24 h; a vacuum (0.2 torr) was applied and the blend was then heated at 120 °C for an additional 96 h to completely remove the solvent. The frequency-dependent impedance properties (from 10 MHz to 10 Hz) of the polymer complexes were measured using an Autolab instrument designed by Eco Chemie. The samples were pressed into disks and loaded into a sealed conductivity cell between stainless-steel blocking electrodes; the films had thicknesses varying from 0.50 to 0.15 mm for these conductivity measurements. The impedance response was measured at 30 °C and the conductivity was calculated from the bulk resistance according to the Eq. (2-2).[33,34]

$$\sigma = \frac{L}{AR_b} \qquad (2\text{-}2)$$

where σ is the conductivity, L is the thickness of the electrolyte film, A is the section area of the stainless-steel electrode, and R_b is the bulk resistance.

2.3. Results and Discussion

2.3.1 PMMA-*co*-PVP Copolymer Characterization. A series of copolymers was prepared using various VP and MMA monomer concentrations. Table 2-1 lists the MMA contents (mol%) of the copolymers, determined through ^{1}H NMR spectroscopy and EA. Because of the compositions of the copolymers determined through ^{1}H NMR spectroscopy were affected by the interaction between water and PMMA-*co*-PVP, their VP contents (mol%) are slightly overestimated. EA provided better accuracy, although the H atom contents determined this way are inaccurate because of compositions of the copolymers were affected by the presence of water. Accordingly, we applied only the EA-determined N and C contents to calculate the VP content using Eq. (2-1). In the following discussion, the sample codes for these copolymers are based on the MMA contents obtained through EA.

We calculated reactivity ratios (r_1 for MMA; r_2 for VP) using the methodology of Kelen and Tudos.[35–37] Table 2-1 summarizes the monomer feed ratios and the resultant compositions

of the copolymers. To minimize errors resulted from changes in the feed ratios, the polymerization was terminated at monomer conversions of less than 10%. The values of r_1 and r_2 are the ratios of the homo-propagation and cross-propagation rate constants for each monomer (i.e., k_{11}/k_{12} and k_{22}/k_{21}, respectively). Figure 2-1 displays the Kelen–Tudos plot for the PMMA-*co*-PVP copolymers. The values of r_1 and r_2 were 0.94 and 0.97, respectively. In a previous study,[38] we defined a copolymerization to be "ideal" when the product $r_1 \times r_2$ was unity. When r_1 and r_2 both equal 1, the two monomers possess equal reactivity toward both propagating species; the behavior of the resulting copolymer is referred to as random or Bernoullian. Thus, the copolymers synthesized through free radical polymerization in this study were essentially random. (i.e., close to an ideal copolymer: $r_1 \times r_2 = 0.91$).

2.3.2. Analyses of OP-POSS/Homopolymer Binary Blends. Figure 2-2 presents DSC thermograms of the PMMA/OP-POSS and PVP/OP-POSS blends. The star-shaped OP-POSS was similar to a linear oligomer of poly(vinyl phenol), i.e., it has a degree of polymerization equal to 8. The glass transition temperature of OP-POSS (25 °C) was lower than that of a typical high-molecular-weight (M_n = 10,000 g/mol) PVPh (150 °C) because of molecular weights and structural differences. Single values of T_g existed in both blends, implying that all of these binary and ternary blends are miscible. Several equations have been suggested to predict the variation of the glass transition temperature of a random copolymer or miscible blend as a function of its composition. In this study, we employed the Kwei equation to predict the variation of the glass transition temperature:

$$T_g = \frac{W_1 T_{g1} + kW_2 T_{g2}}{W_1 + kW_2} + qW_1 W_2 \qquad (2\text{-}3)$$

where W_1 and W_2 are the weight fractions of the compositions, T_{g1} and T_{g2} represent the glass transition temperature of the corresponding blend components, and k and q are fitting constants. Furthermore, the value of q, a parameter corresponding to the strength of hydrogen

bonds in the blend, correlated to the balance between the breaking of the self-association and the forming of the inter-association hydrogen bonds. Figure 2-3 displays the dependence of T_g on compositions of the PVP/OP-POSS and PMMA/OP-POSS blends. We obtained the values of k and q based on non-linear least-squares best fits. In the PVP/OP-POSS blends, q had a value of +100, revealing the presence of a strong intermolecular interaction between PVP and OP-POSS. On the other hand, a negative value of q (–40) was obtained for the PMMA/OP-POSS blends, indicating that the intermolecular hydrogen bonding was weaker than the intramolecular hydrogen bonding.

Figure 2-4 displays partial IR spectra (2700–3700 cm^{-1}) of the PMMA/OP-POSS and PVP/OP-POSS blends. The pure OP-POSS exhibits two bands in the OH stretching region in the IR spectrum; one corresponding to the hydrogen-bonded OH groups (a broad band centered at 3350 cm^{-1}) and the other to "free" OH groups (a shoulder centered at 3525 cm^{-1}). When the PMMA (PVP) was mixed with OP-POSS and the C=O oxygen atoms of PMMA (PVP) interacted with the OH groups of OP-POSS, thus the broad band shifted to higher (lower) frequency at 3450 (3190) cm^{-1}. This behavior reflected the competition between the hydroxyl–hydroxyl and hydroxyl–carbonyl interactions. Additionally, the hydroxyl–carbonyl interactions predominated over the hydroxyl–hydroxyl interactions in the PMMA (PVP)-rich blends; thus, we assigned the band at 3450 (3190) cm^{-1} to be the OH groups interacting with the C=O units. Moskala et al. used the frequency difference ($\Delta\nu$) between the hydrogen-bonded and free OH absorptions to estimate the average strength of the intermolecular interaction.[39] Accordingly, we used the free OH stretching at 3525 cm^{-1} as a reference, the hydroxyl–carbonyl inter-association was weaker than the hydroxyl–hydroxyl self-association interaction in the PMMA/OP-POSS blends, but stronger in the PVP/OP-POSS blends. This finding is consistent with the negative and positive values of q for the PMMA/OP-POSS and PVP/OP-POSS blends, based on Kwei equation.

Figure 2-5 displays the C=O stretching regions in the IR spectra of PVP/OP-POSS and PMMA/OP-POSS blends. In Figure 2-5(a), pure PVP exhibits a broad band centered at 1680 cm^{-1}, corresponding to the "free" C=O groups. Painter et al.[40] reported that the pyrrolidone group strongly self-associates through transitional dipole coupling. Therefore, the signal for "free" C=O groups at 1680 cm^{-1} is not that of "truly free" C=O groups, which would be centered at 1708 cm^{-1}. The signal for C=O stretching was split into two bands at 1680 and 1650 cm^{-1} corresponding to "free" and the hydrogen-bonded C=O groups, respectively; these signals fitted the Gaussian function well. As the concentration of OP-POSS increased, the probability of PVP/OP-POSS interactions increased, resulting in an increased intensity of the hydrogen-bonded C=O band at the expense of the "free" C=O band. We calculated the fraction of the hydrogen-bonded C=O groups (f_b) using Eq. (2-4):[41]

$$f_b^{C=O} = \frac{A_b/1.3}{A_b/1.3 + A_f} \qquad (2\text{-}4)$$

where A_b and A_f denote the peak areas corresponding to the hydrogen-bonded and "free" C=O groups, respectively. In this case, we employed a ratio for the two absorptivities (a_2/a_1) of 1.3 based on a previous calculation.[40] Table 2-2 summarizes the results of curve fitting for the PVP/OP-POSS blends. As expected, the fraction of hydrogen-bonded C=O groups increased upon increasing the OP-POSS content.

Figure 2-5(b) reveals that the PMMA blend system has a sharp (compared with that of the pure PVP) IR band at 1730 cm^{-1} and a shoulder at 1710 cm^{-1}, representing the free and the hydrogen-bonded C=O groups, that also fitted the Gaussian function well. We applied the method described above to analyze the PMMA/OP-POSS blends, but in this case, we used a value of a_2/a_1 of 1.5.[42] Table 2-2 lists the results of curve fitting of the PMMA/OP-POSS system. Again, the fractions of hydrogen-bonded C=O groups increased upon the increase of the OP-POSS content.

In previous studies,[27,28] we confirmed that certain interactions occur between the POSS moieties and OH group. In this study, the situation was more complicated than those in previous studies because the OH groups were attached to the POSS cage. To further understand the interaction phenomena, we employed the Painter–Coleman association model (PCAM) to analyze these systems:[41]

$$B_1 + B_1 \xleftrightarrow{K_2} B_2$$

$$B_h + B_1 \xleftrightarrow{K_B} B_{h+1} (h \geq 2)$$

$$B_h + C_1 \xleftrightarrow{K_c} B_h C$$

$$B_h + A_1 \xleftrightarrow{K_A} B_h A$$

where A, B, and C are descriptors representing the siloxane groups, the phenol groups of the POSS cages, and PMMA, respectively; K_A, K_B, and K_C are their respective association equilibrium constants; K_2 is the equilibrium constant of forming dimers between phenol groups. These equilibrium constants can be expressed in terms of volume fractions:

$$\Phi_B = \Phi_{B1}\Gamma_2\left[1+\frac{K_A\Phi_{A1}}{r_A}+\frac{K_C\Phi_{C1}}{r_C}\right] \quad (2\text{-}5)$$

$$\Phi_A = \Phi_{A1}\left[1+K_A\Phi_{B1}\Gamma_1\right] \quad (2\text{-}6)$$

$$\Phi_C = \Phi_{C1}\left[1+K_C\Phi_{B1}\Gamma_1\right] \quad (2\text{-}7)$$

where

$$\Gamma_1 = \left(1-\frac{K_2}{K_B}\right)+\frac{K_2}{K_B}\left(\frac{1}{1-K_B\Phi_{B1}}\right) \quad (2\text{-}8)$$

$$\Gamma_2 = \left(1-\frac{K_2}{K_B}\right)+\frac{K_2}{K_B}\left(\frac{1}{(1-K_B\Phi_{B1})^2}\right) \quad (2\text{-}9)$$

Where Φ_A, Φ_B, and Φ_C are the volume fractions of the repeat units in the blend, Φ_{A1}, Φ_{B1}, and Φ_{C1} are the volume fractions of the isolated units in the blend, r_A (V_A/V_B) and r_C (V_C/V_B) are the ratios of the segmental molar volumes.[28] Furthermore, we adopted the self-association equilibrium constants of PVPh[45] ($K_2 = 21$ and $K_B = 66.8$), for phenol groups in this study to describe the formation of dimers and multimers, respectively. The

inter-association equilibrium constant (K_C) of the PVPh/PMMA blend has been reported previously to be 37.4.[44] Using the value of K_C together with the phenol group self-association equilibrium constants (K_2 and K_B), we obtained a theoretical curve for the fraction of hydrogen-bonded C=O groups at 25 °C as a function of the weight fraction of OP-POSS content (Figure 2-6). When the value of K_A was equal to 2, the experimental data agreed fairly well with the predictions of the PCAM. A slight deviation was observed at weight fractions less than 0.4 because the most accurate range for determining the fraction of hydrogen-bonded C=O groups was from 0.4 to 0.7, where the bands for both the free and hydrogen bonded C=O bands were well separated and had significant absorbances.[45] The ratio of the inter-association equilibrium constant (K_A) corresponding to the interaction between OH and siloxane groups of POSS cages to the inter-association equilibrium constant (K_C), was 0.05, implying that inter-association between the phenol and siloxane groups of the POSS cages was insignificant and, thus, could be ignored. The structure of the OP-POSS and the hydroxyl–hydroxyl interaction formed through the phenol groups are the reasons for this behavior because both the arms of OP-POSS which were steric barriers and the presence of hydroxyl–hydroxyl interaction blocked the OH groups from interacting with the siloxane groups.

Using the value of the K_B and K_2 above and ignoring inter-association between the phenol and siloxane groups of OP-POSS, we employed the PCAM again to determine the "real" value of K_A for the PMMA/OP-POSS blend. The approximate equations were simplified as follows:[46,47]

$$\Phi_B = \Phi_{B1}\Gamma_2\left[1+\frac{K_A\Phi_{A1}}{r_A}\right] \tag{2-10}$$

$$\Phi_A = \Phi_{A1}\left[1+K_A\Phi_{B1}\Gamma_1\right] \tag{2-11}$$

where

$$\Gamma_1 = \left(1 - \frac{K_2}{K_B}\right) + \frac{K_2}{K_B}\left(\frac{1}{(1 - K_B\Phi_{B1})}\right) \quad (2\text{-}12)$$

$$\Gamma_2 = \left(1 - \frac{K_2}{K_B}\right) + \frac{K_2}{K_B}\left(\frac{1}{(1 - K_B\Phi_{B1})^2}\right) \quad (2\text{-}13)$$

where Φ_A and Φ_B denote the volume fractions of the non-self associated species A (PMMA) and the self-associating species B (OP-POSS), respectively: Φ_{A1} and Φ_{B1} are the corresponding volume fractions of the isolated PMMA and OP-POSS, respectively; r is the ratio of molar volumes (V_A/V_B). Using the least-squares method, we obtained theoretical curves for the fraction of hydrogen-bonded C=O groups at 25 °C as a function of the weight fraction of the OP-POSS content (Figure 2-7). When K_A was equal to 29.0, the experimental data agreed fairly well with the predictions of the PCAM. Table 2-3 lists all the parameters required for the PCAM to estimate the thermodynamic properties of these blends. Furthermore, the inter-association equilibrium constant (K_A = 29.0) of the PMMA/OP-POSS blend system was smaller than that of the self-association equilibrium constant (66.8) of the OP-POSS oligomer; this finding implies that the tendency toward self-association of two OH groups dominates over the hydroxyl–carbonyl interactions in the PMMA/OP-POSS blends. Most importantly, the value of K_A for PMMA/OP-POSS blend system was smaller than those for poly(vinyl phenol) PVPh/PMMA(K_A = 37.4)[44] and ethyl phenol (EPh)/PMMA (K_A = 101)[48] blends, implying that the OH groups in the PMMA/OP-POSS blend system have less of a chance to interact with C=O groups than they do in the other two blends. In a previous study,[44] we found that the value of the inter-association equilibrium constant is affected by the spacing between the hydrogen-bonding functional groups. In this case, the spacing between the OH groups attached to the POSS cage (a star-shaped macromolecule) can be smaller than those of the other two blend systems, making them less accessible for inter-association, resulting in a decrease in the ratio of the inter-association and self-association equilibrium

constants.

We could not, however, use this approach to determine the K_A for the PVP/OP-POSS blend because the pyrrolidone groups exhibited strong self-association through transitional dipole coupling and the signal for "free" carbonyl group at 1680 cm^{-1} was not that of "truly free" C=O groups, which would have been centered at 1708 cm^{-1}. Furthermore, for the value of K_A for the PVP/OP-POSS blends to be calculated accurately, it would have to be less than 6000± 2000 based on the results above.[40] In previous studies,[49–51] we determined that the value of q for the PMMA/PVPh and PVP/PVPh blend systems where 0 and +140, respectively—much greater than those of –40 and +100 for the PMMA/OP-POSS and PVP/OP-POSS blend systems, respectively—indicating that the intermolecular hydrogen bonding in the PMMA/OP-POSS and PVP/OP-POSS blends was weaker than that in the PMMA/PVPh and PVP/PVPh blends. The values of K_A are in good agreement with these results obtained from curve fitting of the Kwei equation.

2.3.3. Analyses of Binary Blend OP-POSS/Copolymers. Figure 2-8 displays the C=O regions for the MMA and VP units in the IR spectra of the MMA61/OP-POSS blend. Table 2-4 summarizes the results of curve fitting. The addition of a small content of OP-POSS (20%) in the blend resulted in a new band at 1658 cm^{-1} assigned to the "hydrogen-bonded" C=O groups of the PVP. The signal for the "hydrogen-bonded" C=O groups of PMMA appeared when the OP-POSS content was increased to 40 wt%. The OH groups of OP-POSS prefer to interact with PVP rather than with PMMA, as evidenced by the difference between the value of K_A for the PMMA/OP-POSS and PVP/OP-POSS blend systems. When the OP-POSS content was greater than 40%, the OH groups interacted simultaneously with both the PMMA and PVP units.

As indicated in Table 2-1, the presence of VP units in each copolymer system resulted in an increase in the value of T_g with all of the DSC traces revealing a single glass transition

temperature, implying that these copolymers are miscible. Figure 2-9 presents DSC thermograms of the MMA61/OP-POSS blend system. Essentially all of the blends displayed the same trend; the presence of OP-POSS results in a lowering of the glass transition temperature of the copolymer. We used the Kwei equation to predict the variation of the glass transition temperature of the miscible blend as a function of its composition. Figure 2-10 illustrates the dependence of T_g on the composition of the MMA81/OP-POSS, MMA61/OP-POSS, and MMA53/OP-POSS miscible blends. Again, based on the non-linear least-squares best fit, the values of k and q were obtained. For the MMA53/OP-POSS blend system, we obtained the largest value of q (+75) implying that the MMA53/OP-POSS blend system featured stronger intermolecular interactions between OP-POSS and itself than did the other two copolymer/OP-POSS blends. As indicated in Figure 2-10, the addition of a lower content of VP (20 wt%) in the PMMA chain resulted in a change in nature of the interaction. The intermolecular hydrogen bonds in the PMMA/OP-POSS blends were weaker than the intramolecular hydrogen bonds. After copolymerization at a 20 wt% VP content, the intermolecular hydrogen bonding became stronger than the intramolecular hydrogen bonding because the OH groups interacted more preferably with the VP segments. Therefore, the value of q increased gradually upon increasing copolymerized-VP content, reflecting the fact that the intermolecular hydrogen bonding of the copolymer/OP-POSS blend system became stronger accordingly.

2.3.4. Analyses of Ionic Conductivity. In a previous study,[34] we found that a polymer electrolyte composed of $LiClO_4$/MMA61 had a higher ionic conductivity at room temperature than did the $LiClO_4$/PMMA, $LiClO_4$/PVP, $LiClO_4$/MMA81, and $LiClO_4$/MMA53 blend systems at the same $LiClO_4$ content. As mentioned above, the interactions between polymer chains are affected by the presence of OP-POSS. In addition, because the mobility of charge carriers is directly related to the mobility of the polymer matrix, we were interested in

comparing the ionic conductivity of ternary and binary blends. Figure 2-11 displays the plots of the ionic conductivity with respect to the MMA content in copolymers at room temperature for $LiClO_4$/PMMA-*co*-PVP and $LiClO_4$/OP-POSS/PMMA-*co*-PVP blends containing a fixed $LiClO_4$ content of 20 wt%. The polymer electrolyte $LiClO_4$/OP-POSS/MMA61 exhibited a higher ionic conductivity at room temperature than did the binary blend of $LiClO_4$/PMMA-co-PVP because the OP-POSS might lead to an increase in the chain mobility of the polymer electrolyte. To clarify the complicated nature of the interactions in the $LiClO_4$/OP-POSS/polymer ternary blend, we are presently performing additional studies that we will discuss in the near future.

2.4. Conclusions

We have employed DSC and FTIR spectroscopy techniques to investigate in detail the miscibility behavior and mechanisms of interaction for polymer blends of OP-POSS and PMMA-*co*-PVP. For the OP-POSS/PMMA blends, the value of K_A of 29 was smaller than those for the PVPh/PMMA (K_A = 37.4) and EPh/PMMA (K_A = 101) blends, implying that the spacing between phenol groups attached to the POSS nanoparticle was smaller than those of the other two blend systems, resulting in a decrease in the ratio of the inter-association and self-association equilibrium constants. Moreover, intermolecular hydrogen bonding became stronger than intramolecular hydrogen bonding after copolymerization with VP content because the OH groups preferred to interact with the VP segments. Furthermore, the presence of OP-POSS in a $LiClO_4$/OP-POSS/MMA61 ternary blend played an important role in enhancing the ionic conductivity of the polymer electrolyte.

References

1. Kuo, S. W.; Lin, H. C.; Huang, W. J.; Huang, C. F.; Chang, F. C. *J. Polym. Sci., Polym. Phys.* **2006**, *44*, 673.

2. Lee, Y. J.; Huang, J. M.; Kuo, S. W.; Chang, F. C. *Polymer* **2005**, *46*, 10056.

3. Zhang, H.; Kulkarni, S.; Wunder, S. L. *J. Phys. Chem. B* **2007**, *111*, 3583.

4. Kopesky, E. T.; Haddad, T. S.; Cohen, R. E.; McKinley, G. H. *Macromolecules* **2004**, *37*, 8992.

5. Li, G. Z.; Wang, L.; Toghiani, H.; Daulton, T. L.; Koyama, K.; Pittman, C. Y. *Macromolecules* **2001**, *34*, 8686.

6. Matejka, L.; Strachota, A.; Plestil, J.; Whelan, P.; Steinhart, M.; Slouf, M. *Macromolecules* **2004**, *37*, 9449.

7. Lin, H. C.; Wang, C. F.; Kuo, S. W.; Tung, P. H.; Huang, C. F.; Lin, C. H.; Chang, F. C. *J. Phys. Chem. B* **2007**, *111*, 3404.

8. Leu, C. M.; Chang, Y. T.; Wei, K. H. *Chem. Mater.* **2003**, *15*, 2261.

9. Leu, C. M.; Chang, Y. T.; Wei, K. H. *Chem. Mater.* **2003**, *15*, 3721.

10. Phillips, S. H.; Haddad, T. S.; Tomcrzak, S. J. *Curr. Opin. Solid State Mater. Sci.* **2004**, *8*, 21.

11. Li, G. Z.; Wang, L. C.; Ni, H. L. *J. Inorg. Organomet. Polym.* **2001**, *11*, 123.

12. Chen, W. Y.; Wang, Y. Z.; Kuo, S. W.; Huang, C. F.; Tung, P. H.; Chang, F. C. *Polymer* **2004**, *45*, 6897.

13. Tamaki, R.; Choi, J.; Laine, R. M. *Chem. Mater.* **2003**, *15*, 793.

14. Lee, Y. J.; Huang, J. M.; Kuo, S. W.; Lu, J. S.; Chang, F. C. *Polymer* **2005**, *46*, 173.

15. Ye, Y. S.; Chen, W. Y.; Wang, Y. Z. *J. Polym. Sci., Part A: Polym. Chem.* **2006**, *44*, 5391.

16. Liu, Y. L.; Chang, G. P.; Hsu, K. Y.; Chang, F. C. *J. Polym. Sci., Part A: Polym. Chem.* **2006**, *44*, 3825.

17. Do Carmo, D. R.; Paim, L. L.; Dias, N. L. *Appl. Surf. Sci.* **2007**, *253*, 3683.

18. Voronkov, M. G.; Lavrent'ev, V. I. *Top. Curr. Chem.* **1982**, 102, 199.

19. Baney, R. H.; Itoh, M.; Sakakibara, A.; Suzuki, T. *Chem. Rev.* **1995**, 95, 1409.

20. Provatas, J. G. *Trends Polym. Sci.* 1997, 5, 327.

21. Loy, D. A.; Shea, K. J. Chem. Rev. 1995, 95, 1431.

22. Lichtenhan, J. D.; In Polymeric Materials Encyclopedia, Salamone, J. C. Ed.; CRC Press: Boca Raton, FL, 1996, 7768.

23. Ni, Y.; Zheng, S. *Chem. Mater.* **2004**, *16*, 5141.

24. Kuo, S. W.; Chang, F. C. *Macromolecules* **2001**, *34*, 4089.

25. Kuo, S. W.; Lin, C. L.; Chang, F. C. *Polymer* **2002**, 3943.

26. Eastwood, E.; Viswanathan, S.; O'Brien, C. P.; Kumar, D.; Dadmun, M. D. *Polymer* **2005**, 3957.

27. Xu, H. Y.; Kuo, S. W.; Chang, F. C. *Macromolecules* **2002**, *35*, 8788.

28. Huang, C. F.; Kuo, S. W.; Huang, W. J.; Chang, F. C. *Macromolecules* **2006**, *39*, 300.

29. Maitra, P.; Wunder, S. L. *Electrochem. Solid-State Lett.* **2004**, *7(4)*, A88.

30. Lin, H. C.; Kuo, S. W.; Huang, C. F.; Chang, F. C.; *Macromol. Rapid Commun.* **2006**, *27*, 537.

31. Xu, Y.; Painter, P. C.; Coleman, M. M. *Polymer* **1993**, *34*, 3010.

32. Luo, L.; Ranger, M.; Lessard, D. G.; Le Garrec, D.; Gori, S.; Leroux, J. C.; Rimmer, S.; Smith, D. *Macromolecules* **2004**, *37*, 4008.

33. Watanabe, M.; Ohashi, S.; Sanui, K.; Ogata, N.; Kobayashi, T.; Ohtaki, Z. *Macromolecules* **1985**, *18*, 1945.

34. Chiu, C. Y.; Yen, Y. J.; Chang, F. C. *Polymer* **2006**, *48*, 1329.

35. Kennedy, J. P.; Kelen, T.; Tüdös, F. J. *Polym. Sci., Polym. Chem. Ed.* **1975**, *13*, 2277.

36. Kelen, T.; Tüdös, F. *Macromol. Sci. Chem.* **1975**, *A9*, 1.

37. Kuo, S. W.; Chang, F. C. *Polymer* **2001**, *42*, 9843.

38. Odian, G.. *Principles of Polymerization*, 4th ed.; John Wiley & Sons: New York, 2004.

39. Moskala, E. J.; Varnell, D. F.; Coleman, M. M. *Polymer* **1985**, *26*, 228.

40. Hu, Y.; Motzer, H. R.; Etxeberria, A. M.; Fernandez-Berridi, M. J.;Iruin, J. J.; Painter, P. C.; Coleman, M. M. *Macromol. Chem. Phys.* **2000**, *201*, 705.

41. Coleman, M. M.; Graf, J. F.; Painter, P. C. *Specific Interactions and the Miscibility of Polymer Blends*; Technomic Publishing: Lancaster, PA, 1991.

42. Moskala, E. J.; Howe, S. E.; Painter, P. C.; Coleman, M. M.; *Macromolecules* **1984**, *17*, 1671.

43. Kuo, S. W.; Chan, S. C.; Chang, F. C. *Polymer* **2002**, *43*, 3653.

44. Lin, C. L.; Chen, W. C.; Liao, C. S.; Su, Y. C.; Huang, C. F.; Kuo, S. W.; Chang, F. C. *Macromolecules* **2005**, *38*, 6435.

45. Coleman, M. M.; Pehlert, G. J.; Painter, P. C. *Macromolecules* **1996**, *29*, 6820.

46. Lee, Y. J.; Kuo, S. W.; Huang, W. J.; Lee, H. Y.; Chang, F. C. *J. Polym. Sci.* **2004**, *42*, 1127.

47. Kuo, S. W.; Chang, F. C. *Macromol. Chem. Phys.* **2002**, *203*, 868.

48. Hu, Y.; Painter, P. C.; Coleman, M. M.; Butera, R. J. *Macromolecules* **1998**, *31(10)*, 3394.

49. Lee, H. F.; Kuo, S. W.; Chang, F. C. *Macromolecules* **2006**, *39*, 5458

50. Chen, W. C.; Kuo, S. W.; Jeng, U. S.; Chang, F. C *Macromolecules* **2008**, *41*, 1401.

51. Kuo, S. W.; Chang, F. C. *Macromolecules* **2001**, *34*, 4089.

Scheme 2-1. Synthesis and chemical structure of OP-POSS.

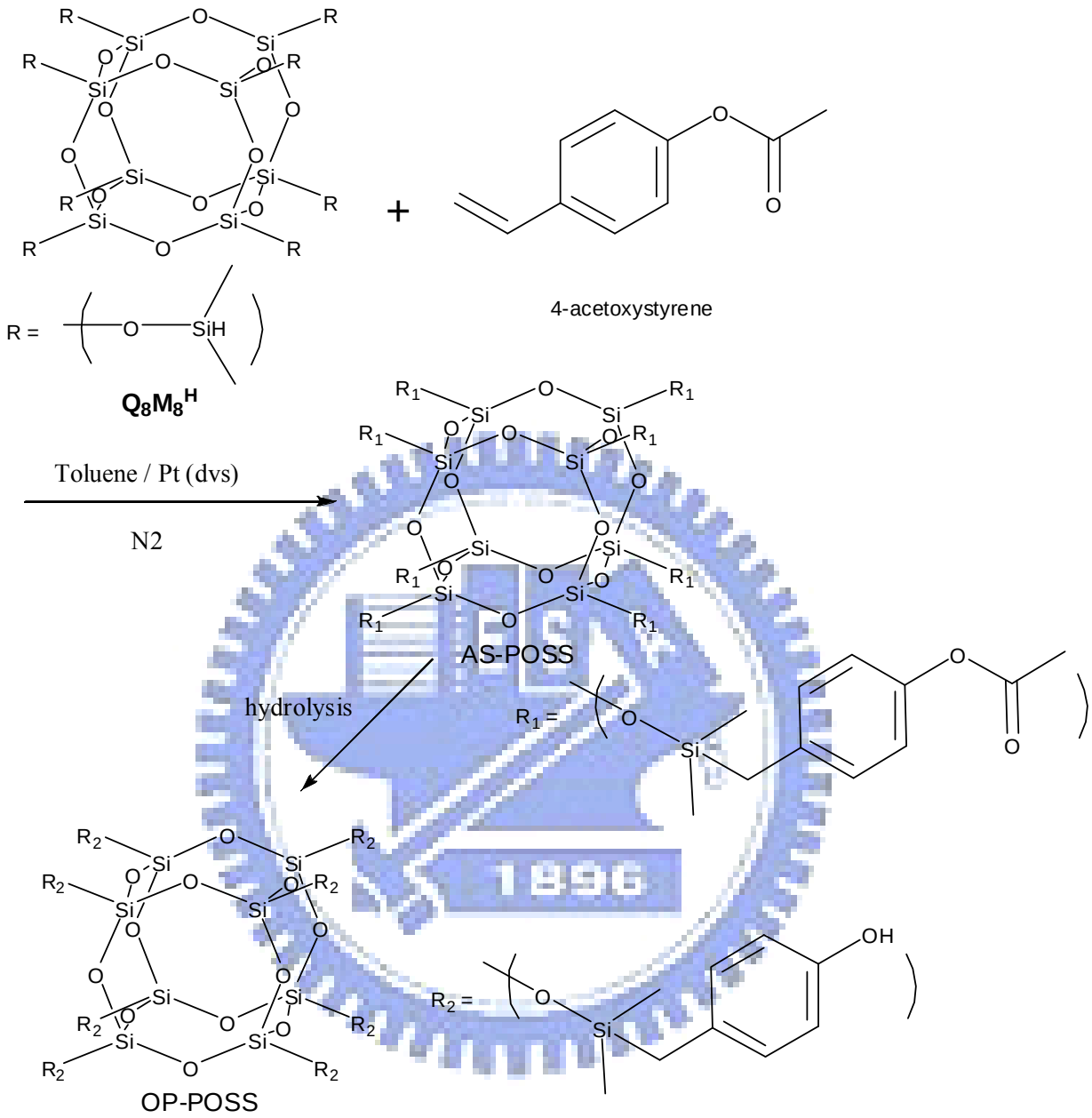

Scheme 2-2. Synthesis of PMMA-*co*-PVP random copolymer.

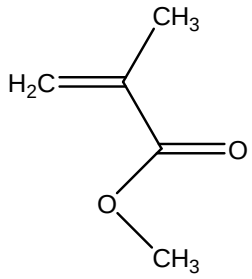

methyl methacrylate (MMA)

+

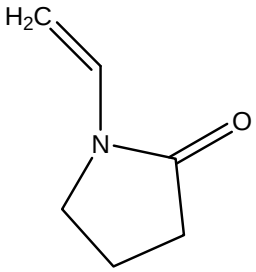

N-vinyl-2-pyrrolidone (VP)

benzene, 80-90°C

AIBN

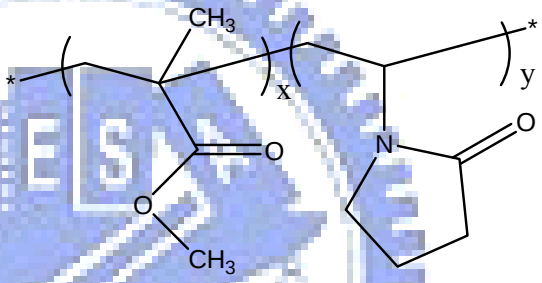

Poly(methyl methacrylate-*co*-vinyl pyrrolidone)

Table 2-1. PMMA-*co*-PVP Copolymer Compositions and Molecular Weights[a].

copolymer abbreviation[b]	monomer feed (mol%)		polymer composition (mol%)				M_n[e]	M_w/M_n[e]	T_g[f] (°C)
			EA[c]		NMR[d]				
	VP	MMA	VP	MMA	VP	MMA			
PMMA	0	100	0	100	0	100	25700	1.76	111
MMA81	18.4	81.6	19.4	80.6	18.7	81.3	22100	2.00	123
MMA61	37.5	62.5	38.5	61.5	40.7	59.3	20300	2.52	134
MMA53	47.4	52.6	46.8	53.2	52.9	47.1	17000	2.29	139
PVP	100	0	100	0	100	0	18200	2.33	181

[a] Polymerization conditions: initiator = AIBN; solvent = benzene; temperature = 80 °C. [b] Labeling based on VP content in the PMMA-*co*-PVP copolymers obtained from EA. [c] Calculated through EA using Eq. (1). [d] Obtained from the ^{1}H NMR spectra. [e] Determined by GPC using polystyrene standards and DMF as the eluent. [f] Characterized from DSC thermograms.

Table 2-2. Curve Fitting of the C=O stretching bands in the FTIR spectra of PVP/OP-POSS and PMMA/OP-POSS blends at room temperature.

	free C=O			hydrogen-bonded C=O			
PVP/POSS	ν, cm^{-1}	$W_{1/2}$,	A_f %	ν, cm^{-1}	$W_{1/2}$,	A_b %	f_b
Pure PVP	1680	28	100				
80/20	1681	31	91.5	1652	18	8.5	6.7
60/40	1685	31	82.8	1653	20	17.2	13.8
50/50	1685	28	67.5	1656	22	32.5	27.0
40/60	1687	23	40.9	1659	28	59.1	52.6
20/80	1690	15	5.9	1660	30	94.1	92.5
	free C=O			Hydrogen-bonded C=O			
PMMA/POSS	ν, cm^{-1}	$W_{1/2}$,	A_f %	ν, cm^{-1}	$W_{1/2}$,	A_b %	f_b
PMMA	1730	20	100				
80/20	1731	21	85.8	1707	25	14.2	10.0
60/40	1732	22	76.3	1707	24	23.7	17.2
50/50	1732	20	68.6	1708	24	31.4	23.4
40/60	1732	19	61.9	1708	23	38.1	29.1
30/70	1732	18	54.6	1708	23	45.4	35.7
20/80	1732	17	49.3	1708	23	50.7	40.7
10/90	1732	18	39.2	1708	23	60.8	50.9

Table 2-3. Self-association and Inter-Association Equilibrium Constants and Thermodynamic Parameters for PMMA/OP-POSS blends at 25°C[a].

	V	M_w	equilibrium constant		
			K_2[b]	K_B[b]	K_A[c]
OP-POSS	1705.2	1978	21.0	66.8	
PMMA	84.9	100			29.0

[a] V: Molar volume (mL/mol); M_w: molecular weight (g/mol); K_2: dimer self-association equilibrium constant; K_B: multimer self-association equilibrium constant; K_A: inter-association equilibrium constant, [b]: ref. 40; [c]: Calculated using the PCAM.

Table 2-4. Curve fitting of the C=O stretching bands in the FTIR spectra of MMA61/OP-POSS (120°C) blends.

	free C=O			hydrogen-bonded C=O				free C=O			H-Bonding C=O			
	ν, cm^{-1}	$W_{1/2}$, cm^{-1}	A_f %	ν, cm^{-1}	$W_{1/2}$, cm^{-1}	A_b%	f_b	ν, cm^{-1}	$W_{1/2}$, cm^{-1}	A_f %	ν, cm^{-1}	$W_{1/2}$, cm^{-1}	A_b%	f_b
MMA61	1683	25	100					1730	26	100				
80/20	1686	26	75.1	1658	23	24.9	20.2	1730	28	100				
60/40	1686	25	49.0	1660	24	51.0	44.5	1730	27	93.0	1710	20	7.0	4.7
50/50	1687	26	42.9	1659	24	57.1	50.5	1730	26	90.6	1710	20	9.4	6.5
40/60	1687	26	28.3	1660	25	71.7	66.1	1730	26	85.4	1710	20	14.6	10.2
20/80	1687	25	10.9	1660	25	89.1	86.3	1730	26	75.7	1710	20	24.3	17.6

Figure 2-1. Kelen–Tudos plot for the PMMA-*co*-PVP copolymers.

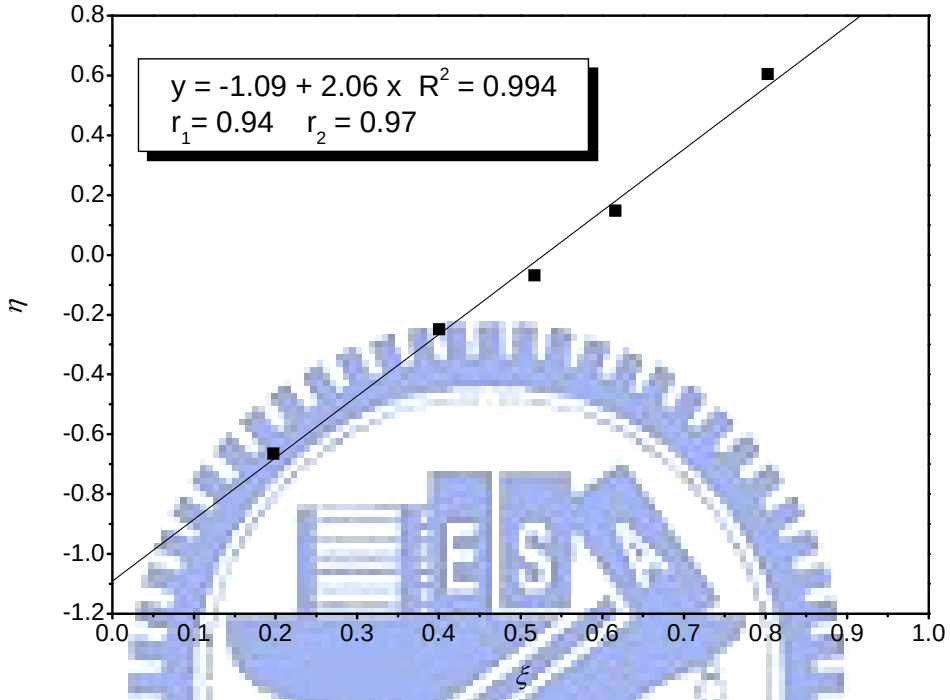

Figure 2-2. DSC scans for (a) PMMA/OP-POSS and (b) PVP/OP-POSS blends of various compositions.

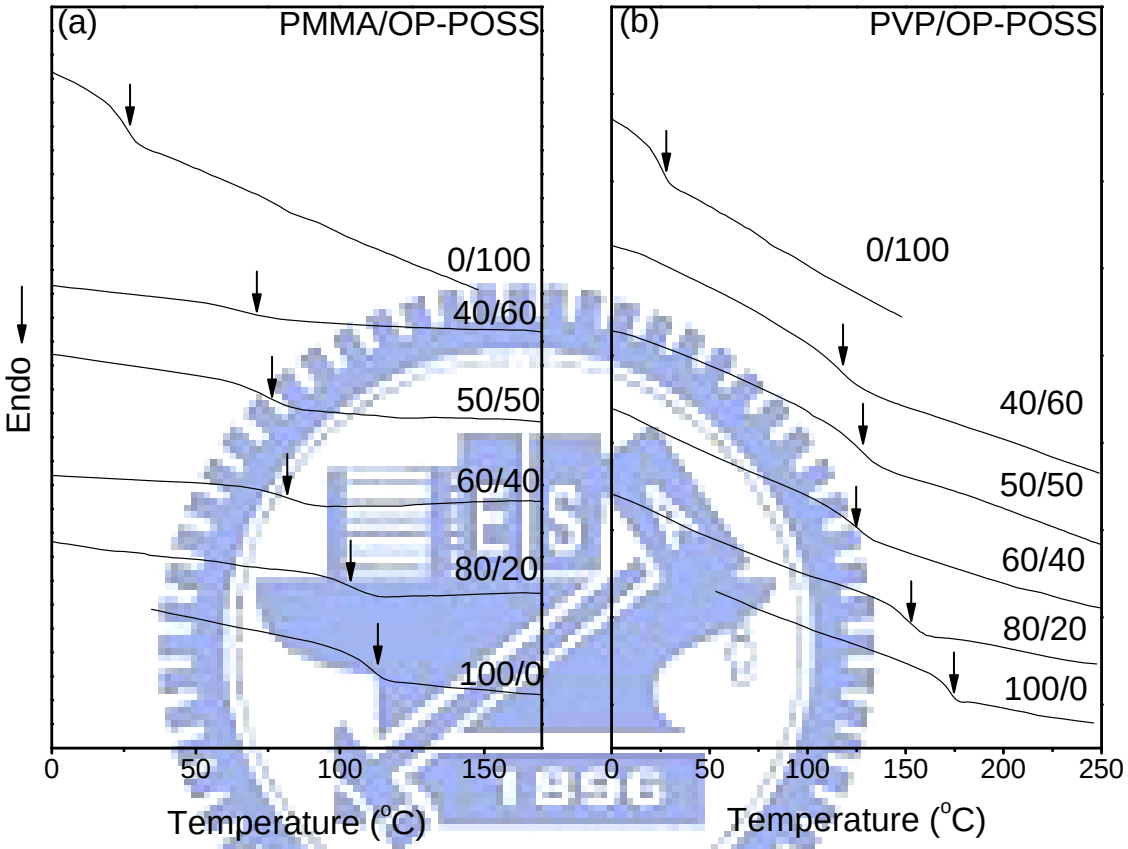

Figure 2-3. Plots of T_g versus (a) the PVP content of PVP/OP-POSS blends and (b) the PMMA content of PMMA/OP-POSS blends.

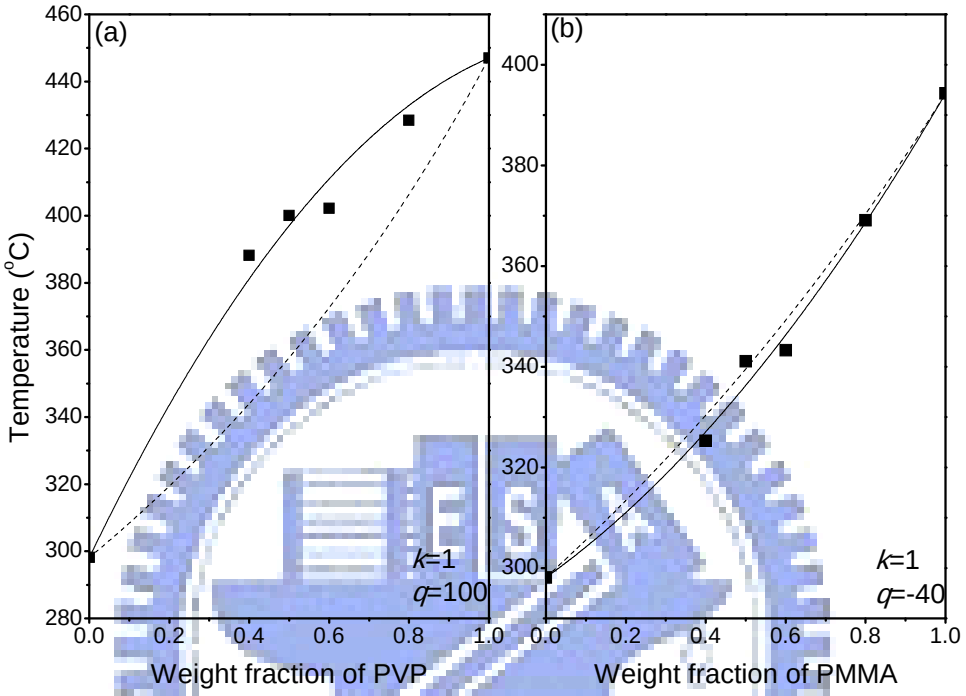

Figure 2-4. Partial IR spectra (OH stretching region) of OP-POSS and P MMA/OP-POSS and PVP/OP-POSS blend systems.

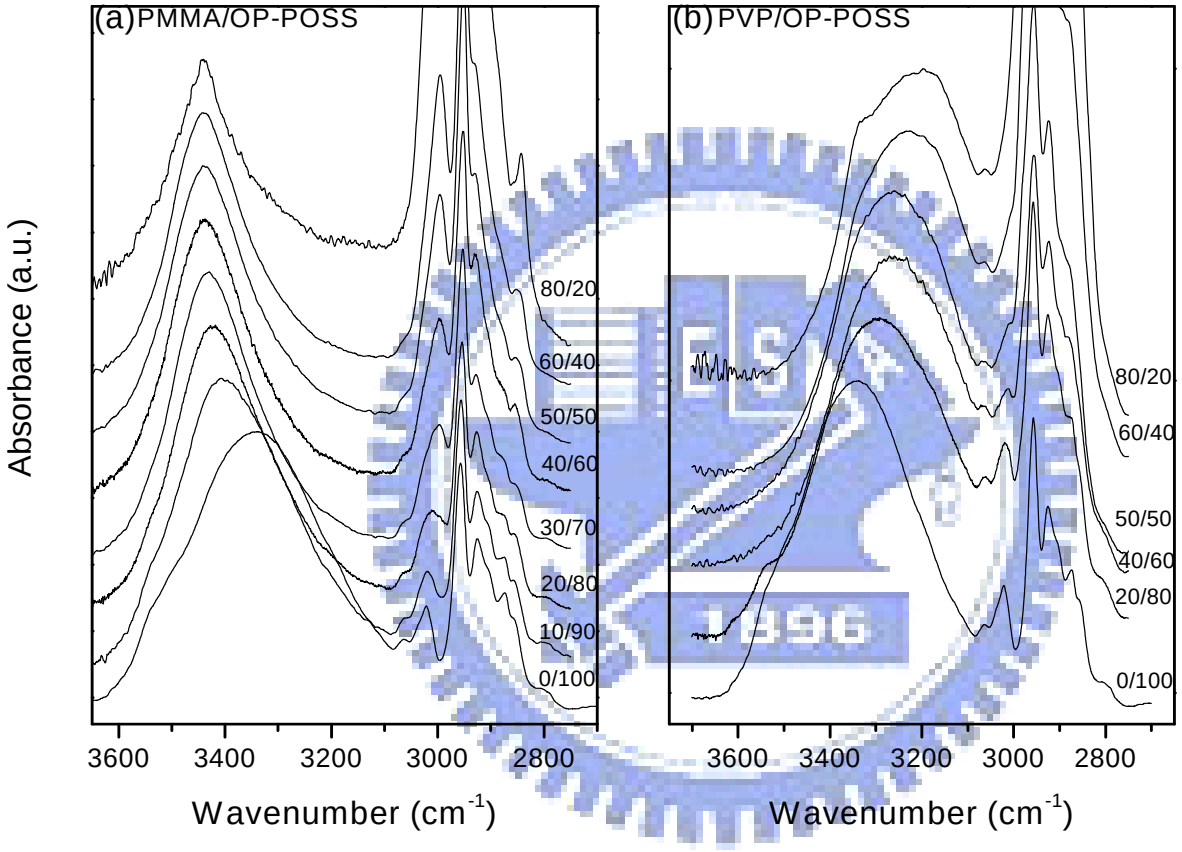

Figure 2-5. Partial IR spectra (C=O stretching region) of (a) PVP/OP-POSS blends at 120 °C and (b) PMMA/OP-POSS blends at 25 °C.

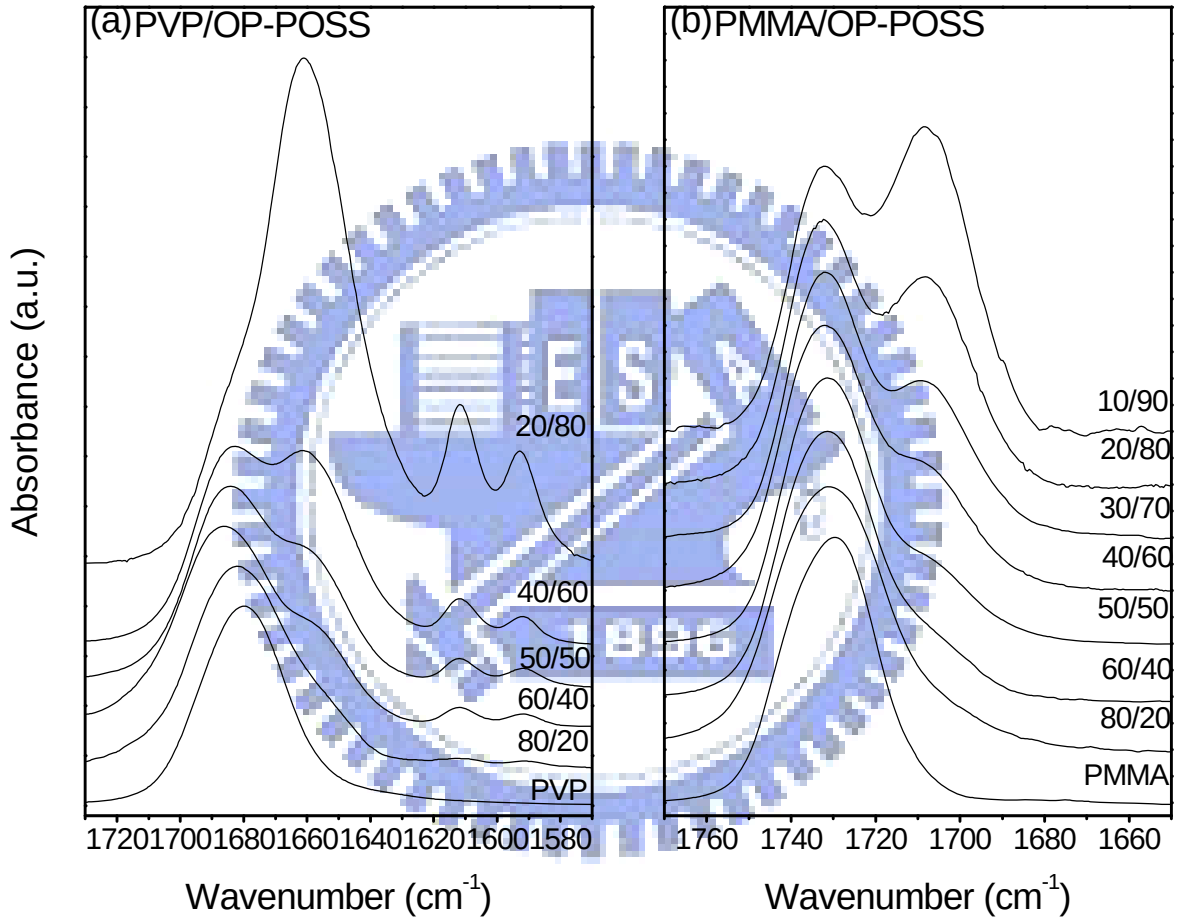

Figure 2-6. Fraction of the hydrogen-bonded C=O groups plotted with respect to the blend composition: (■) FTIR spectroscopy data; (—) theoretical values for PMMA/OP-POSS blends (K_A = 2) at 25 °C.

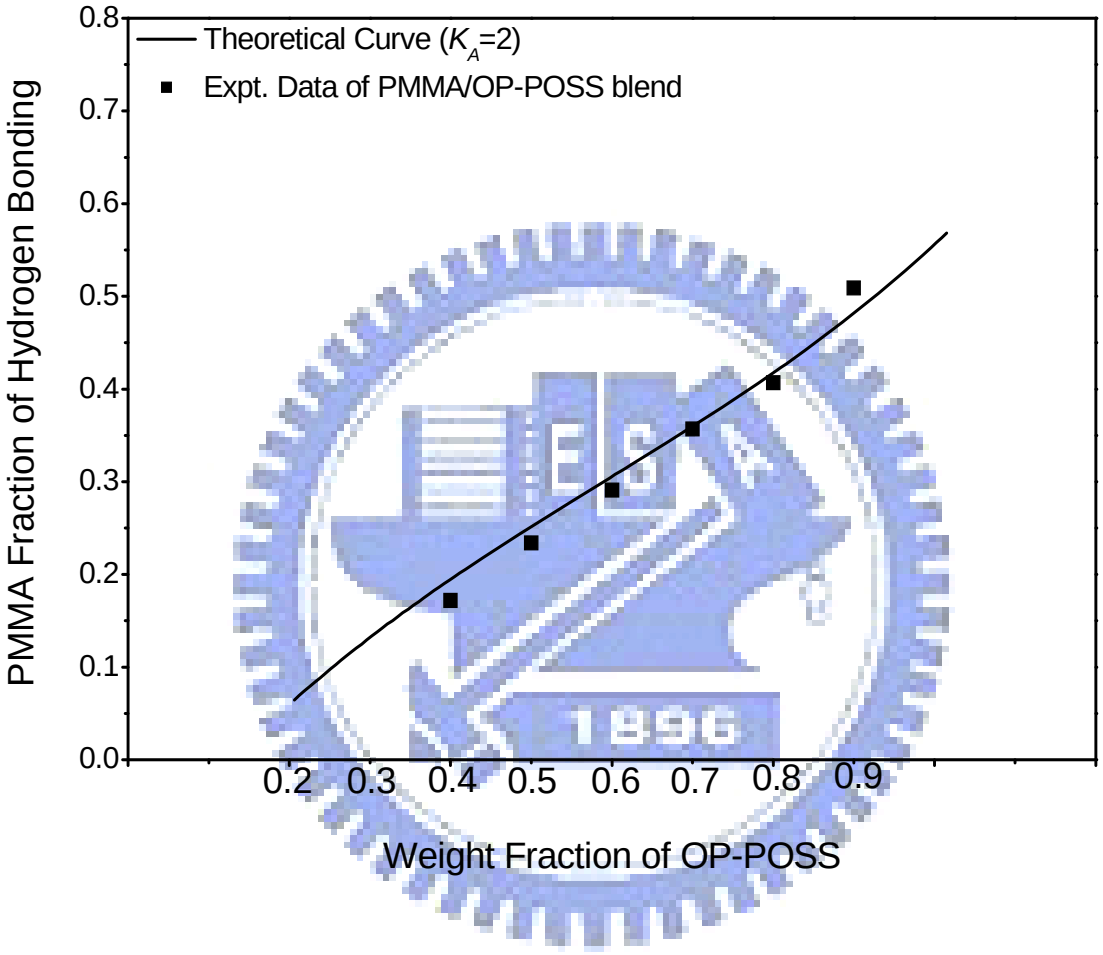

Figure 2-7. Fraction of the hydrogen-bonded C=O groups plotted with respect to the blend composition: (■) FTIR spectroscopy data; (—) theoretical values for PMMA/OP-POSS blends (K_A = 29) at 25 °C.

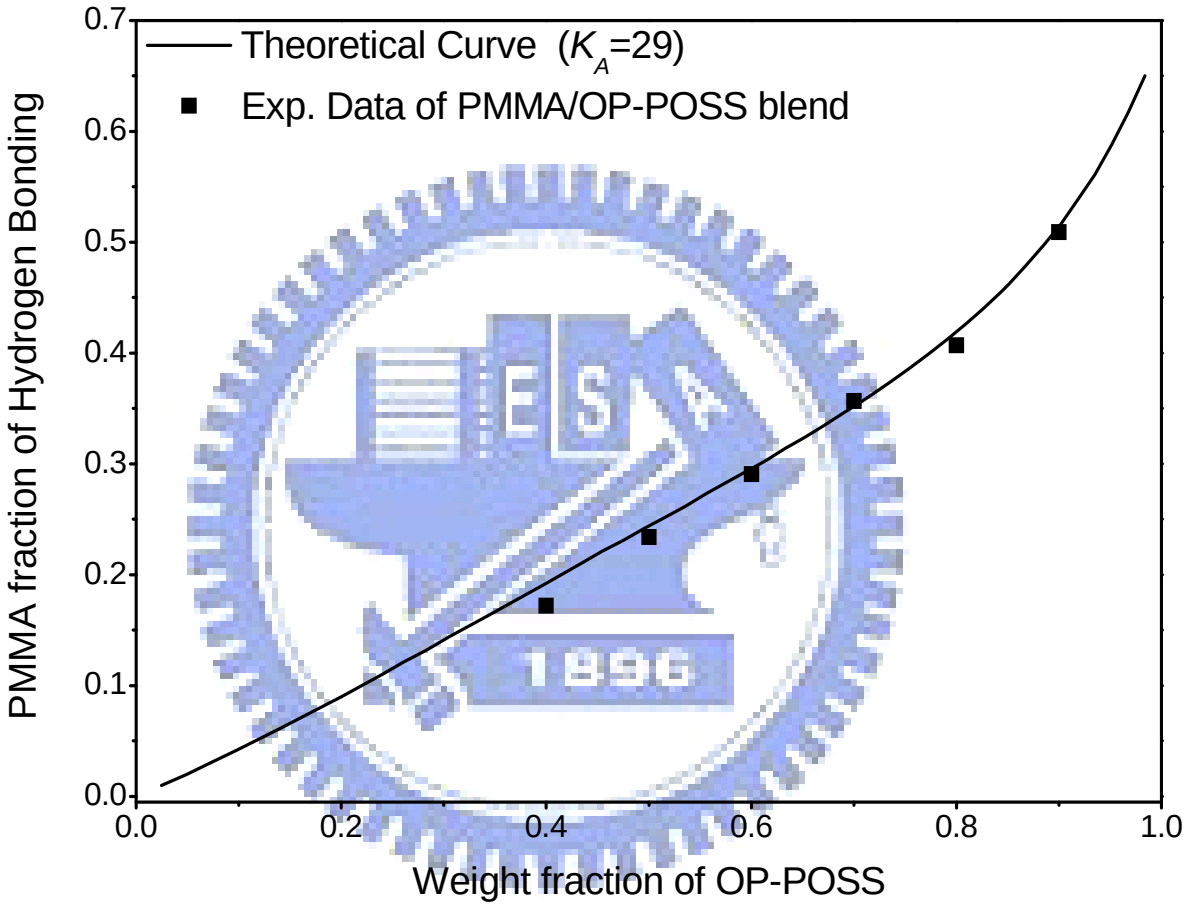

Figure 2-8. Partial IR spectra (1800–1625 cm^{-1}) of the MMA61/OP-POSS blend containing various OP-POSS contents, recorded at 120 °C.

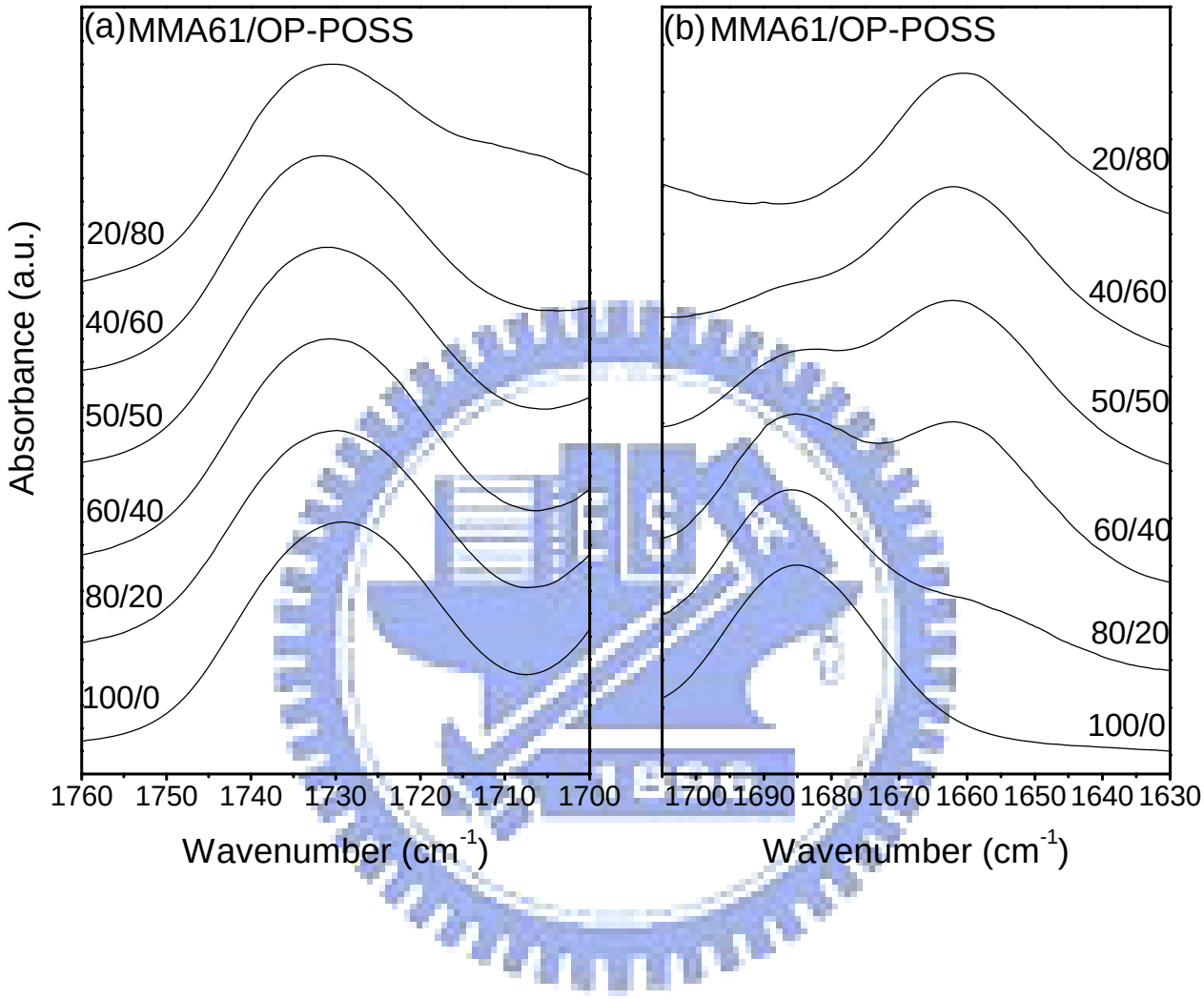

Figure 2-9. DSC scans for MMA61/OP-POSS blends of various compositions.

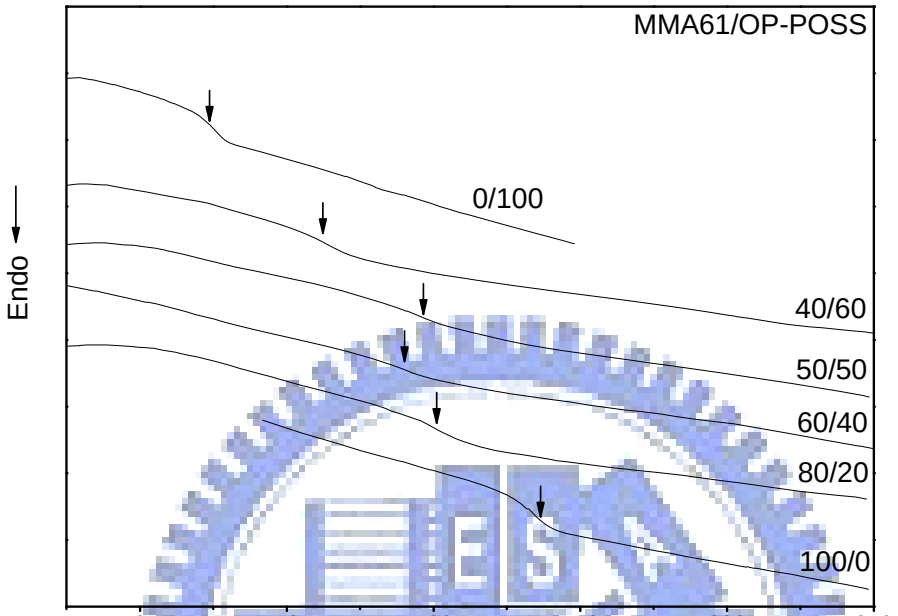

Figure 2-10. Plots of T_g versus (a) the MMA81 content of MMA81/OP-POSS blends, (b) the MMA61 content of MMA61/OP-POSS blends, and (c) the MMA53 content of MMA53/OP-POSS blends.

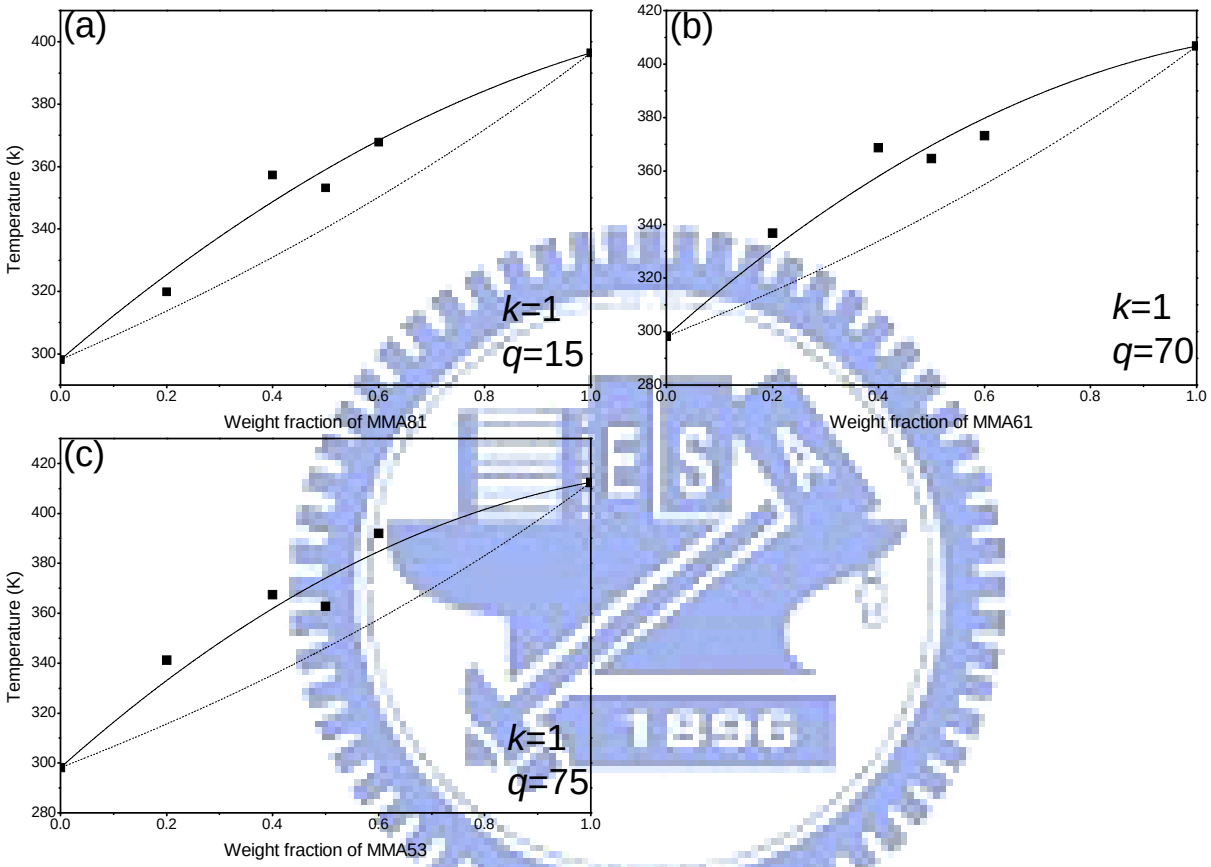

Figure 2-11. Plots of ionic conductivity with respect to the MMA content in PMMA-*co*-PVP copolymers for (■) $LiClO_4$/polymer binary blends and (□) $LiClO_4$/OP-POSS/MMA61 ternary blends.

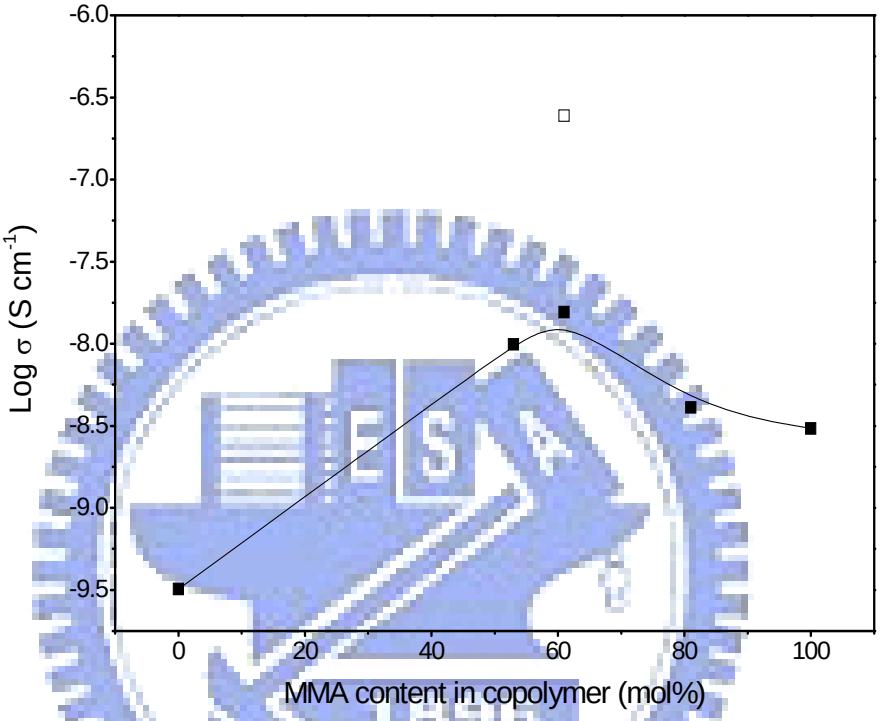

Chapter 3

Effect of $LiClO_4$ on the Thermal and Morphological Properties of Organic/Inorganic Polymer Hybrids

Abstract. This paper describes the thermal properties, morphologies, and interactions within the binary and ternary blends of poly(methyl methacrylate) (PMMA), octa(phenol)octasilsesquioxane (OP-POSS), and $LiClO_4$. In the binary PMMA/OP-POSS blends, the OP-POSS molecules tend to aggregate and result in a decrease (19 °C) in the glass transition temperature. In the ternary PMMA/$LiClO_4$/OP-POSS blends, however, the OP-POSS molecules form small sphere-like domains (20 nm) leading to the composite's glass transition temperature increasing by up to 30 °C. Based on these FTIR spectra, the addition of $LiClO_4$ influenced the probability of hydrogen bonds formed between PMMA and OP-POSS and these SEM micrographs, DSC, and XRD data indicated that the addition of $LiClO_4$ is a convenient and simple approach toward dispersing the OP-POSS nanoparticles within PMMA, where the presence of $LiClO_4$ changes the physical effect of OP-POSS from that of a diluent role to a cross-linker role.

Keywords: hydrogen bonding, polyhedral oligomeric silsesquoixane, ion-dipole interaction.

3.1. Introduction

Composite materials fabricated from organic polymers and inorganic materials are currently attracting great attention for both their fundamental scientific behavior and industrial applications. Polyhedral oligomeric silsesquoixanes (POSSs), which have the general formula $(RSiO1.5)_n$ are prototypical organic/inorganic systems because they are composed of inorganic cores with external organic substituents. Through appropriate control over the functionality of these organic substituents, both mono- and octa-functional macromonomers can be blended or attached covalently to linear thermoplastics or thermosetting networks to form high-performance hybrid materials.[1-18] Other interesting organic/inorganic blend systems

are the polymer electrolytes formed via the dissolution of salts into polar and high-weight macromolecules where strong noncovalent interactions between the macromolecules and the cations of the salts result in changes in the polymers' properties, e.g., its miscibility.[19,20] To our knowledge, the reports which described organic/inorganic composite system featuring both hydrogen bonding interactions, ion-dipole interactions by incorporating the POSS nanoparticles and $LiClO_4$ into polymers are still rare.[21,22] In addition, the interaction and conductivity behaviors of poly(vinyl pyrrolidone-*co*-methyl mechacrylate) (PVP-co-PMMA) with $LiClO_4$ were reported in our previous work[23] and we also indicated that the ionic conductivity of a $LiClO_4$/PMMA-*co*-PVP polymer electrolyte was enhanced after blending with OP-POSS.[24] To further realize the interaction mechanism within these polymer electrolytes incorporated by OP-POSS which is functionalized to behave as a strong proton donor and exhibits improved miscibility with host polymers containing proton acceptors,[25-28] these blends comprising PMMA, $LiClO_4$, and POSS derivatives were prepared and their properties were described at various compositions.

3.2. Experimental Part

3.2.1. Materials. Toluene, tetrahydrofuran (THF), platinum divinyl tetramethyldisiloxane complex [Pt(dvs)], 4-acetoxystyrene (AS), lithium perchlorate ($LiClO_4$), and poly(methyl methacrylate) (PMMA) were purchased from Aldrich Chemical Co. $\mathbf{Q_8M_8^H}$, $C_{16}H_{56}O_{20}Si_{16}$, was obtained from Hybrid Plastics Co. Toluene was fractionally distilled from calcium hydride under a nitrogen atmosphere. $\mathbf{Q_8M_8^H}$, Pt(dvs) and AS were used as received. The oligomers octa(acetoxystyryl)octasilsequioxane (AS-POSS) and octa(phenol)octasilsesquioxane (OP-POSS) were synthesized (Scheme 3-1) according to a procedure described previously.[26] Several PMMA/$LiClO_4$/OP-POSS blends were dissolved in THF (15 wt%) and stirred continuously for 8 h at 25 °C. To prepare the sample for XRD, SEM, and DSC measurements, the solutions were cast into Teflon dishes and dried under a

nitrogen atmosphere at 25 °C for 24 h, under vacuum at about 0.2 torr at 60 °C for 12 h, and then at 120 °C for 8 h to completely remove any residual solvent or water. The compositions of the PMMA/$LiClO_4$/OP-POSS blends are summarized in Table 3-1. The unit phr is a concentration representation: e.g., 100/25/1 refers to a system formed from 100 g of PMMA, 25 g of $LiClO_4$ and 1 g of OP-POSS.

3.2.2. Characterization. Thermal analyses were performed using a DuPont TA 2010 DSC instrument operated at a scan rate of 20 °C/min from -50 to 200 °C. FTIR spectra were recorded over the range 4000–400 cm^{-1} using a Nicolet Avatar 320 FT-IR spectrometer (32 scans; 1 cm^{-1} resolution) operated at 120 °C. To prepare the samples for the FTIR observation, these solutions were cast onto KBr disks and dried as mentioned above. FE-SEM and SEM-DEX images were recorded using a Hitachi-S4200I microscope operated at acceleration voltage of 5–15 kV and ambient temperature. All samples were fractured under cryogenic conditions using liquid nitrogen. X-ray diffraction (XRD) experiments were operated at ambient temperature and performed using the wiggler beamline BL17A1 of the National Synchrotron Radiation Research Center (NSRRC), Taiwan employing a monochromated beam [wavelength (λ): 1.3329 Å]; the XRD pattern was collected by a curved imaging plate (IP: Fuji BAS III: area: 20 × 40 cm^2) having a radius equivalent to the sample-to-detector distance (280 nm).

3.3. Results and Discussion

3.3.1. Morphologies. Figures 3-1 present cross-sectional SEM images, which were employed previously to investigate the distribution of various functional POSS derivatives, of the (a) 100/0/5 and (b) 100/25/5 blends.[5,29-35] The POSS molecules in the 100/0/5 blend appear to aggregate into large domains (bright regions) within the PMMA matrix. In contrast, the OP-POSS molecules in the 100/25/5 blend have formed sphere-like domains having diameters of ca. 20 nm. In our previous studies,[23,36] we examined blends featuring a range of

competitive noncovalent interactions, including carbonyl (PMMA)···hydroxyl (OP-POSS), hydroxyl (OP-POSS)···hydroxyl (OP-POSS), carbonyl (PMMA)···Li^+, and Li^+···ClO_4^- interactions.[37-39] From the knowledge gained from those studies, we suspected that the morphological differences between the 100/0/5 and 100/25/5 blend resulted from the different types of noncovalent interactions within them. Figure 3-2(a) presents IR spectra displaying the ν (ClO_4^-) internal vibration modes of these blends. The bands centered at 626 and 636 cm^{-1} correspond to the signals of the free anion and the contact ion pair, respectively.[40,41] The intensity of the blend for the contact ion pair increased upon increasing the content of OP-POSS, revealing that OP-POSS molecules tend to increase the formation of contact ion pairs. Figure 3-2(b) displays the carbonyl stretching region of IR spectra of the PMMA/$LiClO_4$/OP-POSS blends. The bands at 1730, 1709, and 1700 cm^{-1} correspond to the free C=O groups of PMMA, and those involved in hydrogen bonds (with the OH groups of OP-POSS) and ion–dipole interactions (with Li^+), respectively. In the spectra of the 100/25/0 and 100/25/5 blends, the intensity of the shoulder at 1700 cm^{-1} decreases dramatically in the latter, indicating that the presence of OP-POSS led to a decrease in the number of PMMA C=O groups involved in ion–dipole interactions. The intensities of the hydrogen-bonded C=O of PMMA were identical for the 100/25/5 and 100/0/20 blends, indicating that the fractions of such groups of PMMA were identical.[36] The presence of $LiClO_4$ salts in the ternary blend led to an increase of the probability of forming C=O (PMMA)···OH (OP-POSS) hydrogen bonds. Thus, there must have been a specific interaction occurring between $LiClO_4$ and OP-POSS. Figure 3-2(c) displays the region from 2700 to 3700 cm^{-1} in the IR spectra of the OP-POSS/$LiClO_4$ (phr) binary blends. $LiClO_4$ appears to interact with the OH groups of OP-POSS shifting their broad band to higher frequency. These IR spectra reveal that the interactions between OP-POSS and $LiClO_4$ coexist with the C=O (PMMA)···OH (OP-POSS), OH (OP-POSS)···OH (OP-POSS), C=O (PMMA)···Li^+, and Li^+···ClO_4^- interactions, with

competition between these species resulting in the change in morphology.[42-44] Table 3-1 lists the values of 2θ obtained from XRD analysis of the various blends (Figures 3-3). The signal centered at 10.2° corresponding to the intermolecular distance between PMMA chains[45] remained unchanged after the incorporation of OP-POSS. In contrast, the addition of $LiClO_4$ (25 phr) to the PMMA matrix shifted the 2θ angle from 10.2° to 12.6° which suggests that $Li^+\cdots O{=}C$ coordination resulted in contraction of the polymer chains. The presence of OP-POSS in the 100/25/5 blend resulted in a shift of the2θ angle to 12.6° from that of 10.5° for the 100/25/0 blend. This finding implies that the addition of OP-POSS increases the contracted intermolecular distance between PMMA polymers. For the 100/25/5 blend, the 2θ angle was almost identical to that of 100/0/5, i.e., for the association of PMMA, $LiClO_4$, and OP-POSS. In the 100/25/5 blend, the OP-POSS molecules were dispersed well in the presence of $LiClO_4$, as the SEM image revealed, which has the influence of increasing the contracted intermolecular distance between PMMA chains. As a result of these competing influences, the 2θ angle for the 100/0/5 and 100/25/5 blends remained virtually unchanged.

Figure 3-1 illustrates the proposed mechanism leading to development of the morphologies of the 100/0/5 and 100/25/5 blends. During the initial stage, all of the components in the 100/0/5 and 100/25/5 blends were dissolved and distributed uniformly within the solvent. During the second stage, as the solvent evaporates partially, the $LiClO_4$ in the 100/25/5 blend interacts with both OP-POSS and PMMA and forms sphere-like OP-POSS/$LiClO_4$ domains. During the final stage, as the solvent and water molecules are removed completely, the degree of phase separation in the PMMA/$LiClO_4$/OP-POSS is relatively lower—and, thus, the OP-POSS domains are relatively smaller—than in the PMMA/OP-POSS blends as a result of the competitive interactions.

3.3.2. Thermal Properties. Table 3-1 lists DSC data of the PMMA/$LiClO_4$/OP-POSS blends obtained from Figure 3-4. In the blends lacking the salt, the presence of OP-POSS decreases

the glass transition temperature (T_g) of PMMA as a result of aggregation of the OP-POSS. In contrast, for the 100/25/1 blend, the addition of 25 phr $LiClO_4$ salts to the 100/0/1 blend resulted in a 27 °C increase in T_g. The change was much greater (30 °C) for the 100/0/5 and 100/25/5 systems. In the 100/25/0, 100/0/1, and 100/0/5 blends, the weak associations, i.e., $Li^+\cdots$O=C (PMMA) and C=O (PMMA)$\cdots$OH (OP-POSS) had no effect or a slight decrease in the value of T_g of the composite.[23,34,46,47] In the 100/25/1 and 100/25/5 blends, the combination of the various noncovalent interactions resulted in the formation of OP-POSS/$LiClO_4$ aggregated domains, improving the probability of forming C=O (PMMA)$\cdots$OH (OP-POSS) hydrogen bonds, smaller and better-distributed OP-POSS molecules, and an increase in the value of T_g of the composites.[48-51] In previous studies,[5,52] POSSs were found to affect the glass transition temperatures of nanocomposites through two different effects: one was a restricted effect that enhanced T_g, the other increased the free volume of the system, which reduced T_g. Based on our FTIR, XRD, DSC data, and SEM micrographs, the presence of $LiClO_4$ in the 100/25/5 blend influenced the hydrogen bonds formed between PMMA and OP-POSS, dispersion of OP-POSS, and the intermolecular distance between PMMA chains; thus, the addition of $LiClO_4$ shifted the physical role of OP-POSS from that of a diuent to a restricted role (physical crosslinking). Additionally, the interactions between PMMA, $LiClO_4$, and OP-POSS enhanced the restricted effect of the OP-POSS toward PMMA. Therefore, the glass transition temperature of the composites was enhanced through the simultaneous incorporation of $LiClO_4$ and OP-POSS.

3.4. Conclusions

In the 100/0/1 and 100/0/5 blends, the OP-POSS molecules tended to aggregate into large domains because of the tendency of their OH groups to self-associate rather than form OH$\cdots$C=O hydrogen bonds,[36,53] resulting in a decrease in the value of T_g of the PMMA/OP-POSS composites. In the 100/25/1 and 100/25/5 blends, $LiClO_4$ and OP-POSS

formed a better dispersion of sphere-like OP-POSS/$LiClO_4$ domains as a result of competition among the various interaction pairs. Based on these FTIR spectra, $LiClO_4$ played critical roles through its ion–dipole interaction with PMMA and its specific interactions with OP-POSS, influencing hydrogen bonds formed between PMMA and OP-POSS and dispersion of OP-POSS; the result was an enhancement of the glass transition temperature of these PMMA/OP-POSS composites. Thus, the addition of $LiClO_4$ is a convenient and simple approach toward dispersing the OP-POSS nanoparticles within PMMA polymers, where the presence of $LiClO_4$ changes the physical effect of OP-POSS from that of a diluent to a cross-linker role.

References

1. Kuo, S. W.; Lin, H. C.; Huang, W. J.; Huang, C. F.; Chang, F. C. *J Polym Sci, Polym Phys* **2006**, *44*, 673.
2. Kopesky, E. T.; Haddad, T. S.; Cohen, R. E.; McKinley, G. H. *Macromolecules* **2004**, *37*, 8992.
3. Li, G. Z.; Wang, L.; Toghiani, H.; Daulton, T. L.; Koyama, K.; Pittman, C. Y. *Macromolecules* **2001**, *34*, 8686.
4. Chen, W. Y.; Wang, Y. Z.; Kuo, S. W.; Huang, C. F.; Tung, P. H.; Chang, F. C. *Polymer* **2004**, *45*, 6897.
5. Matejka, L.; Strachota, A.; Plestil, J.; Whelan, P.; Steinhart, M.; Slouf, M. *Macromolecules* **2004,** *37*, 9449.
6. Goldman, M.; Shen, L. *Phys Rev* **1966**, *114*, 321.
7. Leu, C. M.; Chang, Y. T.; Wei, K. H. *Chem Mater* **2003**, *15*, 2261.
8. Lee, Y. J.; Huang, J. M.; Kuo, S. W.; Lu, J. S.; Chang, F. C. *Polymer* **2005**, *46*, 173.
9. Liu, Y. L.; Chang, G. P.; Hsu, K. Y. ; Chang, F. C. *J Polym Sci, Part A: Polym Chem* **2006**, *44*, 3852.
10. Phillips, S. H.; Haddad, T. S.; Tomcrzak, S. J. *Curr. Opin. Solid State Mater Sci* **2004**, *8*, 21.
11. Li, G. Z.; Wang, L. C.; Ni, H. L. *J Inorg Organomet Polym* **2001**, *11*, 123.
12. Kopesky, E. T.; Haddad, T. S.; Cohen, R. E.; McKinley, G. H. *Macromolecules* 2004, 37, 8992.
13. Voronkov, M. G.; Lavrent'ev, V. I. *Top Curr Chem* **1982**, *102*, 199.
14. Baney, R. H.; Itoh, M.; Sakakibara, A.; Suzuki, T. *Chem Rev* **1995**, *95*, 1409.
15. Provatas, J. G. *Trends Polym Sci* **1997**, *5*, 327.
16. Loy, D. A.; Shea, K. J. *Chem Rev* **1995**, *95*, 1431.

17. Lichtenhan, J. D. In: *Polymeric Materials Encyclopedia*, Salamone, J. C. Ed. CRC Press: Boca Raton, FL, **1996**. pp. 7768.

18. Laine, R. M. *J Mater Chem* **2005**, *15*, 44.

19. Chiu, C. Y. ; Chen, H. W. ; Kuo, S. W. ; Huang, C. F.; Chang, F. C. *Macromolecules* **2004**, *37*, 8424.

20. Chiu, C. Y. ; Hsu, W. H. ; Yen, Y. J. ; Kuo, S. W. ; Chang, F. C. *Macromolecules* **2005**, *38*, 6640.

21. Zhang, H. ; Kulkarni, S.; Wunder, S. L. *J Phys Chem B* **2007**, *111*, 3583.

22. Mather, P. T.; Kim, B. S.; Ge, Q.; Liu, C. D. US Pat. 2006:7,067,606.

23. Chiu, C. Y.; Yen, Y. J.; Kuo, S. W.; Chen, H. W.; Chang, F. C. *Polymer* **2007**, *48*, 1329.

24. "Miscibility and Hydrogen Bonding Behavior in Organic/Inorganic Polymer Hybrids Containing Octaphenol Polyhedral Oligomeric Silsesquioxane" Yen, Y. C.; Kuo, S. W.; Huang, C. F.; Chen, J. K.; Chang, F. C. *J Phys Chem B* **2008**, in press.

25. Eastwood, E.; Viswanathan, S.; O'Brien, C. P.; Kumar, D.; Dadmun, M. D. *Polymer* **2005**, *46*, 3957.

26. Kuo, S. W.; Chang, F. C. *Macromolecules* **2001**, *34*, 4089.

27. Ohgi, H.; Yang, H.; Sato, T.; Horii, F. *Polymer* **2007**, *48*, 3850.

28. Huang, C. F.; Kuo, S. W.; Lin, F. J.; Wang, C. F.; Hung, C. J.; Chang, F. C. *Polymer* **2006**, *47*, 7060.

29. Kuo, S. W.; Lin, C. L.; Chang, F. C. *Polymer* **2002**, *43*, 3943.

30. Lin, H. C.; Kuo, S. W.; Huang, C. F.; Chang, F. C. *Macromol Rapid Commun* **2006**, *27*, 537.

31. Liu, H. Z.; Zheng, S. X. *Macromol Rapid Commun* **2005**, *26*, 196.

32. Leu, C. M.; Reddy, G. M.; Wei, K. H.; Shu, C. F. *Chem Mater* **2003**, *11*, 2261.

33. Zhang, C.; Babonneau, F. ; Bonmme, C. ; Laine, R. M. ; Soles, C. L. ; Hristov, H. A. ;

Yee, A. F. *J Am Chem Soc* **1998**, *120*, 8380.

34. Leu, C. M.; Chang, Y. T.; Wei, K. H. *Macromolecules* **2003**, *36*, 9122.

35. Chen, W. Y.; Ho, K. S.; Hsieh, T. H.; Chang, F. C.; Wang, Y. Z. *Macromol Rapid Commun* **2006**, *27*, 452.

36. Lin, C. L.; Chen, W. C. ; Liao, C. S.; Su, Y. C.; Huang, C. F.; Kuo, S. W. ; Chang, F. C. *Macromolecules* **2005**, *38*, 6435.

37. Hameed, N.; Qipeng, G. Q. *Polymer* **2008**, *49*, 922.

38. Lim, J. S.; Noda, I.; Im, S. S. *Polymer* **2007**, *48*, 2745.

39. Ohgi, H.; Sato, T.; Hu, S.; Horii, F. *Polymer* **2006**, *47*, 1324.

40. Mishra, R.; Rao, K. J. *Solid State Ionics* **1998**, *106*, 113.

41. Salomon, M.; Xu, M.; Eyring, E. M.; Petrucci, S. *J Phys Chme* **1994**, *98*, 8234.

42. Choi, S.; Kim, J. H.; Kang, Y. S. *Macromolecules* **2001**, *34*, 9087.

43. Sargsyan, A.; Tonoyan, A.; Davtyan, S.; Schick, C. *Eur Polym J* **2007**, *43*, 3113.

44. Zhang, S.; Runt, J. *J. Phys. Chem. B* **2004**, *108*, 6295.

45. Kim, J.; Sandoval, R. W.; Dettmer, C. M.; Nguyen, S. T.; Torkelson, J. M. *Polymer* In press.

46. Yilgor, I.; Yilgor, E.; Guler, I. G.; Ward, T. C.; Wilkes, G. L. *Polymer* **2006**, *47*, 4105.

47. Sammon, C.; Li, C.; Armes, S. P.; Lewis, A. L. *Polymer* **2006**, *47*, 6123.

48. Kalogeras, I. M.; Neagu, E. R. *Eur Phys J E* **2004**, *14*, 193.

49. Kabomo, M. T.; Blum, F. D.; Kulkeratiyut, S.; Krisanangkura, P. *J Polym Sci Phys* **2008**, *46*, 649.

50. Krakovský, I.; Hanyková, L.; Trchová, M.; Baldrian, J.; Wübbenhorst, M. *Polymer* **2007**, *48*, 2079.

51. Yang, B.; Huang, W. M.; Li, C.; Li, L. *Polymer* **2006**, *47*, 1348.

52. Liu, H.; Zheng, S.; Nie, K. *Macromolecules* **2005**, *38*, 5088.

53. Lin, C. L.; Chen, W. C.; Kuo, S. W.; Chang, F. C. *Polymer* **2006**, *47*, 3436.

Table 3-1. Compositions, 2θ (degrees), and T_g of the binary and ternary blends.

PMMA/$LiClO_4$/OP-POSS (phr)	2θ (degrees)	T_g * (°C)
100/0/0	10.2	116
100/0/1	10.1	97
100/25/0	12.6	115
100/25/1	10.5	124
100/0/5	10.2	97
100/25/5	10.5	127

*: The glass transition temperature (T_g) was obtained as the inflection point of the heat capacity jump.

Scheme 3-1. Synthesis of OP-POSS.

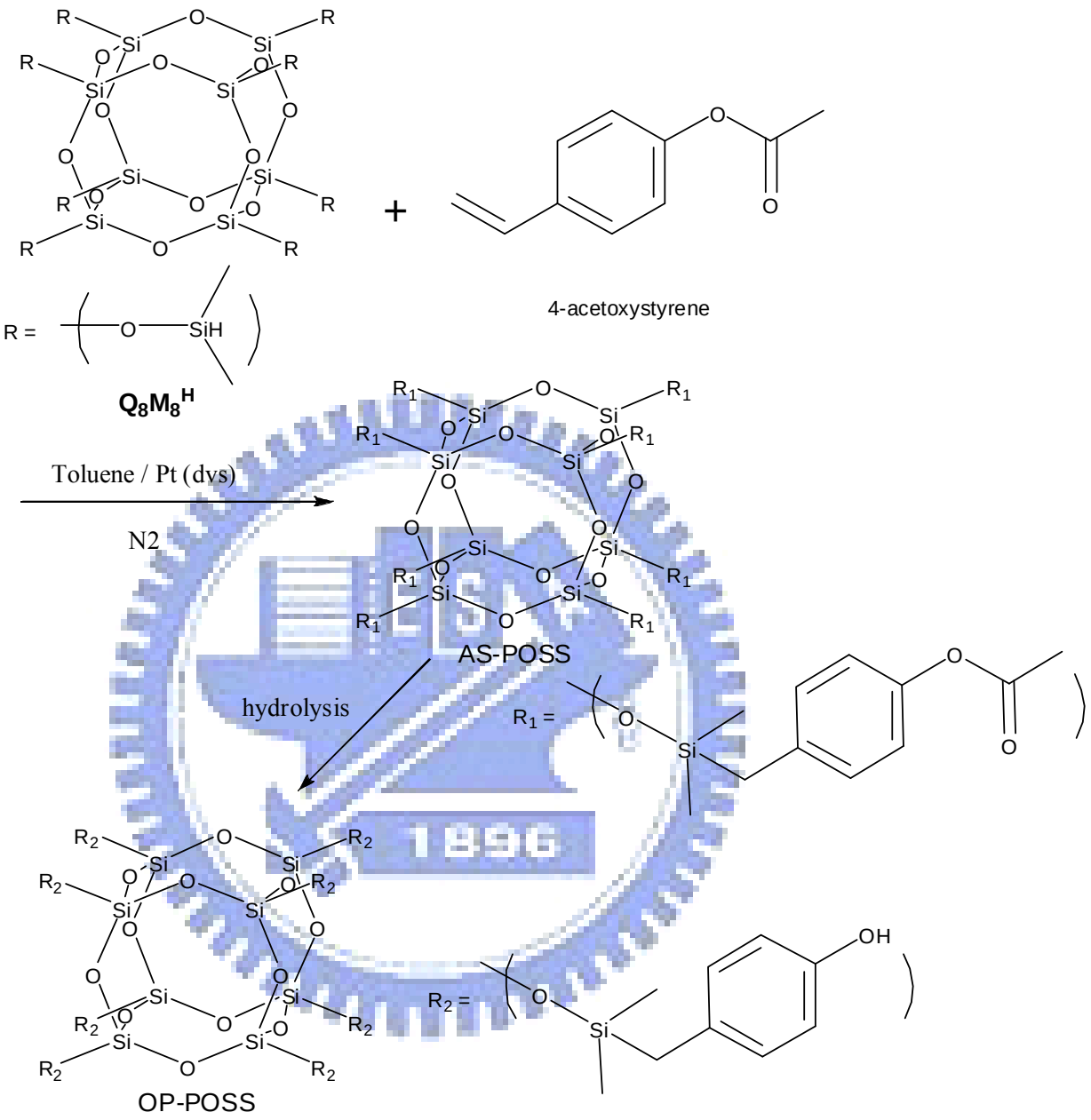

Figure 3-1. FE-SEM micrographs of (a) PMMA/$LiClO_4$/OP-POSS (100/0/5) and (b) PMMA/$LiClO_4$/OP-POSS (100/25/5). (c, d) Schematic representations of the proposed mechanisms of formation of the various OP-POSS domains.

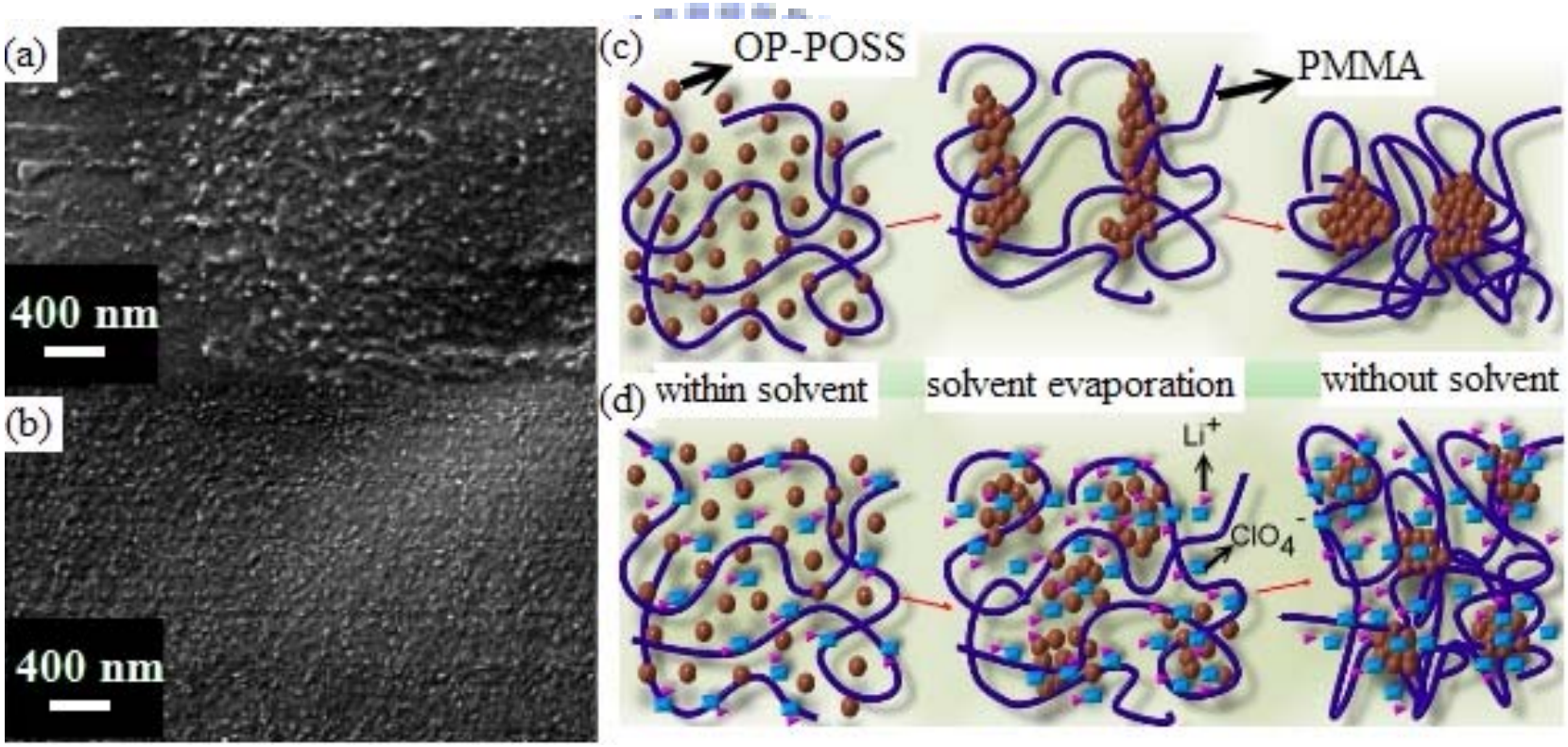

Figure 3-2. IR spectra of various PMMA/$LiClO_4$/OP-POSS blends recorded at 120 °C.

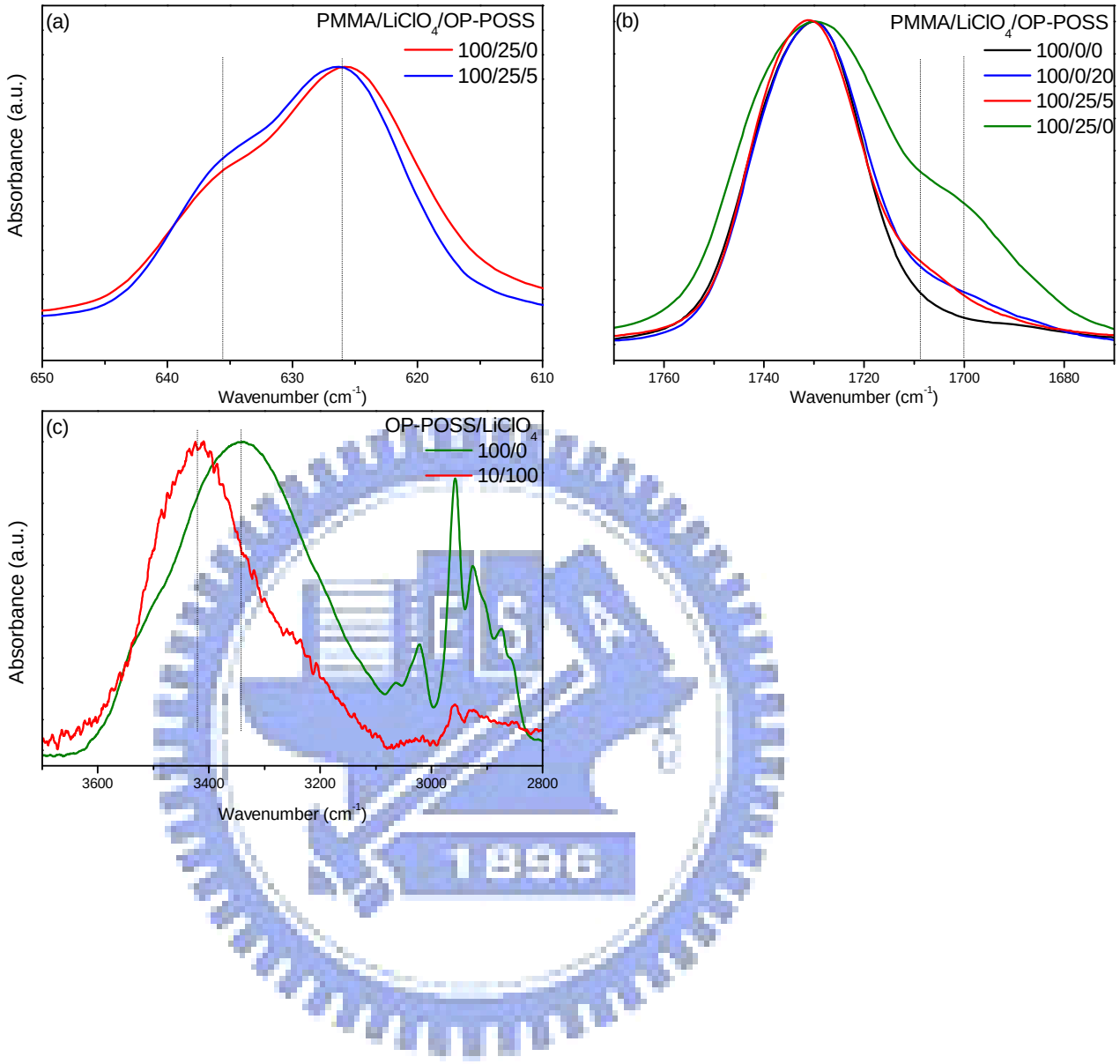

Figure 3-3. XRD patterns of these binary and ternary blends.

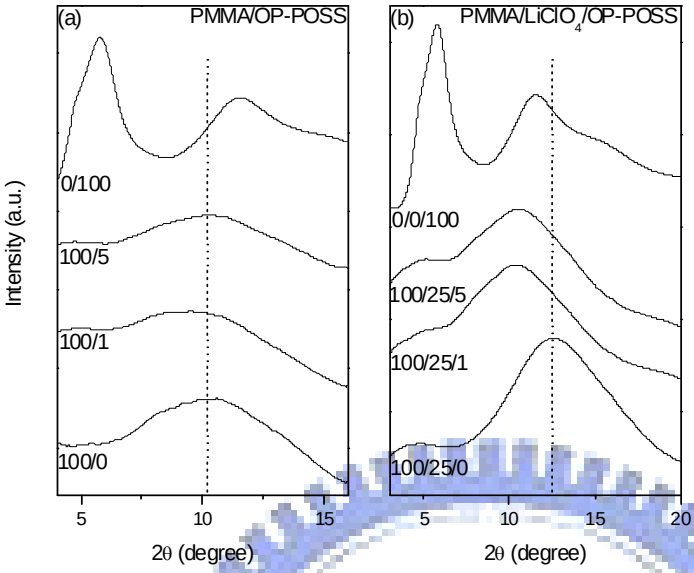

Figure 3-4. DSC curves of these binary and ternary blends.

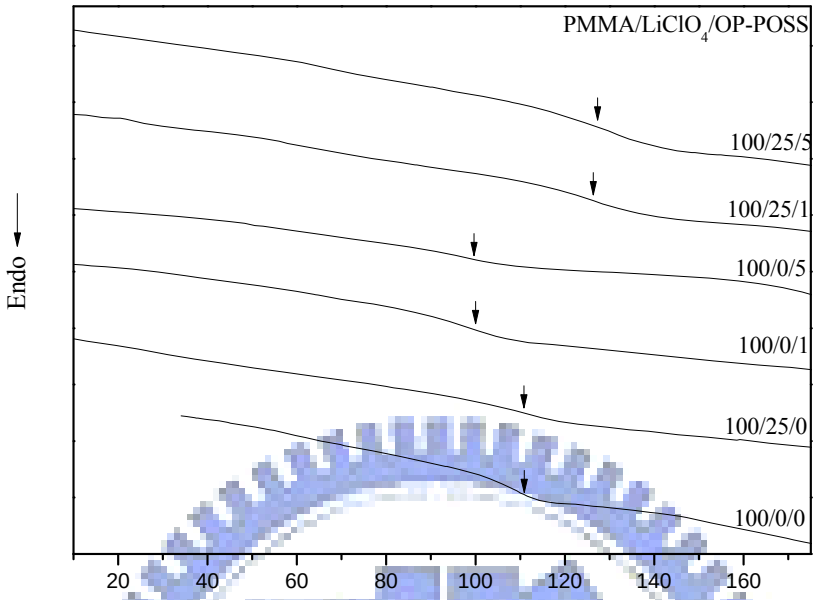

Chapter 4

Effect of Sulfonic Acid Groups on Properties of New Organic/Inorganic Cross-linked Proton Exchange Membrane

Abstract In this study, polyhedral oligomeric silsequoixane (POSS) was incorporated into sulfonated poly(ether ether ketone) (SPEEK), forming a new cross-linked proton exchange membrane (PEM). The distribution of these nano-scale cross-linkers were affected by their sulfonic acid groups and dictated the water behavior and the dispersion and connectivity of hydrophilic domains within these PEMs. A PEM formed by incorporating 17.5 wt% of the cross-linkers (containing POSS molecules and sulfonic acid groups) into SPEEK exhibited high proton conductivity (0.0153 S/cm), low methanol permeability (1.34×10^{-7} cm^2/s), and high selectivity (0.0011 Ss/cm^3).

4.1. Introduction

Proton exchange membrane (PEM) providing ionic pathways for proton transfer is a key component of the direct methanol fuel cell (DMFC). Nafion, one of the most studied material for application as PEM, exhibits both chemical and physical stability at moderate temperature and high proton conductivity through its highly interconnected hydrophilic channels.[1] Sulfonated polymers, such as sulfonated poly(ether sulfone) (SPES), poly(benzimidazole) (SPBI), poly(ether ether ketone) (SPEEK), and polyimide (SPI), are also potential candidates for use in PEMs,[2-13] but their high cost and high methanol permeability limit their applications.[1-13] To overcome these drawbacks, numerous new materials possessing reinforced sulfnoated polymers are often employed.[14-21] Cross-linked PEMs have shown significant advantages in controlling the water behavior, improving the dimension stability, and thermal stability.[22-31] The incorporation of inorganic materials into sulfonated polymers by cross-linking reaction has also been reported.[32-39]

Polyhedral oligomeric silsequoixanes (POSSs), $(RSiO_{1.5})_n$, an intermediate between silica

(SiO_2) and silicone (R_2SiO), are prototypical organic/inorganic systems composed of hydrophobic inorganic cores and externally covered by organic substituents. Through judicious design of the functionalities of these organic substituents, it is possible to create octafunctional or monofunctional macromonomer that can be incorporated into either linear thermoplastics or thermosetting networks to form high performance hybrid materials.[40-54] These POSS hybrid materials are potential candidates for use in PEM because their hydrophobic core and adjustable external functionalities affect the water behavior, dimension stability, and thermal stability of sulfonated polymers but rarely been investigated.[55] In this study, properties of cross-linked PEMs comprising functionalized POSS and sulfonated poly(ether ether ketone) (SPEEK) are presented and discussed.

4.2. Experimental Part

4.2.1. Materials. Toluene, DMSO, 4,4′-diaminodiphenyl ether (ODA), and platinum divinyltetramethyldisiloxane complex [Pt(dvs)] were purchased from Aldrich Chemical Co. Allyl glycidyl ether (AGE) was purchased from Acros Chemical Co. VictrexR PEEK grade 450G extruded pellets were purchased from Victrex. **Q8M8^{H}** was obtained from Hybrid Plastics Co. Toluene and DMSO were distilled from calcium hydride. AGE was purified through vacuum distillation from calcium hydride. **Q8M8^{H}**, Pt(dvs), and ODA were used as received.

4.2.2. Octakis(dimethylsilyloxypropylglycidyl ether)octasilsesquioxane (OG-POSS) Oligomer. The **Q8M8^{H}** oligomer (1.96 mmol) was placed in a dry 50-mL round-bottom flask equipped with a stirrer bar. Anhydrous toluene (30 mL), AGE (16.66 mmol), and Pt(dvs) (1 drop) were added. The reaction mixture was heated at 80 °C under an argon atmosphere for 8 h, the then cooled to room temperature. The activated charcoal was added to the reaction mixture and stirred for 10 min, and then the solution was filtered through a 0.45 mm Teflon membrane. The residual solvent was evaporated; finally, the product, OG-POSS (Scheme 4-1),

was obtained as a colorless, viscous liquid.[43]

4.2.3. Synthesis of 4,4´-Diaminodiphenyl Ether-2,2´-disulfonic Acid (ODADS). ODA (8.00 g, 10.0 mmol) was placed under an argon atmosphere into a 100-mL three-neck flask equipped with a mechanical stirring device and cooled in an ice bath. Conc. H_2SO_4 (95%, 6.8 mL) was added for 10 min. After the ODA had dissolved completely, fuming sulfuric acid (60% SO_3, 14 mL) was added dropwise to the flask. The sulfonation mixture was stirred at 25 °C for 2 h and then it was heated at 80 °C for 4 h. The slurry was cooled to room temperature and then it was carefully poured onto crushed ice (100 g). The filtered white product was redissolved in a NaOH solution (30%, 500 mL), and then it was acidified with conc. HCl. The precipitate was filtered, washed repeatedly with deionized water and methanol, and then dried to constant weight.[10]

4.2.4. Sulfonation of PEEK. The PEEK pellets (20g) were added slowly to conc. H_2SO_4 (95–98 wt%, 500 mL) in a three-neck flask at room temperature under an argon atmosphere. After dissolution, the solution was heated at 55 °C with vigorous stirring for 3 h and then it was added to ice water to form a precipitate (SPEEK). After filtering and washing with distilled water, the SPEEK was converted into its sodium salt through immersion in 1M NaOH for 72 h. The degree of sulfonation (DS) was determined to be 71.8 % through ^{1}H NMR of a SPEEK solution in DMSO-d_6.

4.2.5. Membranes Preparations. Desired amounts of SPEEK, OG-POSS, ODA, and ODADS were dissolved in DMSO to form 15 % polymer solutions and stirred for 24 h at 25 °C. The solutions were cast onto Teflon dishes maintained at 60 °C for 48 h to remove most of the solvent, and then these membranes were dried under vacuum at about 0.2 torr at 60 °C for an additional 48 h to complete the drying process. ^{13}C NMR spectroscopy confirmed that the thermal curing reaction (Scheme 4-1) between OG-POSS and ODA (or ODADS) was complete. Finally, the membrane was peeled from the Teflon dishes through immersion in

deionized water. After immersion in 2 M HCl for 24 h, the film was obtained in acidic form; it was then washed with deionized water until the pH reached 6–7. Table 4-1 summaries these membrane compositions.

4.2.6. Characterization. ^{1}H NMR spectrum was recorded at 25 °C on an INOVA 500 MHz spectrometer. The thermal degradation behavior of the membrane was measured using a thermal gravimetric analyzer (TGA Q100) operated at a heating rate of 20 °C/min from 25 to 800 °C. Dynamic mechanical testing was performed using a DuPont DMA Q800 dynamic mechanical analyzer operated at a heating rate of 5 °C /min from 150 to 350 °C and a frequency of 1.0 Hz. Transmission electron microscopy (TEM) was performed using JEOL JEM-1200CX-II microscope operated at 120 kV. To stain the hydrophilic domains, the membrane was converted into their Pb^{2+} form through immersion in 1 N $Pb(OAC)_2$ solution overnight and then rinsing with water. For TEM observation, the ultra-microtome section of the dried membrane (50-nm slices) was placed on 200-mesh copper grids. The frequency-dependent impedance property (from 10 kHz to 10 Hz) of the polymer complex was measured using an Autolab designed by Eco Chemie. For conductivity measurement, the membrane was placed in a conductivity cell between stainless-steel blocking electrodes at 30 °C. The conductivity was calculated according to equation (4-1)

$$\sigma = \frac{L}{AR_b} \qquad (4\text{-}1)$$

where σ is the conductivity, L is the membranes thickness, A is the section area of the stainless steel electrode, and R_b is the bulk resistance.

The water uptake (WU; %) was calculated using equation (4-2):

$$\text{WU}\ (\%) = \frac{W_{wet} - W_{dry}}{W_{dry}} \times 100\% \qquad (4\text{-}2)$$

where W_{wet} and W_{dry} are the wet weight and dried weight of the membrane, respectively. The completely dried PEM was immersed in deionized water at room temperature for 24 h, then

removed quickly and blotted with filter paper to remove any excess water on the membrane surfaces, and immediately weighed to obtain its wet mass (W_{wet}). The dried weight (W_{dry}) of the membrane was measured after drying at 120 °C for 24 h.

The ion exchange capacity (IEC) was determined through titration with NaOH solution of the acid released from immersing the membrane in acid from into 1 M NaCl solution. The ionic concentration was calculated using equation (4-3):

$$[H^+] = \frac{IEC \times W_d / V_W}{1000} \tag{4-3}$$

where IEC refers to the titrated IEC, W_d is the weight of the dried membrane, and V_w is the volume of the wet membrane.

The number of water molecules per ionic group, λ, was determined using equation (4-4):

$$\lambda = \frac{WU}{18 \times IEC} \tag{4-4}$$

The amount of free water in the fully hydrated membranes was determined using a DuPont TA2010 differential scanning calorimeter. The sample was firstly cooled from 25 to –60 °C and then heated to 50 °C at a rate of 5 °C/min. The mass of free water in the membrane was measured by integrating the area under the cooling curve and comparing it to the measured enthalpy of fusion for water (314 J/g).

Water desorption measurement was performed using the TGA Q100 to determine the weight change of the sample over time at 80 °C. The water desorption coefficient was calculated using equation (4-5):

$$\frac{M_t}{M_\infty} = 4\left(\frac{Dt}{\pi L^2}\right)^{1/2} \tag{4-5}$$

where D is the water desorption coefficient, M_t/M_∞ represents the water desorption, and L is the membrane thickness.

The methanol diffusion coefficient of the membrane was measured using a two-chamber

liquid permeability cell that has been described in detail previously. A 50-mL chamber contained 5 M methanol solution; the other 50-mL chamber was filled with deionized water. The methanol concentration in the water cell was determined periodically using a GC-8A gas chromatograph (SHTMADU, Tokyo, Japan). The methanol permeability was calculated using equation (4-6):

$$C_B(t) = \frac{A}{V_B}\frac{P}{L}C_A(t - t_0) \qquad (4\text{-}6)$$

where V_0 is the initial volume of deionized water, L is the membrane thickness, A is the membrane area, C_A and C_B are the methanol concentrations in the methanol and water chambers, respectively, and P is the methanol diffusion coefficient.[1-39,56]

4.3. Results and Discussion

4.3.1. Morphologies of Cross-linkers. The degree of dispersion of POSS molecules in polymer matrices has great effect on both the thermal and mechanical properties of resulted composite systems.[40-63] In this study, these OG-POSS/ODA and OG-POSS/ODADS cross-linkers were incorporated into PEMs, membrane properties such as the water uptake, IEC, proton conductivity, and methanol permeability are expected to be affected. Previous reports on the morphologies of PEMs and polymers containing various functionalized POSS derivatives have indicated that the microstructure plays a critical role in determining the properties of PEMs.[1-63] Figure 4-1 presents SEM images (cross-sectional views) of OG15 and SOG15 membranes. In Figure 4-1(a), these OG-POSS/ODA cross-linkers (bright part) aggregate into spherical domains in the OG15 membrane whereas these aggregated OG-POSS/ODADS domains are significantly smaller and better dispersed in the SOG15 membrane [shown in Figure 4-1(b)]. In the OG membrane, the OG-POSS/ODA cross-linker tends to aggregate into hydrophobic domains while these sulfonic acid groups of ODADS in the SOG membrane interact with both the C=O and sulfonic acid groups of SPEEK and thus prevent the aggregation of the OG-POSS/ODADS cross-linkers.[64-67] Therefore, large

aggregation of the OG-POSS/ODA cross-linker occurs in the OG membrane system while the OG-POSS/ODADS cross-linker aggregates into fine and well-distributed domains.

4.3.2. Thermal Analysis. Figure 4-2 presents the TGA curves of the (a) SPEEK, OG03, and OG10 membranes and the (b) OG03, OG10, SOG03, and SOG10 membranes, indicating that all curves exhibit two steps of weight loss. The first degradation step above 300 °C corresponds to the degradation of sulfonic acid groups and the second weight loss region above 500 °C is associated with degradation of the SPEEK main chain and the linkages between the OG-POSS and ODA (or ODADS) unit as previously reported.[37,68] These TGA curves suggest that all these membranes are suitable for use as proton conducting materials in terms of thermal stability. Figure 4-2(b) reveals that the thermal stability of SOG10 is slightly better than that of OG10 and the SOG03 membrane has superior thermal stability than OG03. In addition, these plots of the loss factor tan δ as a function of temperature for SOG15 and OG15 membranes presented in Figure 4-2(c) indicate that the glass transition temperature of the former is higher than that of the latter. In previous studies,[64-67] the sulfonic acid group could interact with each other and the C=O group within these PEMs. In this study, these sulfonic acid groups act as them did in previous works, improving the miscibility between SPEEK and the OG-POSS/ODADS cross-linker and the distribution of cross-linkers, resulting in the relatively better thermal properties of these SOG membranes.[69]

4.3.3. Membrane Morphologies. Figure 4-3 displays TEM micrographs of these OG10 and SOG10 membranes where the light regions correspond to hydrophobic domains and these dark regions represent hydrophilic domains (ionic clusters). In Figure 4-3(a), the size of the hydrophilic domains of SPEEK varies from 20 to 100 nm, indicating that the SPEEK membrane is highly phase-separated. These membranes employed for TEM measurement are all anhydrous membranes; when they are fully hydrated, their hydrophilic domains will be connected to yield larger continuous hydrophilic domains and micro-phase separation of these

hydrophilic/hydrophobic domains become more pronounced. Greater phase separation and continuous hydrophilic domains of the hydrated SPEEK membrane allow protons for easier transport through the Grotthus (hopping) and vehicle (diffusion) mechanisms.[70-75] These features, however, also affect the methanol permeability behavior because the methanol permeation occurs in the form of methanol/H_2O complexes (such as $CH_3OH_2^+$ and H_3O^+) through continuous hydrophilic domains. Therefore, the methanol permeability of SPEEK can be retarded through micro-structural changes. Figure 4-3(b) reveals that the OG10 membrane possesses smaller and better-dispersed hydrophilic domains than SPEEK. The presence of OG-POSS/ODA cross-linkers tends to restrict the connection of these hydrophilic domains. In Figure 4-3(c), the size of these hydrophilic domains within the SOG10 membrane is fairly uniform (20 nm) and well dispersed. The difference in the hydrophilic domain size and distribution between the SOG10 and OG10 membranes can be attributed to the presence of the sulfonic acid groups of ODADS. Better distribution of the cross-linker unit in the SOG10 membrane results in better separation of hydrophilic domains as compared with the OG10 and SPEEK membranes. When the OG10 membrane is hydrated, the connectivity of hydrophilic domains is poorer than these SOG10 and SPEEK membranes because of the longer distance between hydrophilic domains, resulting in lower methanol crossover but lower proton conductivity. On the contrary, the SOG membrane exhibits high proton conductivity and less methanol crossover because of better connection and dispersion of these hydrophilic domains.[1–39]

4.3.4. Relationship between water sorption and membrane miscibility. The extent of water molecules in PEMs affects the degrees of proton transfer and methanol permeability. Excess water sorption causes low mechanical strength and poor hydrolytic stability of the PEM and thus unsuitable for fuel cell applications. Therefore, sufficient water sorption is required in a PEM and is of great importance when studying a PEM. Figure 4-4(a) indicates that the ion

exchange capacity (IEC) depends on the content of sulfonic acid group in these SPEEK, OG, and SOG membranes. When the OG-POSS/ODA cross-linker content is increased in the OG membrane, IEC decreases because of lower overall sulfonic acid content. In the SOG membranes, IEC increases with increasing cross-linker content through the presence of the sulfonic acid groups in ODADS.[76–78]

Figure 4-4(b) displays the effect of the cross-linker content on the water uptake of these OG and SOG membranes. All OG membranes exhibit lower water uptake relative to these SPEEK and SOG membranes because of lower content of sulfonic acid groups and greater separation of hydrophilic domains.[32-39] On the other hand, the water uptakes of SOG03 and SOG07 membranes are higher than those of these SPEEK and OG membranes, indicating that these relatively distributed OG-POSS/ODADS cross-linkers enhance the water sorption ability.[76-78] In the SOG10, SOG15, and SOG20 membranes, the water uptake decreases with increasing the cross-linker content as described in the OG membrane. The number of water molecules per sulfonic acid group (λ) is another important factor to determine the water state within a PEM. Figure 4-4(c) reveals the influence of the cross-linker content on λ for these OG and SOG membranes. In the OG system, the addition of the OG-POSS/ODA cross-linker results in a decrease in λ as compared with the SPEEK membrane because of low hydrophilic nature of the cross-linker. However, further addition of the OG-POSS/ODA cross-linker leads to increase in λ, which has rarely been observed in other cross-linked systems,[21-39,76-78] indicating that the cross-linker containing OG-POSS possesses specific effect on the water behavior of a PEM. On the other hand, in the SOG03 membrane, λ increases as compared with these SPEEK and OG membranes because the presence of the OG-POSS/ODADS cross-linker enhances the water sorption ability.[76-78] Nevertheless, λ decreases in all the other SOG membranes with adding these cross-linkers as previously reported. [76-78]

Table 4-2 lists that the bound water ratios affecting the proton transfer and methanol

permeability within a PEM. The bound water ratios of the OG membranes were all higher than that of the SPEEK membrane and increase upon increasing the cross-linker content as previous studies.[76-78] In contrast, the bound water ratio of the SOG03 membrane decreases as a result of the excess water sorption caused by the relative distributed OG-POSS/ODADS cross-linker. However, the bound water ratio increases upon further addition of OG-POSS/ODADS cross-linkers.[78] The water behavior of these OG and SOG membranes are dependent upon the nature of cross-linkers and the characteristic of OG-POSS.

4.3.5. Proton conductivity, methanol permeability, and selectivity. Figure 4-5(a) presents the proton conductivity of the membranes as a function of the cross-linker content, indicating that all these OG membranes exhibit lower proton conductivity, which decreases upon increasing the cross-linker content, than the SPEEK membrane. For all these OG membranes, the addition of the cross-linker reduces the degree of water sorption and causes separation of these hydrophilic domains and lower water desorption coefficient (see Table 4-2), thus these OG membranes exhibit relatively lower proton conductivity.[55] The water desorption coefficients of the SOG03, SOG07, and SOG10 membranes are higher than that of the SPEEK membrane, representing that these relatively distributed OG-POSS/ODADS cross-linkers result in connected hydrophilic domains. Therefore, these proton conductivities of these membranes are close or higher than that of the SPEEK membrane. In the SOG15 and SOG20 membranes, the effect of the epoxy network predominated over both the morphology and the water behavior, thus the proton conductivity decreases.

Methanol permeability [Figure 4-5(b)] is correlated to proton conductivity because methanol molecules are transported through the hydrophilic channels, which also function as the proton transport medium.[1–39] As mentioned above, the OG-POSS/ODA cross-linker in the OG membrane dictates the distribution of these hydrophilic domains causing the lower water sorption, lower free water content, and greater separation of hydrophilic domain, thus all OG

membranes exhibit methanol permeability lower than that of the SPEEK membrane. For the SOG membranes, methanol permeabilities of these SOG03 and SOG07 membranes are slightly higher or equal to the SPEEK membrane because of the excess water sorption and the decrease in the bound water ratio. For the SOG10, SOG15, and SOG20 membranes, however, the methanol permeability decreases upon increasing the cross-linker content because of the increased bound water ratio. The selectivity of the OG and SOG membranes is calculated and employed to judge whether they would be suitable for PEM applications [Figure 4-5(c)].[25,33,79] All these OG membranes exhibit selectivity lower than the SPEEK membrane where the methanol permeability and proton conductivity were both reduced after the incorporation of OG-POSS/ODA as a result of the separation of hydrophilic domains, lower water sorption, and higher bound water ratio. Because the reduction in the proton conductivity is greater than that in the methanol permeability, the selectivities (performances) of all the OG membranes are lower than that of the SPEEK membrane. On the other hand, these SOG membranes exhibit higher selectivity that the SPEEK membrane. Although the SOG03 and SOG07 possess higher methanol permeability as compared with these SPEEK and OG membranes, they also possess higher proton conductivity, thus they exhibit relatively higher selectivities. For these SOG10, SOG15, and SOG20 membranes, the methanol permeability decreases while proton conductivity is unchanged with increasing the cross-linker content, thus their selectivites are higher than those of these SOG03 and SOG07 membranes. The proton conductivity remains unchanged because these relatively distributed OG-POSS/ODADS cross-linkers result in complex connection of these separated hydrophilic domains as observed in these SEM and TEM micrographs. Figure 4-6 illustrates the proposed mechanisms of proton transfer within these PEMs. The SOG membranes possess better and complex connection of their separated hydrophilic domains, hindering the degree of methanol crossover from mass transfer without affecting the proton conductivity; therefore, they exhibit

higher proton conductivity, lower methanol permeability, and higher performance as compared with those OG and SPEEK membranes.

4.4. Conclusions A new cross-linked proton exchange membrane comprising SPEEK and an epoxy network containing OG-POSS nanoparticles was prepared. From a comparison of the properties of the OG and SOG membranes, the OG-POSS/ODADS cross-linkers within SOG membranes were better distributed because of the sulfonic acid groups attached to the cross-linkers. Better distribution of the OG-POSS/ODADS cross-linker causes increased bound water ratio and complex connection of these separated hydrophilic domains within the SOG membrane, therefore they (SPEEK/OG-POSS/ODADS membranes) possess relatively higher proton conductivities (0.0182 S/cm), lower methanol permeabilities (1.08 x 10^{-7} cm^2/s), and higher selectivity (0.0011 Ss/cm^3).

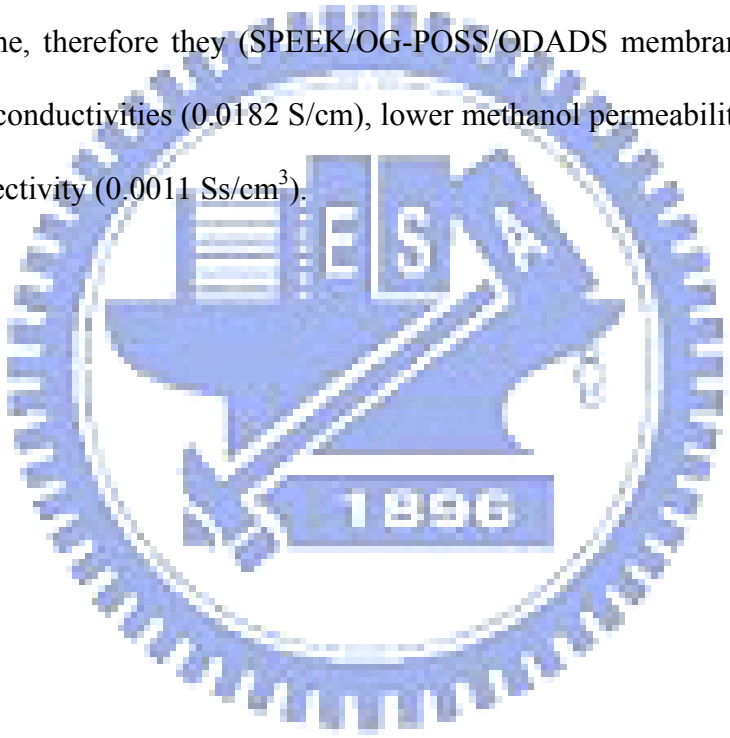

References

1. Hickner, M. A.; Ghassemi, H.; Kim, Y. S.; Einsla, B. R.; McGrath, J. E. *Chem. Rev.* **2004**, *104*, 4587.

2. Wang, F.; Hickner, M.; Kim, Y. S.; Zawodzinski, T. A.; McGrath, J. E. *J. Membrane. Sci.* **2002**, *197*, 231.

3. Rozière, J.; Jones, D. J.; *Annu.Rev. Mater. Res.* **2003**, *33*, 503.

4. Xing, P. X.; Robertson, G. P.; Guiver, M. D.; Mikhailenko, S. D. Kaliaguine, S. *Macromolecules* **2004**, *37*, 7960.

5. Wang, Z.; Ni, H. Z.; Zhao, C. J.; Li, X. F.; Zhang, G.; Shao, K.; Na, H. *J. Membrane. Sci.* **2006**, *285*, 239.

6. Schönberger, F.; Jochen Kerres, J. *J. Polym. Sci Pol Chem.* **2007**, *45*, 5237.

7. Patric Jannasch, P. *Curr. Opin. Colloid. Interface Sci.* **2003**, *8*, 96.

8. Fu, Y. Z.; Manthiram, A. Guiver, M. D. *Eelctrochem. Commun.* **2007**, *9*, 905.

9. Xing, P. X.; Robertson, G. P.; Guiver, M. D.; Mikhailenko, S. D.; Wang, K. P.; Kaliaguine, S. *J. Membrane. Sci.* **2004**, *229*, 95.

10. Fang, J. H.; Guo, X. X.; Harada, S.; Watari, T.; Tanaka, K.; Kita, H.; Okamoto, K. *Macromolecules* **2002**, *35*, 9022.

11. Zhou, Z. L.; Dominey, R. N.; Rolland, J. P.; Maynor, B. W.; Pandya, A. A.; M. DeSimone, J. M. *J. Am. Chem. Soc.* **2006**, *128*, 12963.

12. Miyatake, K.; Chikashige, Y.; Eiji Higuchi, E.; Masahiro Watanabe, M. *J. Am. Chem. Soc.* **2007**, *129*, 3879.

13. Asano, N.; Aoki, M.; Suzuki, S.; Miyatake, K.; Uchida, H.; Watanabe, M. *J. Am. Chem. Soc.* **2006**, *128*, 1762.

14. Xu, K.; Li, K.; Khanchaitit, P.; Wang, Q. *Chem. Mater.* **2007**, *19*, 5937.

15. M. Tsui, E. M.; Cortalezzi, M. M.; Wiesner, M. R. *J. Membrane. Sci.* **2007**, *306*, 8.

16. Subbaraman, R.; Ghassemi, H.; Zawodzinski, T. A. *J. Am. Chem. Soc.* **2007**, *128*, 2238.

17. Yamaguchi, T.; Zhou, H.; Nakazawa, S.; Hara, N.; *Adv. Mater.* **2007**, *19*, 592.

18. Grunzinger, S. J.; Watanabe, M.; Fukagawa, K.; Kikuchi, R.; Tominaga, Y.; Hayakawa, T.; Kakimoto, M. *J. Power. Sources.* **2008**, *175*, 120.

19. Yang, Y. S.; Shi, Z. Q.; Holdcroft, S. *Macromolecules* **2004**, *37*, 1678.

20. Shi, Z. Q.; Holdcroft, S. *Macromolecules* **2005**, *38*, 4193.

21. Farhat, T. R.; Hammond, P. T. *Adv. Funct. Mater.* **2005**, *15*, 945.

22. Ding, F. C.; Wang, S. J.; Xiao, M.; Meng Y. Z. *J. Power. Sources.* **2007**, *164*, 488.

23. Cho, K. Y.; Jung, H. Y.; Shin, S. S.; Choi, N. S.; Sung, S. J.; Park, J. K.; Choi, J. H.; Park, K. W.; Sung, Y. E. *Electrochim. Acta*. **2004**, *50*, 589.

24. Lee, C. H.; Park, H. B.; Chung, Y. S.; Lee, Y. M.; Freeman, B. D. *Macromolecules* **2006**, *39*, 755.

25. Fu, T. Z.; Zhao, C. J.; Zhong, S. L.; Zhang, G.; Shao, K.; Zhang, H. Q.; Wang, J.; Na, H. *J. Power. Sources.* **2007**, *165*, 708.

26. Qiao, J. L.; Hamaya, T.; Okada, T. *Chem. Mater.* **2005**, *17*, 2413.

27. Zhong, S. L.; Fu, T. Z.; Dou, Z. Y.; Zhao, C. J.; Na, H. *J. Power. Sources.* **2006**, *162*, 51.

28. Gasa, J. V.; Boob, S.; Weiss, R. A.; Shaw, M. T. *J. Membrane. Sci.* **2006**, *269*, 177.

29. Yamaki, T.; Kobayashi, K.; Asano, M.; Kubota, H.; Yoshida, M. *Polymer* **2004**, *45*, 6569.

30. Park, H. B.; Lee, C. H.; Sohn J. Y.; Lee, Y. M.; Freeman, B. D.; Kim, H. J. *J Membrane. Sci.* **2006**, *285*, 432.

31. Kim, D. S.; Guiver, M. D.; Nam, S. Y.; Yun, T. I.; Seo, M. Y.; Kim, S. J.; Hwang, H. S.; Rhim, J. W. *J. Membrane. Sci.* **2006**, *281*, 156.

32. Kim, D. S.; Liu, B. J.; Guiver, M. D. *Polymer* **2006**, *47*, 7871.

33. Chen, W. F.; Kuo, P. L. *Macromolecules* **2007**, *40*, 1987.

34. Shahi, V. K. *Solid. State. Ionics.* **2007**, *177*, 3395.

35. Vona, M. L. D.; Marani, D. D'Ottavi, C.; Trombetta, Marcella.; Traversa, E.; Beurroies, I.; Knauth, P.; Licoccia, S. *Chem. Mater.* **2006**, *18*, 69.

36. Kim, D. S.; Park, H. B.; Rhim, J. W.; Lee, Y. M. *J. Membrane. Sci.* **2004**, *240*, 37.

37. Su, Y. H.; Liu, Y. L.; Sun, Y. M.; Lai, J. Y.; Wang, D. M.; Gao, Y. Liu, B.; Guiver, M. D. *J. Membrane. Sci.* **2007**, *296*, 21.

38. Chen, S. W.; Holmberg, B.; Li, W. Z.; Wang, X.; Deng, W. Q.; Munoz, R.; Yan Y. S. *Chem. Mater.* **2006**, *18*, 5669.

39. Chang, Y. W.; Wang, E.; Shin, G.; Han, J. E.; Mather, P. T. *Polym. Adv. Technol.* **2007**, *18*, 535.

40. Kuo, S. W.; Lin, H. C.; Huang, W. J.; Huang, C. F.; Chang, F. C. *J. Polym. Sci., Polym. Phys.* **2006**, *44*, 673.

41. Kopesky, E. T.; Haddad, T. S.; Cohen, R. E.; McKinley, G. H. *Macromolecules* **2004**, *37*, 8992.

42. Li, G. Z.; Wang, L.; Toghiani, H.; Daulton, T. L.; Koyama, K.; Pittman, C. Y. *Macromolecules* **2001**, *34*, 8686.

43. Chen, W. Y.; Wang, Y. Z.; Kuo, S. W.; Huang, C. F.; Tung, P. H.; Chang, F. C. *Polymer* **2004**, *45*, 6897

44. Matejka, L.; Strachota, A.; Plestil, J.; Whelan, P.; Steinhart, M.; Slouf, M. *Macromolecules* **2004**, *37*, 9449.

45. Tamaki, R. ; Choi, J.; Laine, R. M. *Chem. Mater.* **2003**, *15*, 793.

46. Goldman, M.; Shen, L. *Phys. Rev.* **1966**, *114*, 321.

47. Kaplan, D. S. *J. Appl. Polym. Sci.* **1976**, *20*, 1615.

48. Leu, C. M.; Chang, Y. T.; Wei, K. H. *Chem. Mater.* **2003**, *15*, 2261.

49. Leu, C. M.; Chang, Y. T.; Wei, K. H. *Chem. Mater.* **2003**, *15*, 3721.

50. Lee, Y. J.; Huang, J. M.; Kuo, S. W.; Lu, J. S.; Chang, F. C. *Polymer* **2005**, *46*, 173.

51. Lee, Y. J.; Huang, J. M.; Kuo, S. W.; Chang, F. C. *Polymer* **2005**, *46*, 10056.

52. Ye, Y. S.; Chen, W. Y.; Wang, Y. Z. *J. Polym. Sci., Part A: Polym. Chem.* **2006**, *44*, 5391.

53. Liu, Y. L.; Chang, G. P.; Hsu, K. Y.; Chang, F. C. *J. Polym. Sci., Part A: Polym. Chem.* **2006**, *44*, 3852.

54. do Carmo, D. R.; Paim, L. L.; Dias, N. L. *Appl. Surf. Sci.* **2007**, *253*, 3683.

55. Chang, Y. W.; Wang, E.; Shin, G.; Han, J. E.; Mather, P. T. *Polym. Advan. Technol.* **2007**, *18*, 535.

56. Watari, T.; Wang, H. Y.; Kuwahara, K.; Tanaka, K.; Kita, H.; Okamoto, K. *J. Membr. Sci.* **2003**, *219*, 137.

57. Phillips, S. H.; Haddad, T. S.; Tomcrzak, S. *J. Curr. Opin. Solid State Mater. Sci* **2004**, *8*, 21.

58. Li, G. Z.; Wang, L. C.; Ni, H. L. *J. Inorg. Organomet. P.* **2001**, *11*, 123.

59. Liu, H. Z.; Zheng, S. X. *Macromol. Rapid Commun*. **2005**, *26*, 196.

60. Leu, C. M.; Reddy, G. M.; Wei, K. H.; Shu, C. F. *Chem. Mater*. **2003**, *11*, 2261.

61. Zhang, C.; Babonneau, F.; Bonmme, C.; Laine, R. M.; Soles, C. L.; Hristov, H. A.; Yee, A. F. *J. Am. Chem. Soc.* **1998**, *120*, 8380.

62. Leu, C. M.; Chang, Y. T.; Wei, K. H. *Macromolecules* **2003**, *36*, 9122.

63. Chen, W. Y.; Ho, K. S.; Hsieh, T. H.; Chang, F. C.; Wang, Y. Z. *Macromol. Rapid Commun*. **2006**, *27*, 452.

64. Devrim, Y. G.; Rzaev, Z.; Piskin, E. *Macromol. Chem. Phys.* **2007**, *208*, 175.

65. Robertson, G. P.; Mikhailenko, S. D.; Wang , K. P.; Xing, P. X.; Guiver, M. D.; Kaliaguine, S. *J. Membr. Sci.* **2003**, *219*, 113.

66. Zhang, H. B.; Pang, J. H.; Wang, D.; Li, A. Z.; Li, X. F.; Jiang, Z. H. *J. Membr. Sci.* **2005**, *264*, 56.

67. Gao, Y.; Robertson, G. P.; Guiver, M. D.; Jian, X.; Mikhailenko, S. D.; Wang, K.;

Kaliaguine, S. *J. Polym. Sci. Part A: Polym. Chem.* **2003**, *41*, 2731.

68. Yu, J. F.; Ngo, T.; McLean, G. *Chem. Mater.* **2005,** *17,* 387-394

69. Liu, H. Z.; Zheng, S.; Nie, K. M. *Macromolecules* **2005**, *38*, 5088.

70. Jamróz, D.; Maréchal, Y. *J. Phys. Chem. B.* **2005**, *109*, 19664.

71. Kornyshev, A. A.; Walbran, S. *J. Chem. Phys.* **2001**, *114*, 10039.

72. Kornyshev, A. A.; Kuznetsov, A. M.; Spohr, E.; Ulstrup, J. *J. Phys. Chem. B.* **2003**, *107*, 3351.

73. Eikerling, M. ; Kornyshev, A. A.; Kuznetsov, A. M. ; Ulstrup, J. ; Walbran, S. *J. Phys. Chem. B.* **2001**, *105*, 3646.

74. Siu, A.; Schmeisser, J.; Holdcroft, S. *J. Phys. Chem. B.* **2006**, *110*, 6072.

75. Choi, P. G.; Jalani, N. H.; Datta, R. *J. Electrochem. Soc.* **2005**, *152*, E123.

76. Lin, C. W.; Huang, Y. F.; Kannan, A. M. *J. Power. Sources.* **2007**, *164*, 449.

77. Lin, C. W.; Huang, Y. F.; Kannan, A. M. *J. Power. Sources.* **2007**, *171*, 340 .

78. Lee, C. H.; Park, H. B.; Chung, Y. S.; Lee, Y. M.; Freeman, B. D. *Macromolecules* **2006**, *39*, 755.

79. Zhao, C. J.; Wang, Z.; Bi, D. W.; Lin, H. D.; Shao, K.; Fu, T. Z.; Zhong, S. L.; Na, H. *Polymer* **2007**, *48*, 3090.

Scheme 4-1. Structure of the organic/inorganic networks.

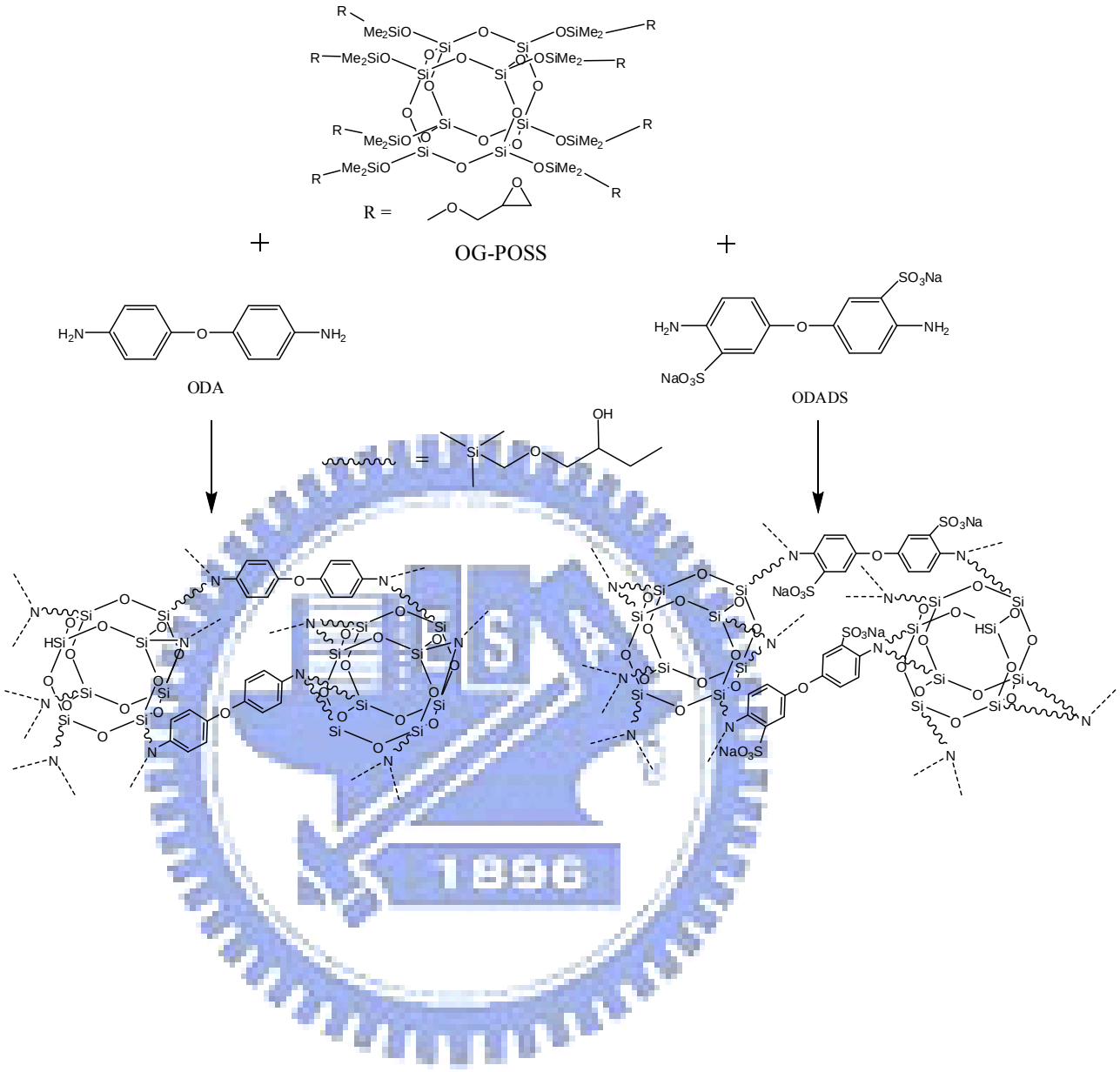

Table 4-1. Compositions of semi-interpenetrating network proton exchange membranes

	SPEEK (g)	OG-POSS (g)	ODA (g)	cross-linker content (wt%)
OG03	2	0.06	0.0124	3.5
OG07	2	0.14	0.0290	7.8
OG10	2	0.2	0.0414	10.8
OG15	2	0.3	0.0621	15.3
OG20	2	0.4	0.0829	19.4
	SPEEK (g)	OG-POSS (g)	ODADS (g)	cross-linker content (wt%)
SOG03	2	0.06	0.0249	4.1
SOG07	2	0.14	0.0580	9.0
SOG10	2	0.2	0.0829	12.4
SOG15	2	0.3	0.1243	17.5
SOG20	2	0.4	0.1657	22.0

Table 4-2. Properties of crossl-linked proton exchange membranes.

	water uptake (%)	IEC (mequiv/g)	λ (H_2O/SO_3H)	water desorption coefficient (cm^2/s)	bound water ratio [bound]/[total]	Methanol Permeability (cm^2/s)	Proton Conductivity (S/cm)	Selectivity (Ss/cm3)
SPEEK	53.0	1.99	14.82	7.32×10^{-5}	46.1	1.96×10^{-7}	0.0152	7.24×10^{-4}
OG03	32.9	1.71	10.38	7.50×10^{-5}	49.1	1.33×10^{-7}	0.0077	5.78×10^{-4}
OG07	27.0	1.38	10.38	3.31×10^{-5}	55.6	1.02×10^{-7}	0.0055	5.39×10^{-4}
OG10	23.5	1.02	11.48	1.48×10^{-5}	60.8	8.8×10^{-8}	0.0036	4.88×10^{-4}
OG15	19.3	0.93	12.2	7.34×10^{-5}	67.8	6.3×10^{-8}	0.0028	4.44×10^{-4}
OG20	16.8	0.79	13.85	5.98×10^{-5}	73.6	3.7×10^{-8}	0.0015	4.05×10^{-4}
SOG03	84.5	2.54	18.51	1.87×10^{-4}	35.2	2.03×10^{-7}	0.0182	8.96×10^{-4}
SOG07	68.6	2.88	13.26	1.35×10^{-4}	45.3	1.95×10^{-7}	0.0177	9.07×10^{-4}
SOG10	49.5	3.07	7.97	1.00×10^{-4}	57.4	1.67×10^{-7}	0.0171	1.02×10^{-3}
SOG15	40.3	3.26	7.30	7.24×10^{-5}	68.2	1.34×10^{-7}	0.0153	1.14×10^{-3}
SOG20	34.2	3.36	6.91	5.50×10^{-5}	74.5	1.08×10^{-7}	0.0119	1.11×10^{-3}

Figure 4-1. SEM micrographs (cross-sectional views) of the (a) OG15 and (b) SOG15 membranes.

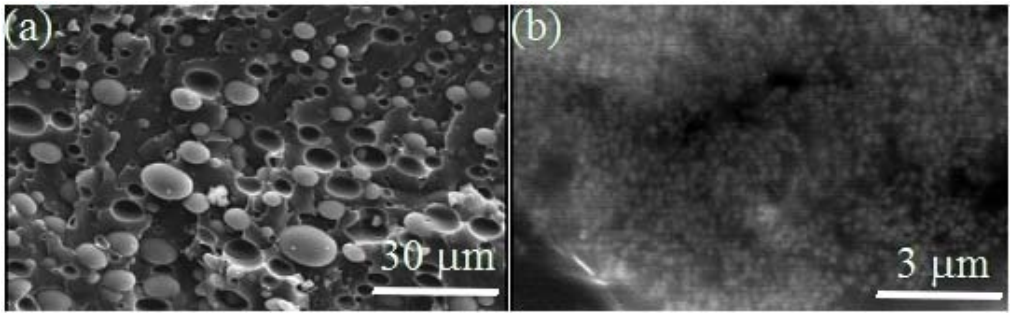

Figure 4-2. TGA curves of the (a) SPEEK, OG03, and OG10 membranes and the (b) OG03 and SOG03 membranes. (c) Corresponding loss factors (tan δ).

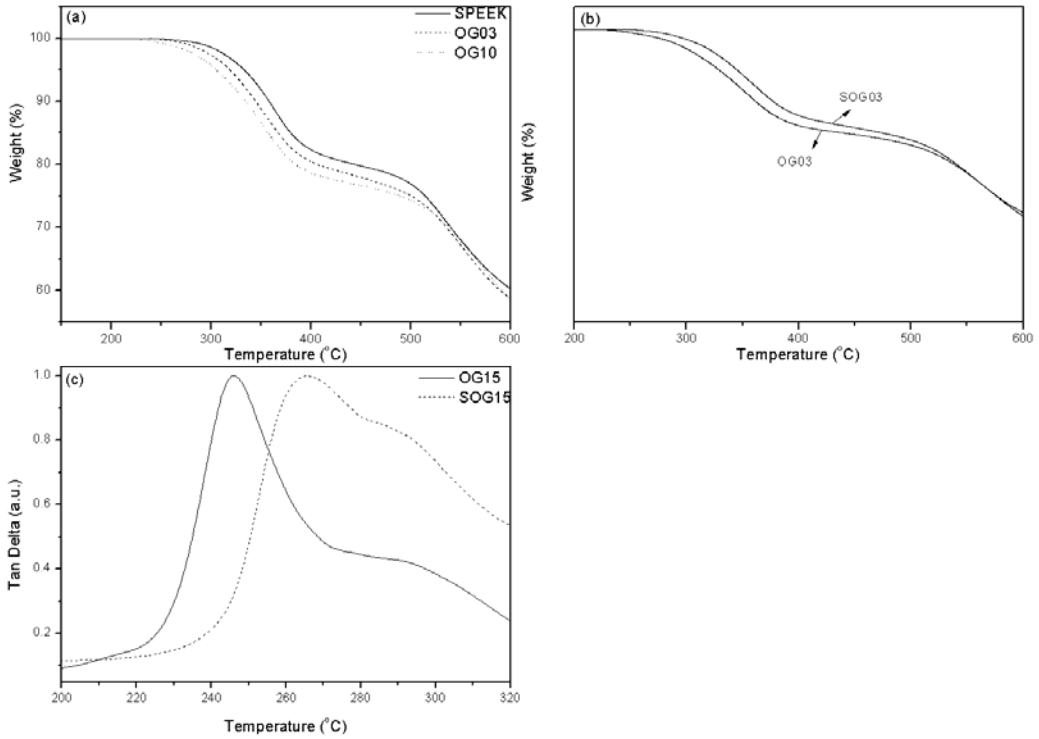

Figure 4-3. TEM micrographs of the (a) SPEEK, (b) OG10, and (c) SOG10 membranes.

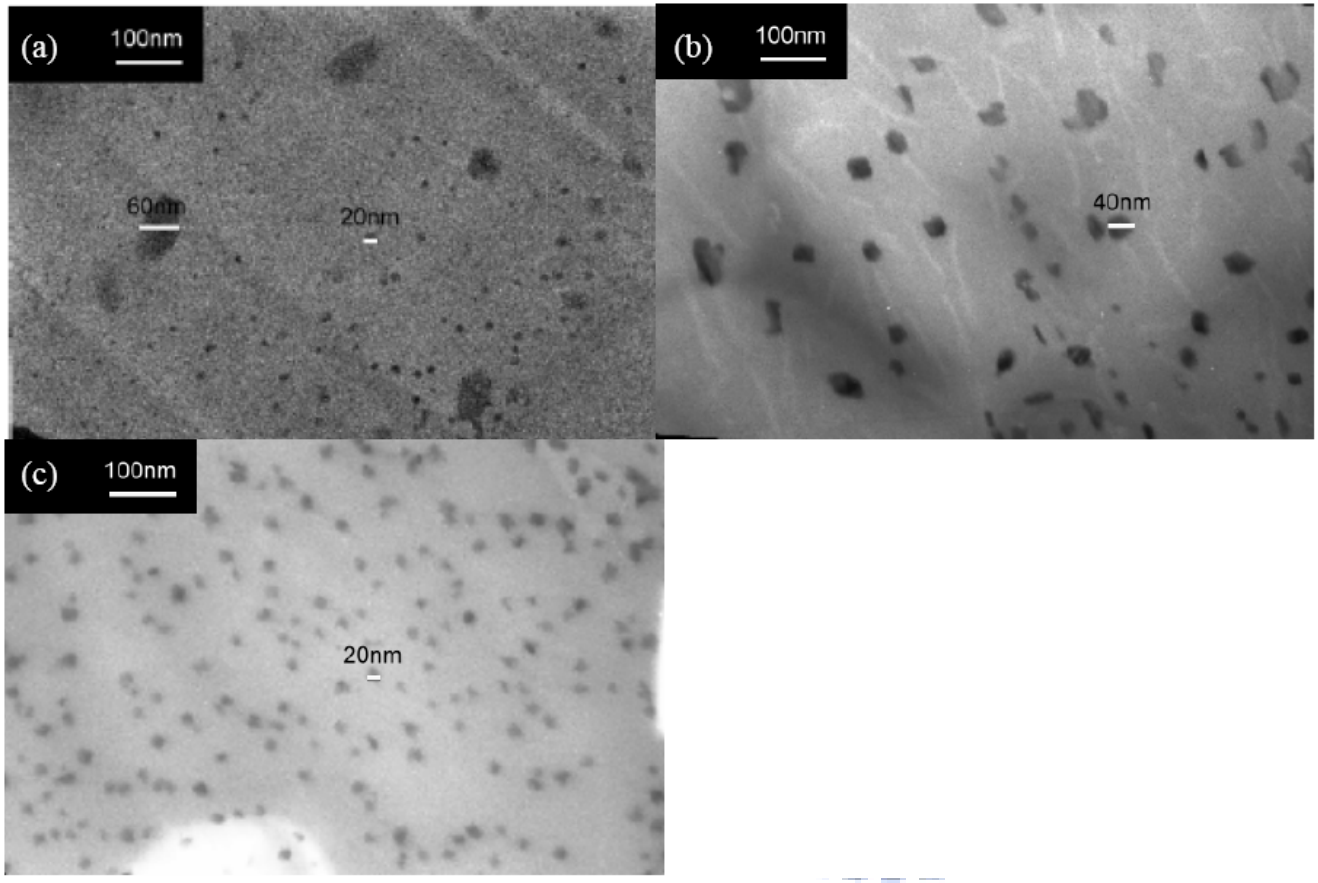

Figure 4-4. (a) IEC values (b) water uptakes, and (c) values of λ plotted with respect to the cross-linker content for the SPEEK, OG, and SOG membranes.

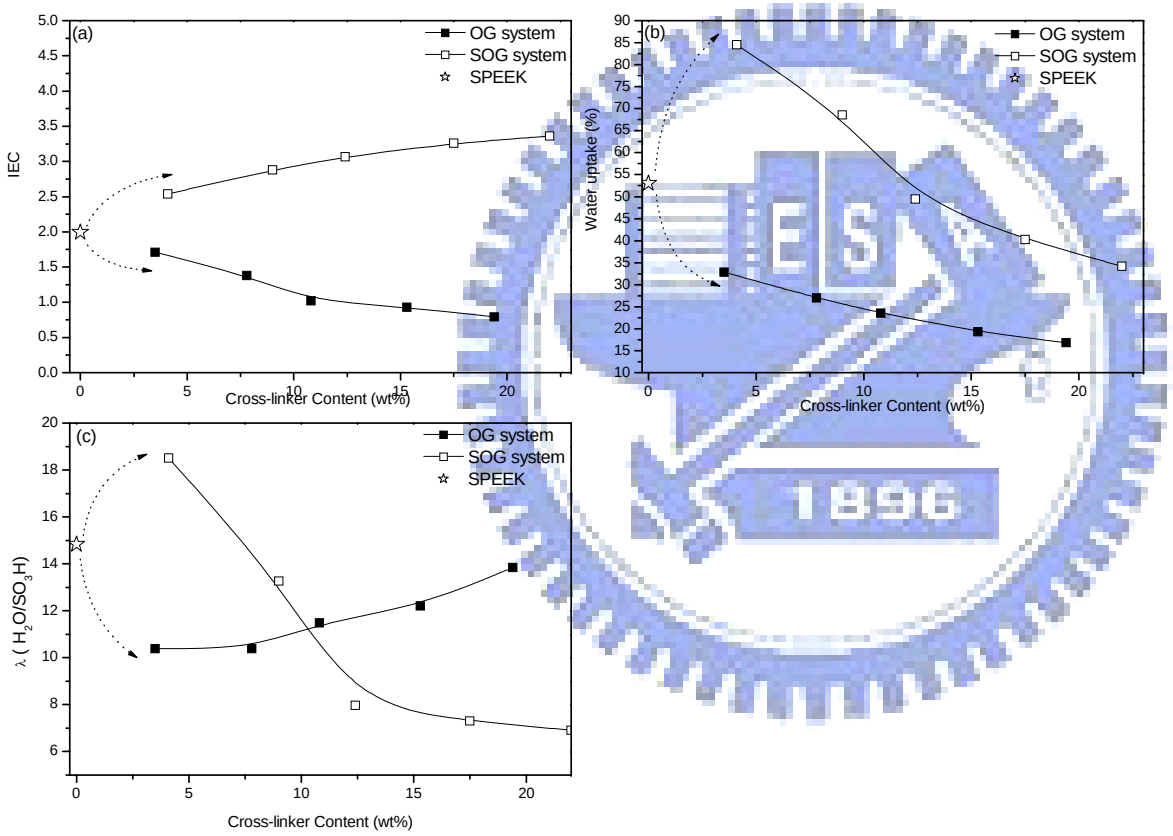

Figure 4-5. (a) Proton conductivities, (b) methanol permeabilities, and (c) selectivities plotted with respect to cross-linker content for SPEEK, OG, and SOG membranes.

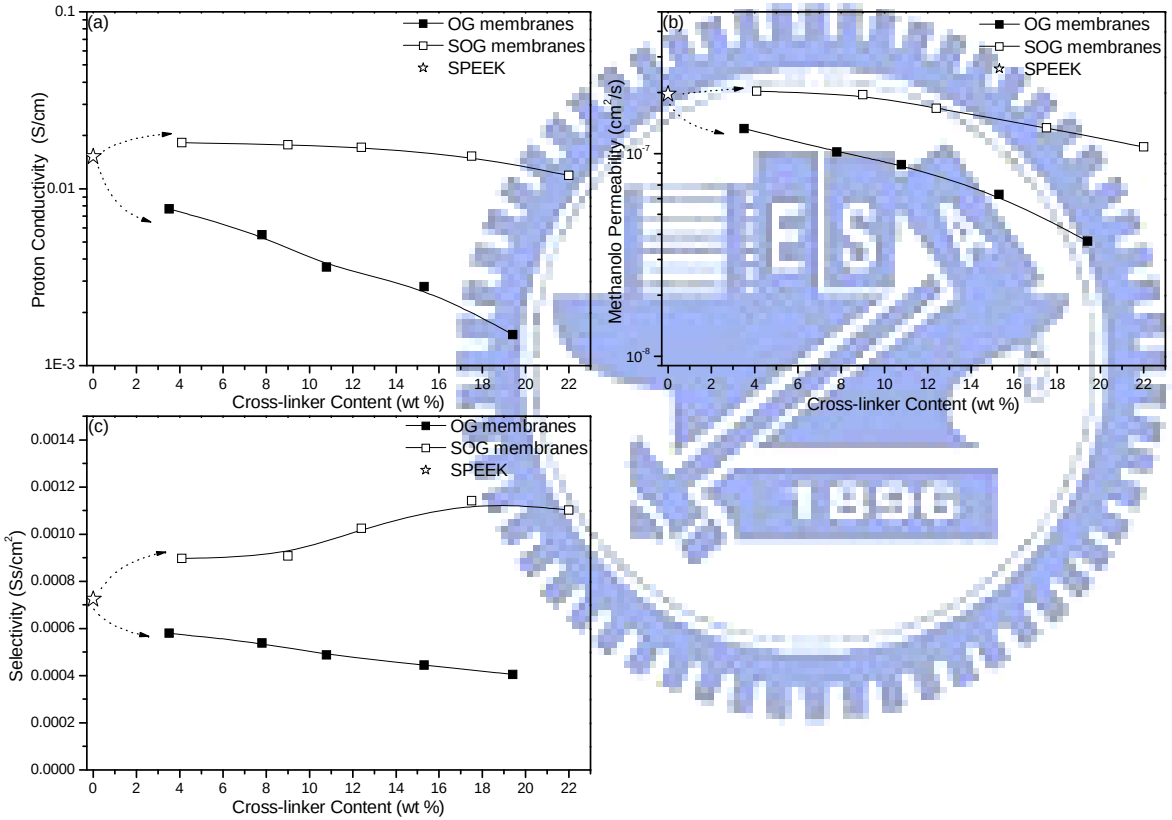

Figure 4-6. Proposed mechanisms of proton transfer within the (a) SPEEK (b) OG, and (c) SOG membranes

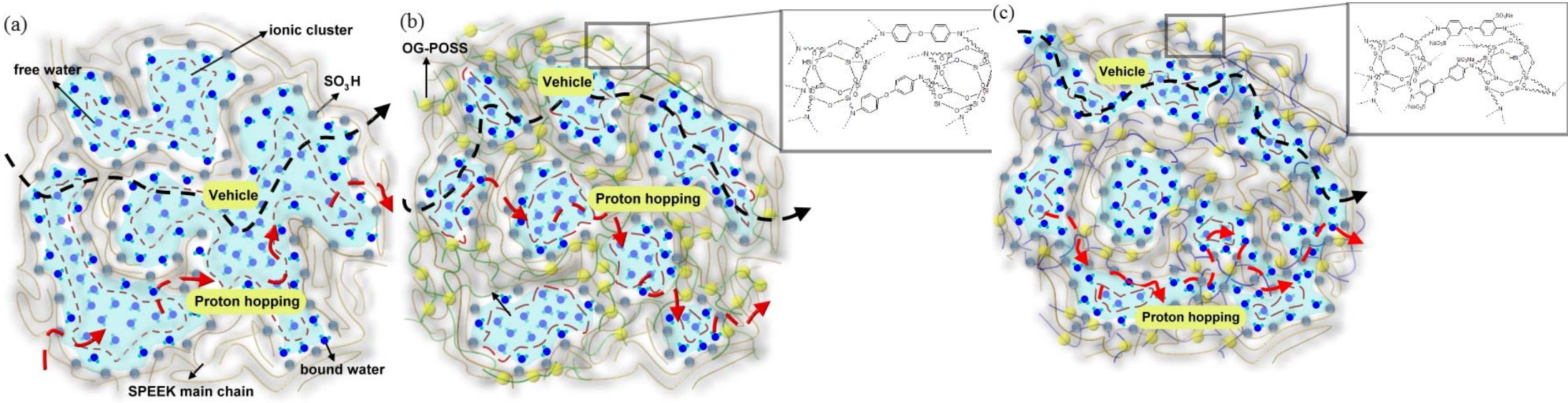

Chapter 5

Conclusions

According to the above, we can conclude that (1) for the OP-POSS/PMMA blends, the value of K_A of 29 was smaller than those for the PVPh/PMMA (K_A = 37.4) and EPh/PMMA (K_A = 101) blends, implying that the spacing between phenol groups attached to the POSS nanoparticle was smaller than those of the other two blend systems, resulting in a decrease in the ratio of the inter-association and self-association equilibrium constants, (2) the addition of $LiClO_4$ is a convenient and simple approach toward dispersing the OP-POSS nanoparticles within PMMA polymers, where the presence of $LiClO_4$ changes the physical effect of OP-POSS from that of a diluent to a cross-linker role, and (3) from a comparison of the properties of the OG and SOG membranes, the selectivity of SOG membranes is higher because of the sulfonic acid groups attached to the cross-linkers, resulting in increased bound water ratio and complex connection of these separated hydrophilic domains.

Publication List

1. Ying-Chieh Yen, Shiao-Wei Kuo, Chih-Feng Huang, Jem-Kun Chen, and Feng-Chih Chang* "***Miscibility and Hydrogen-Bonding Behavior in Organic/Inorganic Polymer Hybrids Containing Octaphenol Polyhedral Oligomeric Silsesquioxane***" *J. Phys. Chem. B.* **2008**, *112*, 10821.
2. Ying-Chieh Yen, Yun-Sheng Ye, Chih-Chia Cheng, Hsiu-Mei Chen, Hwo-Shuenn Sheu, Feng-Chih Chang* "***Effect of LiClO4 on the thermal and morphological properties of organic/inorganic polymer hybrids***" *Polymer* **2008**, *49*, 3625.
3. Chih-Chia Cheng, Chih-Feng Huang, Ying-Chieh Yen, Feng-Chih Chang* "A ‘‘***Plug and Play’’ Polymer Through Biocomplementary Hydrogen Bonding***" *Journal of Polymer Science: Part A: Polymer Chemistry* **2008**, *46*, 6416.
4. Yun-Sheng Ye, Ying-Chieh Yen, Wen-Yi Chen, Chih-Chia Cheng, Feng-Chih Chang* "***A Simple Approach Toward Low-Dielectric Polyimide Nanocomposites: Blending the Polyimide Precursor with a Fluorinated Polyhedral Oligomeric Silsesquioxane***" *Journal of Polymer Science: Part A: Polymer Chemistry* **2008**, *46*, 6296.
5. Chun-Yi Chiu, Ying-Jie Yen, Shiao-Wei Kuo, Hsien-Wei Chen, Feng-Chih Chang* "***Complicated phase behavior and ionic conductivities of PVP-co-PMMA-based polymer electrolytes***" *Polymer* **2007**, *48*, 1329.
6. Chun-Yi Chiu, Wen-Ho Hsu, Ying-Jie Yen, Shiao-Wei Kuo and Feng-Chin Chang* "***Miscibility Behavior and Interaction Mechanism of polymer Electrolytes Comprising LiClO4 and MPEG-block-PCL Copolymers***" *Macromolecules* **2005**, *38*, 6640.

Introduction to the Author

English Name: Yen, Ying-Chieh

Chinese Name: 嚴英傑

Birthday: 1981.12.31

Address: 251 臺北縣淡水鎮新民街 222 巷 20 號 2 樓

E-mail: jiestars@gmail.com

Education:

2000.09 ~ 2004.06 **B.S.**, Department of Chemical Engineering, National Taiwan University, Taipei, Taiwan, ROC.

2004.09 ~ 2008.10 **Ph.D.**, Department of Applied Chemistry, National Chiao Tung University, Hsinchu, Taiwan, ROC.